1-1-2014

Effect of Substrate Ligand Presentation on the Motility of Human T-Lymphocytes

George Aaron Dominguez
University of Pennsylvania, gdom@seas.upenn.edu

Effect of Substrate Ligand Presentation on the Motility of Human T-Lymphocytes

Abstract
EFFECT OF SUBSTRATE LIGAND PRESENTATION ON THE MOTILITY OF HUMAN T-LYMPHOCYTES

George Aaron Dominguez

Daniel A. Hammer

T lymphocyte homing and migration is critical for host defense and immunity. T lymphocytes must be captured from blood flow, tether and roll on the endothelial surface, engage chemokine receptors, and firmly adhere and migrate to sites of inflammation or to secondary lymphoid organs. How adhesive ligands, soluble factors such as chemokines, and fluid shear flow influence the motility of T lymphocytes is important for understanding this dynamic cascade of events. In this thesis, primary human T lymphocyte motility was quantified on various adhesive ligands (haptokinesis) in the presence of chemokines (chemokinesis) and in response to fluid flow. Through the use of microcontact printing onto PDMS surfaces we created surfaces that presented ligand at controlled densities either alone or in combination. The adhesive ligands ICAM-1, VCAM-1, and fibronectin were used to quantify cell migration in the absence of chemokine revealing different modes of T lymphocyte motility with ICAM-1 having an overall greater contribution. Using the homeostatic chemokines CCL19, CCL21, and CXCL12, we demonstrated that motility is biphasic and is dependent upon ICAM-1 concentration, and by presenting chemokines in combination, we can drive motility to higher levels than what was seen with each chemokine individually. Finally we demonstrated that directed migration either upstream or downstream of fluid flow is dependent upon the presence of ICAM-1, VCAM-1, or a combination of the two and the shear rate used. We have been able to show that adhesive ligands, chemokines, and shear flow all work in concert to promote robust primary human T lymphocyte adhesion and migration on microcontact printed PDMS surfaces. This research further elucidates how T lymphocytes interpret these signals for controlling homing to and motility within secondary lymphoid organs and the mechanisms of their migration.

Degree Type
Dissertation

Degree Name
Doctor of Philosophy (PhD)

Graduate Group
Bioengineering

First Advisor
Daniel A. Hammer

EFFECT OF SUBSTRATE LIGAND PRESENTATION ON THE MOTILITY OF HUMAN T-LYMPHOCYTES

George Aaron Dominguez

A DISSERTATION

in

Bioengineering

Presented to the Faculties of the University of Pennsylvania

in

Partial Fulfillment of the Requirements for the

Degree of Doctor of Philosophy

2014

Supervisor of Dissertation

_____

Daniel A. Hammer

Alfred G. and Meta A. Ennis Professor of Bioengineering and Chemical and Biomolecular Engineering

Graduate Group Chairperson

_____

Jason A. Burdick, Professor of Bioengineering

Dissertation Committee

Jason A. Burdick (Chair), Professor of Bioengineering
Janis K. Burkhardt, Associate Professor of Pathology and Laboratory Medicine
Matthew J. Lazzara, Assistant Professor of Chemical and Biomolecular Engineering

EFFECT OF SUBSTRATE LIGAND PRESENTATION ON THE MOTILITY OF HUMAN T-LYMPHOCYTES

This thesis is dedicated to my parents:

Albert and Brenda Dominguez

ACKNOWLEDGMENTS

I would first like to thank my advisor, Daniel Hammer, who has challenged me and fostered my growth as an independent scientist and researcher. I would also like to thank my current thesis committee, Jason Burdick, Jan Burkhardt, and Matt Lazzara as well as previous members, Chris Chen and Casim Sarkar, for their helpful questions, discussions, input, and interest in this work.

Without a doubt, I am extremely grateful to the members of the Hammer Lab for being great colleagues as well as friends. Randi Saunders, Olga Shebanova, Brendon Ricart, Dooyoung Lee, and Lauren Pepper welcomed me into the lab as a member of the Cell Group. They taught me several skills and techniques that provided me with the foundation for my dissertation research. Everyone else in the lab when I joined including Risat Jannat, Michael Beste, Dalia Levine, Greg Robbins, and Josh Katz were all welcoming and made the lab a great place to work. Everyone who has joined since I have been here including, Neha Kamat, Nimil Sood, Laurel Hind, Steven Henry, Kevin Vargo, Amy Chevalier, Nick Anderson, Joanna MacKay, Chen Gao, Woo-Sik Jang, and Seung Chul Park, you all have continued to teach me new things, offer helpful discussions, and make the Hammer lab a second home. I would also like to thank Eric Johnston for all of his technical expertise and guidance which without, my dissertation would not have been possible. A special shout out to Laurel and Kevin for being great colleagues and lab mates. The tea breaks, happy hours, and discussions were definitely some great times.

I would like to thank my friends that I have made here in Philadelphia. Y'all are truly my second family and have supported me through much of my journey here at Penn.

Finally I would like to thank my family. My parents, Albert and Brenda Dominguez, are my biggest fans and without their continuous support and love my dissertation research would not have been possible. I would also like thank my best friends, Gavin Cook and Leigh Ann Couch, for always being there. Y'all's love and support are something I could not go without. Y'all are both truly family – the brother and sister I never had.

ABSTRACT

EFFECT OF SUBSTRATE LIGAND PRESENTATION ON THE MOTILITY OF HUMAN T-LYMPHOCYTES

George Aaron Dominguez

Daniel A. Hammer

T lymphocyte homing and migration is critical for host defense and immunity. T lymphocytes must be captured from blood flow, tether and roll on the endothelial surface, engage chemokine receptors, and firmly adhere and migrate to sites of inflammation or to secondary lymphoid organs. How adhesive ligands, soluble factors such as chemokines, and fluid shear flow influence the motility of T lymphocytes is important for understanding this dynamic cascade of events. In this thesis, primary human T lymphocyte motility was quantified on various adhesive ligands (haptokinesis) in the presence of chemokines (chemokinesis) and in response to fluid flow. Through the use of microcontact printing onto PDMS surfaces we created surfaces that presented ligand at controlled densities either alone or in combination. The adhesive ligands ICAM-1, VCAM-1, and fibronectin were used to quantify cell migration in the absence of chemokine revealing different modes of T lymphocyte motility with ICAM-1 having an overall greater contribution. Using the homeostatic chemokines CCL19, CCL21, and CXCL12, we demonstrated that motility is biphasic and is dependent upon ICAM-1 concentration, and by presenting chemokines in combination, we can drive motility to higher levels than what was seen with each chemokine individually. Finally we demonstrated that directed migration either upstream or downstream of fluid flow is dependent upon the presence of ICAM-1, VCAM-1, or a

combination of the two and the shear rate used. We have been able to show that adhesive ligands, chemokines, and shear flow all work in concert to promote robust primary human T lymphocyte adhesion and migration on microcontact printed PDMS surfaces. This research further elucidates how T lymphocytes interpret these signals for controlling homing to and motility within secondary lymphoid organs and the mechanisms of their migration.

TABLE OF CONTENTS

LIST OF TABLES

LIST OF FIGURES

CHAPTER 1: INTRODUCTION

"Though many lay unburied, birds and beasts would not touch them, or died after tasting them…The bodies of dying men lay one upon the other…[But] those who had recovered from the disease…had now no fear for themselves; for the same man was never attacked twice - never at least fatally."

Thucydides, History of the Peloponnesian War, 431-428 B.C.

MOTIVATION

The immune system relies upon the ability of leukocytes to home and migrate to sites of inflammation or to tissues that facilitate further cell activation [1, 2]. T-lymphocytes are a class of leukocytes that naturally circulate throughout the body in search of antigen presenting cells (APCs) within secondary lymphoid organs (SLOs) that trigger their activation. This behavior, known as immune surveillance, is controlled by various adhesion ligands and chemokines that permit access to these SLOs [3]. In order for this to occur, T-lymphocytes must exit blood flow, firmly adhere to the blood endothelium, resist large hemodynamic forces, and migrate in response to gradients of adhesion ligands and/or chemokines [4]. Defects in T lymphocyte function, motility, and homing can lead various pathologies that impair immune function and health; therefore, it is critical to understand how these factors contribute to T lymphocyte motility and what extent adhesive ligands, chemokines, and fluid flow modulate them.

Integrins expressed on the T lymphocyte surface are critical for cell activation and facilitating interactions with other leukocytes. Particularly, Lymphocyte Function

Associated-antigen 1 (LFA-1) and Very Late Antigen-4 (VLA-4) are necessary to mediate transient and firm adhesions for migration (haptokinesis) to the blood endothelium during leukocyte extravasation [5]. Ligation of chemokine receptors with their cognate chemokine(s) provides intracellular signals that increase integrin activation and drive motility in response to a gradient (chemotaxis) or a local uniform concentration (chemokinesis) [6, 7]. Furthermore, in order for T lymphocytes to migrate on the blood endothelium, resistance to shear caused by fluid flow must be established via LFA-1- and VLA-4-mediated interactions (mechanotaxis). Elucidating how these factors contribute to T lymphocyte adhesion and motility is critical in understanding their function. Thus, the objective of this thesis, as outlined in the specific aims below, is to determine how adhesive ligands, chemokines, and shear flow work together in driving T lymphocyte adhesion and motility.

Specific Aim 1a: Characterize the motility of primary human T-lymphocytes on microcontact printed PDMS surfaces.

Integrin-ligand interactions are critical for T-lymphocyte trafficking and motility in the body. In this aim, we quantify the haptokinetic responses of T-lymphocytes to ICAM-1 and VCAM-1 on microcontact printed (μCP) PDMS substrates. T-lymphocytes will be seeded onto these integrin-binding proteins and their displacements will be tracked over time to calculate the differences in the random motility coefficients as a function of ligand composition and concentration. We hypothesize that biphasic motility will be observed for both ligands.

Specific Aim 1b: Characterize the chemokinetic behavior of primary human T-lymphocytes in response to the homeostatic chemokines CCL19 and CCL21.

It is well known that CCL19 and CCL21 are required for T-lymphocyte homing to secondary lymphoid organs (SLOs) through binding of the CCR7 chemokine receptor. In this aim, we quantify the chemokinetic responses of T-lymphocytes to CCL19 and CCL21 individually and in a combinatorial fashion to further elucidate the motility observed within SLOs. We hypothesize that there will be a peak in motility at a specific concentration of chemokine that will be near the K_D of the CCR7 receptor and, through combinatorial chemokine signaling, we will observe synergistic effects in migration through dual CCR7 ligation.

Specific Aim 2: Quantify the motility of primary human T-lymphocytes on ICAM-1, VCAM-1 and combined ICAM-1/VCAM-1 PDMS surfaces under shear flow.

During the homing of T lymphocytes to SLOs, cells must be captured from blood flow and migrate before diapedesis through the blood endothelium. The hemodynamic forces experienced by cells can be large and vary in magnitude throughout the body. In this aim, we quantify the ability of T-lymphocytes to migrate on ICAM-1, VCAM-1, and combined ICAM-1/VCAM-1 μCP PDMS surfaces as a function of shear rate and ligand density. We expect T-lymphocytes to elicit different modes of migration specifically in the direction of motility (mechanotaxis). Furthermore, it is also known that VCAM-1 engagement is capable of increasing β_2-dependent adhesion leading to changes migration. By presenting cells with various combinations of both ICAM-1 and VCAM-1, a synergetic response in adhesion should be observed further modulating directional migration under fluid flow

further elucidating the contributions of ICAM-1 and VCAM-1 to T-lymphocyte motility specifically under fluid flow.

REFERENCES

1. Springer, T.A., *Traffic signals for lymphocyte recirculation and leukocyte emigration: the multistep paradigm.* Cell, 1994. **76**(2): p. 301-14.
2. Butcher, E.C. and L.J. Picker, *Lymphocyte homing and homeostasis.* Science, 1996. **272**(5258): p. 60-6.
3. von Andrian, U.H. and C.R. Mackay, *T-cell Function and Migration: Two Sides of the Same Coin.* N Engl J Med, 2000. **343**(14): p. 1020-34.
4. Ley, K., et al., *Getting to the site of inflammation: the leukocyte adhesion cascade updated.* Nat Rev Immunol, 2007. **7**(9): p. 678-689.
5. Hyun, Y.-M., C. Lefort, and M. Kim, *Leukocyte integrins and their ligand interactions.* Immunologic Research, 2009. **45**(2-3): p. 195-208.
6. Miller, M.J., et al., *Autonomous T cell trafficking examined in vivo with intravital two-photon microscopy.* Proc Natl Acad Sci U S A, 2003. **100**(5): p. 2604-9.
7. Stachowiak, A.N., et al., *Homeostatic lymphoid chemokines synergize with adhesion ligands to trigger T and B lymphocyte chemokinesis.* J Immunol, 2006. **177**(4): p. 2340-8.

CHAPTER 2: BACKGROUND

IMMUNITY

Immunity is the ability to avoid infection and disease through sufficient biological defenses. This concept dates back to the 5th century BC when Thucydides wrote of individuals who recovered from illness during the Plague of Athens but were then able to nurse the sick without contracting it a second time. Along with Thucydides, scientists such as Edward Jenner, Robert Koch and Louis Pasteur led to the evolution of a field of medicine known as immunology. This is the study of the immune system and all the physical, chemical, and physiological components involved in its formation and function.

The immune system can be further separated into two forms of distinct yet interconnected kinds of immunity: innate and adaptive. At the heart of them are leukocytes - cells that defend the body against pathogens and foreign material by eliciting their immune functions. These dynamic and diverse groups of cells are capable of, but not limited to, recognizing and engulfing foreign pathogens, eliciting an allergic reaction, targeting cells for destruction, and providing immunity against a variety of diseases. These functions are all critical for the ability of the cells to "get to where they need to be"; in other words, they must migrate to their target sites rapidly, efficiently, and effectively. Defects in this process lead to complications in the immune response and increase the risk of death from infection.

OVERVIEW OF T-LYMPHOCYTES

Beginnings of T-Lymphocyte Biology

Although the concept of immunity has been recognized for over 2500 years, it was not until the early 1900's that lymphocytes were first implicated in allograft rejection of a foreign tissue. James Murphy recognized that tumor cells were difficult to inject and grow in adult organisms but could be grown in chick embryos. Upon injection of adult lymphoid tissue near the site of tumor cell implantation, rapid destruction of the cells occurred illustrating protection and graft rejection [1-3]. In 1964, it was first demonstrated that small lymphocytes continuously re-circulate from the thoracic duct, to blood, through secondary lymphoid tissue, and back to the thoracic duct [4]. Jacques Francis Albert Pierre Miller was the first to identify the essential role of the thymus in immune function and proposed the existence of the two major subsets of lymphocytes in mammals: T and B [5-7]. In 1975, the phenotypic and functional separation of $CD8^+$ and $CD4^+$ cells was established [8-10]. In the years that have past, we have seen a flurry of research and understanding in T lymphocyte biology that has led to novel technologies and therapeutics used to improve health and fight disease. Masopust et al. provides a thorough review of the history in the discovery of T lymphocytes [11].

The Career of a T-Lymphocyte

T lymphocytes develop from progenitors that are derived from the pluripotent hematopoietic stem cells in the bone marrow and migrate through the blood to the thymus, where they mature; for this reason they are called thymus-dependent (T) lymphocytes. Once cells leave the thymus, they are known as naïve and must determine whether antigen present poses a threat to the body. This is achieved through interactions with dendritic

cells found in secondary lymphoid organs [8]. Encounter with an antigen induces proliferation of T lymphocyte clones, yielding approximately 1000 times more descendants having identical antigenic specificity. After acquiring effector functions, they home to sites of inflammation where they interact with other leukocytes and parenchymal cells to elicit their immune functions [9]. Most effector cells die after antigen clearance but some remain for long-term protection against a re-exposure to antigen (T_{MEM}). A variety of molecules, such as integrins, adhesive ligands, and chemokines, are involved and work in concert to promote proper T lymphocyte homing, migration, and activation [12].

LEUKOCYTE HOMING AND MIGRATION

Leukocyte Homing

A successful immune response is critically dependent on the ability of leukocytes to leave blood circulation and enter the tissue space. This process involves a series of well-defined adhesive events involving primary adhesion molecules permitting the cell to be captured from flow and slow down (tethering/rolling), exposure to a chemoattractant stimulus through binding of a G-protein-coupled receptor, and then firm adhesion and arrest mediated by increased integrin activation [12-16]. These steps are necessary for migration and eventual leukocyte diapedesis through the blood endothelium permitting access to sites of inflammation or entrance to lymphoid tissue. This process is illustrated in Figure 2.1 and is known as leukocyte adhesion cascade and extravasation.

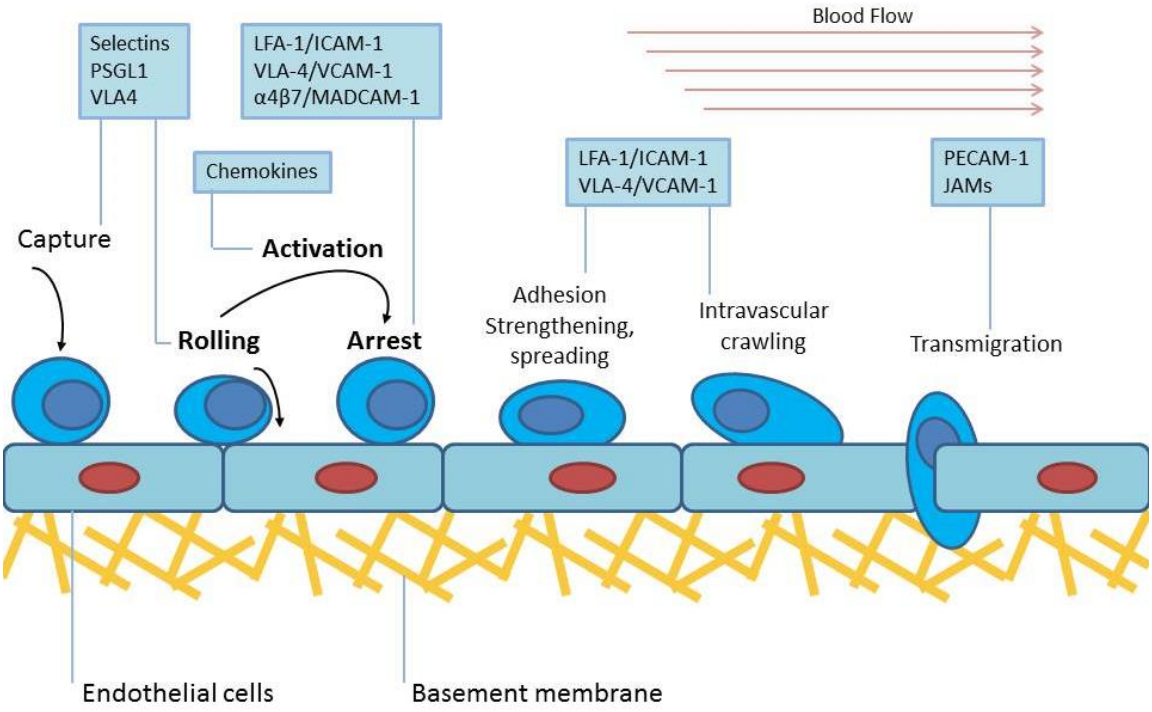

Figure 2.1. Overview of the leukocyte adhesion cascade and extravasation. Cells are captured from flow and undergo tethering/rolling via selectin molecules as well as integrins. Upon chemokine activation, cells arrest and undergo adhesion strengthening to support intravascular crawling and transmigration. Illustration redrawn from [16].

T-lymphocytes in circulation are covered in short microvilli containing bundles of actin filaments with low-affinity adhesion molecules such as L-selectin and the $\alpha_4\beta_1$ (VLA-4) integrin concentrated at the tips [17]. These molecules foster the tethering and rolling events upon the blood endothelium. Other adhesion molecules are involved in firm adhesion events, such as the $\alpha_L\beta_2$ (LFA-1) integrin, and are either distributed randomly on the cell surface or completely excluded from the tips [18]. Upon chemokine engagement, the microvilli collapse exposing firm adhesion molecules converting previous transient rolling interactions into stable, firm adhesions thus supporting subsequent transmigration through the endothelium [19].

T-Lymphocyte Motility

Leukocytes demonstrate rapid movement and flexibility in migrating through their environment compared to slower moving cells such as fibroblasts and endothelial cells. These frequent shape changes and dynamic cytoskeletal rearrangements have therefore led to their mode of migration being described as amoeboid. It has been demonstrated that some leukocytes migrate three-dimensionally through tissue without the need for integrins while in two-dimensions they are required [20]. This has led to questions as to what are the molecular requirements that promote leukocyte motility.

Migrating T-lymphocytes exhibit “hand mirror” morphology with a large cell body comprised of the nucleus followed by a narrow trailing uropod which projects above the surface [21]. Their mode of migration is driven by protrusion of actin-rich pseudopodia at the leading edge with contractile forces at the rear all controlled by members of the Rho GTPase famly of proteins, including RhoA, Rac1, and Cdc42 [22, 23]. Integrins mediate adhesion through interactions with their ligands via signals transmitted from inside the cell

termed "inside-out" signaling in response to chemoattractant binding to G_i-protein-coupled receptors. These signals elicit the transition from rolling to firm adhesion specifically through increased avidity and affinity of integrins [8, 9].

T-Lymphocyte Integrins: LFA-1 and VLA-4

Integrins are heterodimeric, transmembrane receptors that consist of an α and β chain linking the extracellular environment to the cell via adhesions ligands [24]. Adhesions are crucial for both the development and homeostasis of multicellular organisms [25]. Within the immune system, integrins participate in leukocyte attachment to blood endothelium and antigen presenting cells (APCs), cytotoxic killing, and extravasation of cells into lymph nodes or target tissues. Integrins predominantly expressed by leukocytes consist of a β_2 subunit coupled with one of several α subunits ($\alpha_L\beta_2$, $\alpha_M\beta_2$), or the α_4 subunit with its β_1 subunit counterpart ($\alpha_4\beta_1$ and $\alpha_4\beta_7$), and are capable of binding several adhesive ligands (Figure 2.2). Particularly, the integrins known as Lymphocyte Function-Associated Antigen-1 (LFA-1; $\alpha_L\beta_2$) and Very Late Antigen-4 (VLA-4; $\alpha_4\beta_1$) are critical for T lymphocyte activation and for facilitating interactions with other leukocytes, such as dendritic cells and B-lymphocytes, in order to elicit effector functions [12, 13, 26, 27]. In this thesis, we will focus on LFA-1- and VLA-4-mediated adhesion and motility in response to the engineered microenvironment.

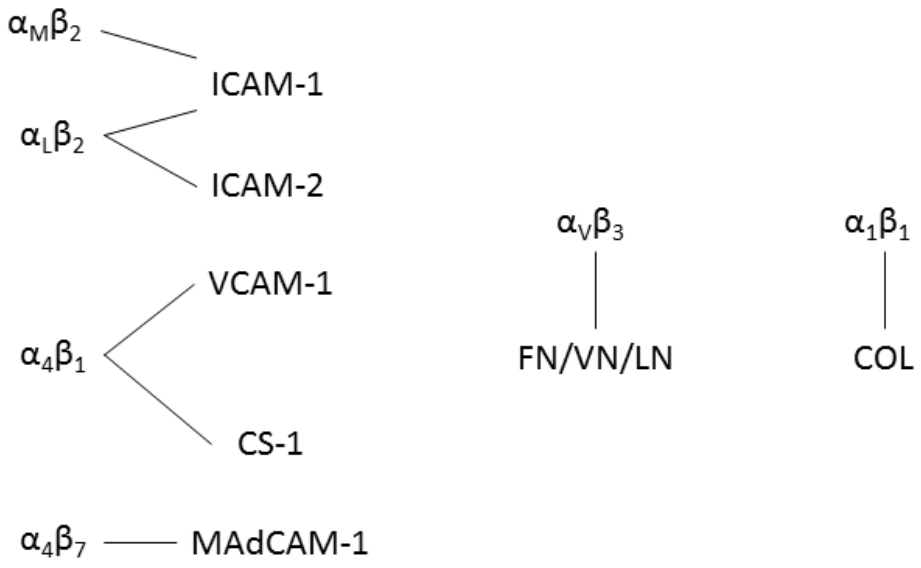

Figure 2.2. Leukocyte integrins and their ligands. Leukocyte integrins bind to liagnds found on the vascular endothelium as well as to components of the extracellular matrix (ECM). ICAM-1, intracellular adhesion molecule-1. ICAM-2, intracellular adhesion molecule-2. VCAM-1, vascular adhesion molecule-1. CS-1, connecting segment-1 of fibronectin. FN, fibronectin. VN, vitronectin. LN, laminin.

LFA-1 is expressed exclusively by leukocytes and is known to be involved in recruitment to inflammatory sites and lymphoid tissues as well as adhesions to other leukocytes [13]. Patients with leukocyte adhesion deficiency (LAD) lack the β_2 subunit and thus the ability to clear pathogens leading to recurrent infections and death at an early age. LFA-1 binds to a family of cell adhesion molecules known as intercellular adhesion molecules (ICAMs) which include ICAM-1, ICAM-2, ICAM-3, ICAM-4, and ICAM-5 [28-32]. The principal adhesion molecules used for migration are ICAM-1 and ICAM-2 and are involved in regulating LFA-1 function through outside-in signaling. ICAM-1 is expressed constitutively only at low levels on vascular endothelial cells and on some leukocytes [33]. Increase in ICAM-1 expression on multiple cell types has been shown to be induced by stimulation with inflammatory cytokines such as interleukin (IL)-1, tumor necrosis factor (TNF) α, interferon (IFN) γ or with lipopolysaccharide (LPS) [34-36]. Interactions between LFA-1 and ICAM-1 is accomplished through binding of the D1 domain of ICAM-1's five immunoglobulin (Ig)-like domains and requires LFA-1 activation [37].. The affinity and avidity of LFA-1 can be regulated through inside-out signaling, as well, by upstream regulators such as Rap-1 [38]. Calcium and diacylglycerol-regulated guanine nucleotide exchange factor I (CalDAG-GEFI) regulates Rap-1 activity and is known to be directly involved in LFA-1 activation induced by chemokines and PMA activation [39, 40]. Regulator of adhesion and polarization enrich in lymphocytes (RAPL), an effector molecule associated with Rap-1, is also involved in integrin activation triggered through chemokine engagement promoting LFA-1 dependent adhesion [41, 42].

VLA-4 is expressed by most resting lymphocytes, eosinophils, and monocytes, and plays a role in the development and differentiation of several tissue and cell types [43-45].

VLA-4 is expressed by bone marrow $CD34^+$ hematopoietic stem cells and is required for mobilization and homing of peripheral blood progenitors [93]. VLA-4 is capable of binding to fibronectin through the connecting segment-1 (CS-1) domain and to vascular cell adhesion molecule-1 (VCAM-1). This integrin is vital for competent immune function and has a tightly regulated multi-step function during rolling and arrest of leukocytes on the endothelium [46, 47]. VLA-4 is also involved in formation of the immunological synapse and cytoskeletal adaptor molecules, such as Rap-1, paxillin, and talin, regulate the adhesiveness [48]. As with LFA-1, Rap-1 also participates in the inside-out triggering of increased VLA-4 activation allowing for ligand binding and cell adhesion [49]. VLA-4 is known to be implicated in numerous autoimmune diseases and chronic inflammation such as multiple sclerosis, Crohn's disease, asthma, stroke, rheumatoid arthritis, and inflammatory bowel disease and is commonly a target for therapeutics of these diseases [50-55].

VLA-4's principal ligand, VCAM-1, contains 7 Ig-like domains and has been shown to be expressed in lymph nodes and the bone marrow to be used for the regulation of leukocyte homing [56]. Within the lymph nodes, VCAM-1 is expressed by postcapillary high endothelial venule (HEV) cells and follicular dendritic cells with increased expression induced by cytokines, high levels of reactive oxygen species (ROS), oxidized low density lipoprotein (oxLDL), high glucose, and turbulent shear stress [57]. Unlike LFA-1/ICAM-1 interactions, VLA-4 is capable of binding to two different domains (D1 or D4) depending upon the level of integrin activation; low affinity VLA-4 readily binds to the D1 domain of VCAM-1 while increased integrin activation is required for binding to the D4 domain

[58]. Thus, the binding of T lymphocytes to VCAM-1 domains is regulated by the activation state of VLA-4.

These integrins are critical for recruitment of leukocytes into sites of inflammation and lymphoid tissues through interactions with the blood endothelium under shear flow. It is known that cells respond to mechanical forces and are able to sense shear flow deformation (mechanoresponsive) [59]. Other cells types are known to respond to mechanical forces such as endothelial cells which align themselves along the direction of fluid flow [60, 61]. Under flow, VLA-4 participates in transient adhesion events, such as tethering and rolling, allowing for the capture of T-lymphocytes from fluid flow leading to firm arrest on VCAM-1 [46, 47]. Shear flow is known to stabilize and strengthen adhesion contacts mediated through LFA-1 and VLA-4 interactions [62-65]. These firm adhesions have been shown to be mandatory for T-lymphocyte migration on the endothelium and transendothelial migration (TEM) [66-69].

In this thesis, all T-lymphocytes were activated using phytohemagglutinin-M (PHA-M) leading to T-cell receptor (TCR) stimulation [70]. It has also been shown that upon activation, expression levels of LFA-1 and VLA-4 do not change but the activation level does increase to support cognate ligand binding [24, 71, 72]. Under such activation, T-lymphocytes migrate on adhesive ligand without chemokine, which we employ in this work.

T-Lymphocyte Polarity and Motility

In order for T-lymphocytes to respond to cues from the environment, cells must polarize and organize their intracellular machinery required for migration. This polarization is generally considered in terms of two distinct regions: the “front” and the

"rear." The front leading edge, or lamellipodium, is an F-actin rich region of the cell that is broad and flat driving the cell forward through actin polymerization and formation of new adhesions to the substratum independent of myosin II crosslinking [73, 74]. Projections from the lamellipodium, known as filopodia, are thin, finger-like protrusions that assist in leading edge attachment and migration. The real trailing edge, or uropod, is generally characterized by the retraction of old adhesions from the substratum and is much smaller than its leading edge counterpart. These two regions of the cell are believed to be governed by distinct signaling molecules and pathways. Molecules typically found near the leading edge of a migrating cell are PI3K, Rac, Cdc42, and most molecules associated with actin polymerization such as ARP 2/3 and WASP [75-77]. WASP has also been found to be required for optimal chemotaxis *in vitro* and *in vivo* [78-80]. Within the rear of the cell, molecules such as PTEN, Rho, ROCK, and myosin II are found contributing to actomyosin contraction allowing for cell forward propulsion [81]. Since Rho is downstream of chemokine GPCRs and is required for increased integrin affinity, it is believed that Rho is located near the site of GPCR signaling that then activates ROCK to result in actomyosin contraction necessary to generate forward thrust (Figure 2.3) [82-84]. Although the molecular players in polarity and migration have been identified, there is still much debate about the precise combination of molecules and signaling pathways that govern overall migration [85].

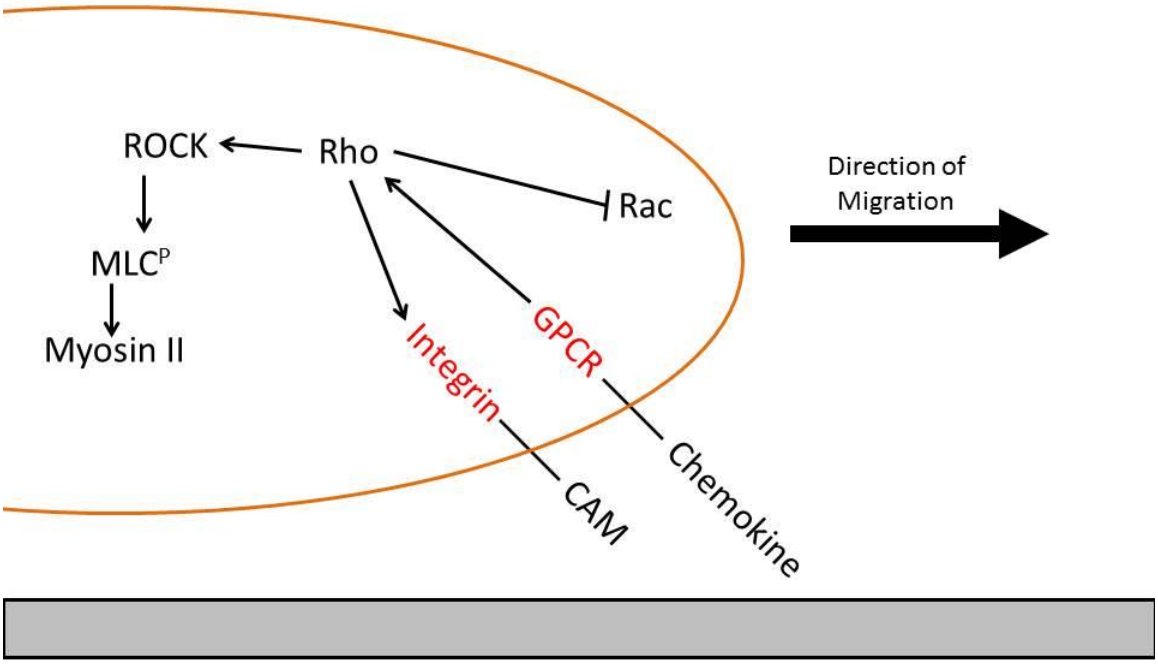

Figure 2.3. Adherent contractile zone found in migrating T lymphocytes along the cell and substratum interface. Rho may be used downstream from chemokine receptors and integrins to activate ROCK promoting myosin II contractility. MLC, myosin light chain. CAM, cell adhesion molecule. Illustration redrawn from [84].

Amoeboid Cell Motility

Although many molecules and signaling pathways such as PI3K, Rac, Cdc42, and Rho are conserved across numerous cell types, there are important distinctions to be made between amoeboid and mesenchymal migration. Amoeboid migration can be considered as a primitive mode of cell migration as even prokaryotes and lower level eukaryotes are able to display this mode of fast migration. Unlike cells displaying mesenchymal migration, these cells to do not use long-lasting, highly stable focal adhesions and typically lack stress fibers. This is not surprising seeing as these cells are highly dynamic and must be able to manipulate their body shape and cytoskeleton to alter their migration paths. They are capable of squeezing through small spaces such as tight junctions and pores within three-dimensional matrices where cells displaying mesenchymal migration typically require extracellular matrix remodeling through proteolysis and matrix metalloprotease (MMP) activity.

Classical models of amoeboid migration are typically done in the slime-mold *Dictyostelium discoideum* [77, 86, 87] and fish keratocytes [88, 89]. The most classic and heavily studied model for amoeboid motility in immune cells has been neutrophils [90, 91], and most recently, dendritic cells [92-95].

Dynamics of Migration

The coordinated motion of a cell plays a key role in development, angiogenesis, wound healing, cancer metastasis, immunity, and many other physiological processes. Often times, this motion is directed by external cues such as adhesion molecules (e.g. ICAM-1, VCAM-1), attractants (e.g. chemokines) and/or mechanical force (e.g. shear flow). Coordinated cell movement and migration is generally believed to have a purpose

(such as in the immune response) thus irregularities in this dynamic process can lead to pathologies [96, 97]. The random motility of cells can be used to quantify the conditions necessary to efficiently perform a search to locate randomly distributed target items such as a pathogen or antigen presenting cell.

A normal cell's trajectory resembles those of normal Brownian particles and is characterized by the mean-squared displacement, MSD, defined as

$$MSD(t) = \langle [x(t + t_0) - x(t_0)]^2 + [y(t + t_0) - y(t_0)]^2 \rangle$$

where $\langle ... \rangle$ denotes the combined average over all starting times t_0 and cell paths for a population [98]. Random walk theories have long been used to model animal displacements such as foraging behavior, predator-prey relationships, etc.; furthermore, these theories have also been used to model mammalian cell migration as uncorrelated random walks assuming that cells maintain no memory of previously taken steps [99, 100]. In theory, cells will move 'nowhere' on average, and their expected mean-squared displacement is linear with time. This is often used to convey the difference between a random walk versus directed motion such as chemotaxis where the *root* mean-squared displacement is linear with time [101]. Random walk is also known as Brownian motion which can be characterized by a mean-squared displacement proportional to $\sim t^{\alpha}$ for long time (t) intervals with $\alpha = 1$ indicating random diffusion. Anomalous diffusion arises when $\alpha \neq 1$ with subdiffusive behavior observed when $\alpha < 1$, superdiffusive with $\alpha > 1$, and ballistic motion when $\alpha = 2$. Recent evidence has demonstrated that Madin-Darby canine kidney (MDCK) cells, mammary epithelial cells (MCF-10A), human neutrophils, and *D. discoideum* move spontaneously in random directions and exhibit superdiffusive motion [90, 102-104]. Work shown in Harris et al. discusses that murine CD8+ T lymphocytes

undergo Lévy walks (a form of superdiffusive motion) to control the pathogen *Toxoplasma gondii* [105]. They propose that this type of motion occurs in order to increase the frequency of finding rare targets with more than an order of magnitude increase in efficiency compared to Brownian motion walkers by covering more territory. This strategy is used by a number of animals including monkeys and marine life to increase foraging efficiency [106-108]. In contrast, Miller et al. demonstrated that naïve murine T-lymphocytes undergo random walks within SLOs [109]. Here, in this thesis, we characterize the motility of activated human T-lymphocytes *in vitro* on engineered surfaces presenting ICAM-1 and VCAM-1

CHEMOTACTIC CYTOKINES (CHEMOKINES)

Chemokine Signaling

Lymphocytes express a variety of chemokine receptors (CCRs) that allow them to navigate throughout the body. The unique combination of CCRs expressed on a cell is thought to provide direction toward, retention within, and egress from a specific organ. As previously noted, T-lymphocytes are capable of binding to CCL19 and CCL21 via the CCR7 receptor as well as CXCL12 via the CXCR4 receptor which are required for entry into SLOs.

Chemokines themselves are small (approximately 8 – 14 kDa) and structurally related chemotactic cytokines that direct cell migration for a variety of leukocytes via their cognate binding interactions with G-protein coupled receptors (GPCRs) [110, 111]. Chemokines can be subdivided into 4 distinct groups (CXC, CX3C, CC, and C) according to the positioning of the first two closely paired and highly conserved cysteines of the

amino acid sequence [112]. Currently, over 40 chemokines are known in the human genome, most having homologues in mice. The main cell types directed by chemokines are neutrophils, dendritic cells, monocytes, macrophages, and lymphocytes, all of which have a role in host defense. In addition to providing directional cues, it has been suggested that chemokines also play fundamental roles in the development, homeostasis, and function of the immune system [110, 111, 113]. Furthermore, chemokines are also used outside of the immune system in a variety of cell types, including cells of the central nervous system or endothelial cells, where they can produce either angiogenic or angiostatic effects [114, 115]. This thesis will focus on the chemokines involved in the homing of T lymphocytes to SLOs specifically CCL19 and CCL21 with a less emphasis on CXCL12.

Chemokine receptors are a family of 7-transmembrane GPCRs found predominantly on leukocytes [112, 116]. Chemokine receptors are generally composed of approximately 350 amino acids, and have conserved structural motifs. The N-terminus generally has a short section of acidic residues oriented into the extracellular space binding to specific chemokines. The seven helical transmembrane domains orient into a barrel shape butted by three intracellular and three extracellular hydrophilic loops; the intracellular C-terminus contains hydroxyl groups (serine and threonine) providing sites for phosphorylation which in turn regulate receptor signaling [116]. Although chemokine receptors bear significant homology in their primary sequences, they typically bind only a small number of ligands, often only a single one. The chemokine receptor is named for the subtype of chemokine it binds, and is numbered according to an agreed-upon standard [110]. Our focus is on the CCR7 and, to a lesser extent, CXCR4 receptors for our investigation into T-lymphocyte adhesion and chemokinesis.

Chemokines and T-lymphocytes

CCR7 is a typical member of the 7-transmembrane domain GPCR family. Its two known ligands CCL19 and CCL21 exhibit similar affinities for receptor binding (~10 nM) [92, 117]. Signaling is thought to proceed by activation of a G-protein of the Gαi subfamily which may or may not be precoupled to the receptor. CCR7 binds the α-subunit of the G-protein and releases the βγ-subunit potentially activating both for downstream signaling. It has not been established which of CCR7's effects are downstream of the α and βγ subunits though preliminary evidence points to PI3K activity downstream of the βγ subunit [118]. Following activation, GPCRs eventually become desensitized and ultimately downregulated through a series of events occurring near the cytoplasmic carboxyl terminus. In one of the few studies of CCR7 phosphorylation, CCL19 was shown to induce significantly more phosphorylation than CCL21 in a human T cell lymphoma cell line [119, 120]. Once the GPCR is phosphorylated, arrestins are recruited to then induce clathrin-mediated endocytosis. CCL19 has been shown to induce a lower steady-state level of CCR7 surface expression by higher rates of endocytosis in a human T cell lymphoma cell line [120]. Also, it has been shown that CCL19 is able to desensitize a T lymphocyte's responsiveness to CCL21, but not vice versa [117]. *In vivo*, this may allow cells to respond first to CCL21 expressed on afferent lymphatic vessels, then subsequently to CCL19 to drive homing and migration to SLOs [121-123]. Cumulatively, significant evidence suggests that although CCL19 and CCL21 have similar affinities for CCR7, their downstream regulation has the potential to activate distinct physiological responses.

Furthermore, deletion of CCR7 or its ligands, CCL19 and CCL21, in the *plt/plt* mouse does not fully impair dendritic cell migration to lymph nodes (although it is

abnormal), implying that the process is complex and that additional chemokine-receptor pairs are likely to be involved. Within this same model, T lymphocytes show a delayed yet still intact immune response that is markedly prolonged [124]. For T lymphocytes, it is known that these chemokines are required for homing to the lymph node although the relative contributions of CCR7/CCL21 and CXCR4/CXCL12 signaling to T lymphocyte migration are not well studied. Recent research has shown that dendritic cells respond CCL19, CCL21, and CXCL12 differently during chemotaxis [92]. Other studies have shown that T lymphocytes are capable of chemotaxing to CCL19 and CCL21 in a microfluidic device eliciting different responses to chemokine concentration [125, 126]. In one study, the effects of the two chemokines were shown to not be additive [127]. Although these chemokine–receptor pairs may function independently of one another, combinatorial signaling is most likely required for effective homing and migration. These ideas are investigated in this thesis in the context of CCR7-mediated chemokinesis.

RECEPTOR-LIGAND KINETICS FOR CHEMOKINESIS

Monovalent Ligands Binding to a Monovalent Receptor

Receptor-ligand kinetics can be used to describe how a chemokine interacts with its cognate receptor, and thus, how the cells respond to that chemokine in solution. For equilibrium binding for the simple reversible reaction scheme between a monovalent free receptor R and a monovalent free ligand L to form a receptor/ligand complex C, the reaction can be written as

$$R + L \leftrightarrow C$$

where the relevant rate constants are the association rate constant k_f and the dissociation rate constant k_r. We can solve for the time rate of change for receptor/ligand complex C

as a function of free receptor number R and the ligand concentration L using principles of mass action kinetics described as

$$\frac{dC}{dt} = k_f RL - k_r C$$

Assuming steady state conditions ($\frac{dC}{dt} = 0$), the receptor-ligand binding kinetic equation can be solved as

$$C = \frac{RL}{K_D}$$

where $K_D = \frac{k_r}{k_f}$ which is known as the equilibrium dissociation constant. A small value of K_D indicates a high affinity of the receptor for the ligand; the avidin/biotin bond is one of the highest affinity bonds in nature with a $K_D = 10^{-15}M$ [128]. If we then assume that ligand concentration is constant, we can solve for receptor/ligand complexes at equilibrium, C_{eq}, and is described as

$$C_{eq} = \frac{R_T L}{K_D + L}$$

where R_T is the total number of receptors on the cell surface [98].

Differential Receptor Occupancy and the K_D: The Driving Force for Chemokinesis

The theory of differential receptor occupancy tells us that there is an ideal number of bound receptor complexes in a system that can achieve ideal chemokinesis [129]. If $[L] \ll K_D$ then $C_{eq} \approx 0$ and the cell will not be able to sense the presence of the chemokine. On the contrary, if $[L] \gg K_D$ then $C_{eq} \approx R_T$ meaning all available receptors are occupied preventing the cell from sensing the chemokine. When the concentration of chemokine is near the K_D then $C_{eq} \approx 0.5R_T$ and only half the receptors are bound. This provides enough

ligand around the cell to engage the receptors allowing for intracellular signaling to drive chemokines and/or chemotaxis.

The random motility coefficient for cells undergoing migration in a uniform field of chemokine (chemokinesis) has been shown to induce migration in a typical bell-shaped does-response curve with increasing chemokine concentration [92, 130]. This means that the random motility coefficient will increase with chemokine concentration until a peak is reached followed by a decline. For chemotaxis studies, values of the mean concentration near the K_D of the receptor are known to enhance directed migration [92, 131, 132].

These principles have been applied to experimentally determine the concentration of chemokine to support optimal migration of cells in both chemokinesis and chemotaxis assays; for instance, recent evidence has shown that CCR7 expressed by dendritic cells have a K_D ranging between 1 to 10 nM which is near the K_D previously observed for CCL19/CCL21/CCR7 interactions [92, 117]. Since T-lymphocytes express the same receptor, CCR7, it is of interest to determine if T lymphocytes respond in the same way as dendritic cells or if the same chemokine-receptor interactions govern their motility differently.

LITHOGRAPHY FOR CELL MIGRATION

PDMS

Polydimethylsiloxane (PDMS) is part of a family of organic silicon polymers referred to as silicones. PDMS is the most widely used silicone for biological applications, and its rheological properties allow it to be cast against three-dimensional structures whose

features are permanently maintained after curing. PDMS is ideal for microscopy because it is optically clear and is stiff enough to withstand large amounts of pressure permitting it to be used for microfluidics [133]. The shear modulus of PDMS is also easily varied from ~100 kPa to ~10 MPa by varying the ratio of elastomer to curing agent [134].

While PDMS is not fully biocompatible, it is inert, non-toxic, and non-flammable. After curing, the PDMS is both hydrophobic and methyl-terminated. The predominant – Si surface chemistry makes it difficult for polar solvents like water to wet the surface; this makes it attractive for binding hydrophobic compounds such as proteins. Plasma or UV ozone treatments can be used to oxidize the surface creating silanol (Si – OH) groups which increase its affinity for binding hydrophobic compounds. The oxidized surfaces are only stable for approximately 30 minutes due to hydrophobic recovery.

Overall, PDMS is an ideal candidate to be used for microcontact printing (μCP) due to (1) it can be readily made to generate micron-scale features on a substrate of a large area, (2) PDMS has low surface energy allowing to be separated from the template during fabrication and after stamping, and (3) it is relatively inert so it does not react with many chemicals [135].

Photolithography and Soft Lithography

Photolithography was developed in the 1950's and involves patterns of arbitrary complexity to be etched into very flat surfaces. A thin layer of photoresist is deposited on a flat silicon wafer via spin-coating. The desired pattern is then created in the photoresist by shining collimated light though a high resolution photomask. There are two types of photoresist; negative photoresists cure when exposed to light while positive photoresists degrade upon exposure to light [136]. Once a master is created, a negative replica can be

cast with PDMS by pouring degassed PDMS over the master and then curing at 25 – 150 ºC to fully crosslink the polymer. Soft lithography builds upon this and was invented by George Whitesides in the late 1990's using photomasks, polymer-based stamps and molds in various combinations to fabricate or replicate patterns [137]. There are two main steps involved. First, the fabrication of a pattern onto a substrate creating a 'master', and second, the use of that pattern to produce features negatively defined by the pattern's relief structure in an elastomeric substrate. The master is created using photolithography on silicon substrates. The term "soft" comes from the use of elastomeric materials, especially PDMS. This platform is commonly used to create features on the micron scale but can be scaled down to the nanometer scale [138, 139].

Microcontact Printing

Most classical adhesion and motility assays involve preparing two-dimensional surfaces by adsorbing an adhesive ligand onto glass or polystyrene with subsequent blocking with a solution of bovine serum albumin (BSA). The BSA is meant to block bare regions of the substrate that would otherwise encourage non-specific cell-substrate interactions. It has been demonstrated that some leukocytes are capable of interacting with BSA-blocked surfaces; specifically, it has been shown that human neutrophils bind to BSA through the use of the integrin Mac-1 ($\alpha_M\beta_2$) [90]. Microcontact printing allows for the creation of surfaces that do not support these type of non-specific interactions. Over the past decade, interests have increased in further understanding of the cell and how it interacts with its external environment. There have been rapid advances in the ability to engineer surfaces with geometrically patterned regions of adhesive ligand surround by non-

adhesive regions to provide insight into how the structure of the cell, surrounding extracellular matrix, and cell-cell interactions drive specific cell functions [140-143].

Methods to pattern adhesive ligand has proliferated greatly over the past decade [144]. The most commonly used technique is known as microcontact printing which was originally developed by George Whitesides and colleagues over two decades ago [137]. For this technique, flat PDMS stamps are used to transfer "inked" material onto a substrate. This technique has been used to pattern PDMS spin-coated substrates with various geometric patterns of ligand [142, 143].

The use of microcontact printing is extensively employed in this work to create surfaces that present adhesive ligand with or without chemokine in order to study the haptokinesis and chemokinesis of human primary T-lymphocytes. Furthermore, we demonstrate that these surfaces can be combined with a parallel flow chamber assay to investigate how shear flow dictates their migration in response to varying shear rates or ligand concentrations.

REFERENCES

1. Silverstein, A.M., *The lymphocyte in immunology: from James B. Murphy to James L. Gowans.* Nat Immunol, 2001. **2**(7): p. 569-71.
2. Murphy, J.B., *Studies in Tissue Specificity : Ii. The Ultimate Fate of Mammalian Tissue Implanted in the Chick Embryo.* J Exp Med, 1914. **19**(2): p. 181-6.
3. Murphy, J.B., *Factors of Resistance to Heteroplastic Tissue-Grafting : Studies in Tissue Specificity. Iii.* J Exp Med, 1914. **19**(5): p. 513-22.

4. Gowans, J.L. and E.J. Knight, *The Route of Re-Circulation of Lymphocytes in the Rat.* Proc R Soc Lond B Biol Sci, 1964. **159**: p. 257-82.

5. Miller, J.F., *Immunological function of the thymus.* Lancet, 1961. **2**(7205): p. 748-9.

6. Miller, J.F. and G.F. Mitchell, *The thymus and the precursors of antigen reactive cells.* Nature, 1967. **216**(5116): p. 659-63.

7. Mitchell, G.F. and J.F. Miller, *Immunological activity of thymus and thoracic-duct lymphocytes.* Proc Natl Acad Sci U S A, 1968. **59**(1): p. 296-303.

8. Cantor, H. and E.A. Boyse, *Functional subclasses of T lymphocytes bearing different Ly antigens. II. Cooperation between subclasses of Ly+ cells in the generation of killer activity.* J Exp Med, 1975. **141**(6): p. 1390-9.

9. Shiku, H., et al., *Expression of T-cell differentiation antigens on effector cells in cell-mediated cytotoxicity in vitro. Evidence for functional heterogeneity related to the surface phenotype of T cells.* J Exp Med, 1975. **141**(1): p. 227-41.

10. Kisielow, P., et al., *Ly antigens as markers for functionally distinct subpopulations of thymus-derived lymphocytes of the mouse.* Nature, 1975. **253**(5488): p. 219-20.

11. Masopust, D., et al., *A brief history of CD8 T cells.* European Journal of Immunology, 2007. **37**(S1): p. S103-S110.

12. von Andrian, U.H. and C.R. Mackay, *T-cell Function and Migration: Two Sides of the Same Coin.* N Engl J Med, 2000. **343**(14): p. 1020-34.

13. Springer, T.A., *Traffic signals for lymphocyte recirculation and leukocyte emigration: the multistep paradigm.* Cell, 1994. **76**(2): p. 301-14.

14. Butcher, E.C. and L.J. Picker, *Lymphocyte homing and homeostasis.* Science, 1996. **272**(5258): p. 60-6.

15. Rose, D.M., J. Han, and M.H. Ginsberg, *Alpha4 integrins and the Immune Response.* Immunol Rev, 2002. **186**: p. 118-24.

16. Ley, K., et al., *Getting to the site of inflammation: the leukocyte adhesion cascade updated.* Nat Rev Immunol, 2007. **7**(9): p. 678-689.

17. Majstoravich, S., et al., *Lymphocyte microvilli are dynamic, actin-dependent structures that do not require Wiskott-Aldrich syndrome protein (WASp) for their morphology*. Blood, 2004. **104**(5): p. 1396-1403.

18. Stein, J.V., et al., *L-selectin–mediated Leukocyte Adhesion In Vivo: Microvillous Distribution Determines Tethering Efficiency, But Not Rolling Velocity.* The Journal of Experimental Medicine, 1999. **189**(1): p. 37-50.

19. Nijhara, R., et al., *Rac1 mediates collapse of microvilli on chemokine-activated T lymphocytes.* J Immunol, 2004. **173**(8): p. 4985-93.

20. Lammermann, T., et al., *Rapid leukocyte migration by integrin-independent flowing and squeezing.* Nature, 2008. **453**(7191): p. 51-55.

21. Smith, A., et al., *A talin-dependent LFA-1 focal zone is formed by rapidly migrating T lymphocytes.* The Journal of Cell Biology, 2005. **170**(1): p. 141-151.

22. Sánchez-Madrid, F. and M. Angel del Pozo, *Leukocyte polarization in cell migration and immune interactions.* The EMBO Journal, 1999. **18**(3): p. 501-511.

23. Jacobelli, J., et al., *Confinement-optimized three-dimensional T cell amoeboid motility is modulated via myosin IIA-regulated adhesions.* Nat Immunol, 2010. **11**(10): p. 953-961.

24. Kinashi, T., *Intracellular signalling controlling integrin activation in lymphocytes.* Nat Rev Immunol, 2005. **5**(7): p. 546-59.

25. Hynes, R.O., *Integrins: versatility, modulation, and signaling in cell adhesion.* Cell, 1992. **69**(1): p. 11-25.

26. Rose, D.M., et al., *The Affinity of Integrin α4β1 Governs Lymphocyte Migration.* The Journal of Immunology, 2001. **167**(5): p. 2824-2830.

27. Hyun, Y.-M., C. Lefort, and M. Kim, *Leukocyte integrins and their ligand interactions.* Immunologic Research, 2009. **45**(2-3): p. 195-208.

28. Marlin, S.D. and T.A. Springer, *Purified intercellular adhesion molecule-1 (ICAM-1) is a ligand for lymphocyte function-associated antigen 1 (LFA-1).* Cell, 1987. **51**(5): p. 813-819.

29. de Fougerolles, A.R., et al., *Characterization of ICAM-2 and evidence for a third counter-receptor for LFA-1.* J Exp Med, 1991. **174**(1): p. 253-67.

30. de Fougerolles, A.R., X. Qin, and T.A. Springer, *Characterization of the function of intercellular adhesion molecule (ICAM)-3 and comparison with ICAM-1 and ICAM-2 in immune responses.* J Exp Med, 1994. **179**(2): p. 619-29.

31. Tian, L., et al., *Binding of T lymphocytes to hippocampal neurons through ICAM-5 (telencephalin) and characterization of its interaction with the leukocyte integrin CD11a/CD18.* Eur J Immunol, 2000. **30**(3): p. 810-8.

32. Ihanus, E., et al., *Characterization of ICAM-4 binding to the I domains of the CD11a/CD18 and CD11b/CD18 leukocyte integrins.* Eur J Biochem, 2003. **270**(8): p. 1710-23.

33. Rothlein, R., et al., *A human intercellular adhesion molecule (ICAM-1) distinct from LFA-1.* J Immunol, 1986. **137**(4): p. 1270-4.

34. Dustin, M.L., et al., *Induction by IL 1 and interferon-gamma: tissue distribution, biochemistry, and function of a natural adherence molecule (ICAM-1).* J Immunol, 1986. **137**(1): p. 245-54.

35. Pober, J.S., et al., *Two distinct monokines, interleukin 1 and tumor necrosis factor, each independently induce biosynthesis and transient expression of the same antigen on the surface of cultured human vascular endothelial cells.* J Immunol, 1986. **136**(5): p. 1680-7.

36. Pober, J.S., et al., *Overlapping patterns of activation of human endothelial cells by interleukin 1, tumor necrosis factor, and immune interferon.* J Immunol, 1986. **137**(6): p. 1893-6.

37. Lawson, C. and S. Wolf, *ICAM-1 signaling in endothelial cells.* Pharmacol Rep, 2009. **61**(1): p. 22-32.

38. Katagiri, K., et al., *Rap1 is a potent activation signal for leukocyte function-associated antigen 1 distinct from protein kinase C and phosphatidylinositol-3-OH kinase.* Mol Cell Biol, 2000. **20**(6): p. 1956-69.

39. Kawasaki, H., et al., *A Rap guanine nucleotide exchange factor enriched highly in the basal ganglia.* Proc Natl Acad Sci U S A, 1998. **95**(22): p. 13278-83.

40. Ghandour, H., et al., *Essential role for Rap1 GTPase and its guanine exchange factor CalDAG-GEFI in LFA-1 but not VLA-4 integrin mediated human T-cell adhesion.* Blood, 2007. **110**(10): p. 3682-90.

41. Kinashi, T. and K. Katagiri, *Regulation of lymphocyte adhesion and migration by the small GTPase Rap1 and its effector molecule, RAPL*. Immunol Lett, 2004. **93**(1): p. 1-5.

42. Katagiri, K., M. Imamura, and T. Kinashi, *Spatiotemporal regulation of the kinase Mst1 by binding protein RAPL is critical for lymphocyte polarity and adhesion*. Nat Immunol, 2006. **7**(9): p. 919-28.

43. Lobb, R.R. and M.E. Hemler, *The pathophysiologic role of alpha 4 integrins in vivo.* J Clin Invest, 1994. **94**(5): p. 1722-8.

44. Luo, B.H., C.V. Carman, and T.A. Springer, *Structural basis of integrin regulation and signaling.* Annu Rev Immunol, 2007. **25**: p. 619-47.

45. Gonzalez-Amaro, R., M. Mittelbrunn, and F. Sanchez-Madrid, *Therapeutic anti-integrin (alpha4 and alphaL) monoclonal antibodies: two-edged swords?* Immunology, 2005. **116**(3): p. 289-96.

46. Alon, R., et al., *The integrin VLA-4 supports tethering and rolling in flow on VCAM-1*. J Cell Biol, 1995. **128**(6): p. 1243-53.

47. Berlin, C., et al., *α4 integrins mediate lymphocyte attachment and rolling under physiologic flow.* Cell, 1995. **80**(3): p. 413-422.

48. Sims, T.N. and M.L. Dustin, *The immunological synapse: integrins take the stage.* Immunol Rev, 2002. **186**: p. 100-17.

49. Reedquist, K.A., et al., *The small GTPase, Rap1, mediates CD31-induced integrin adhesion.* J Cell Biol, 2000. **148**(6): p. 1151-8.

50. Yednock, T.A., et al., *Prevention of experimental autoimmune encephalomyelitis by antibodies against alpha 4 beta 1 integrin.* Nature, 1992. **356**(6364): p. 63-6.

51. Ghosh, S., et al., *Natalizumab for active Crohn's disease.* N Engl J Med, 2003. **348**(1): p. 24-32.

52. Laberge, S., et al., *Role of VLA-4 and LFA-1 in allergen-induced airway hyperresponsiveness and lung inflammation in the rat.* Am J Respir Crit Care Med, 1995. **151**(3 Pt 1): p. 822-9.

53. Offner, H., et al., *Splenic atrophy in experimental stroke is accompanied by increased regulatory T cells and circulating macrophages.* J Immunol, 2006. **176**(11): p. 6523-31.

54. Laffon, A., et al., *Upregulated expression and function of VLA-4 fibronectin receptors on human activated T cells in rheumatoid arthritis.* J Clin Invest, 1991. **88**(2): p. 546-52.

55. Podolsky, D.K., *Inflammatory bowel disease (1).* N Engl J Med, 1991. **325**(13): p. 928-37.

56. Ren, G., et al., *Inflammatory cytokine-induced intercellular adhesion molecule-1 and vascular cell adhesion molecule-1 in mesenchymal stem cells are critical for immunosuppression.* J Immunol, 2010. **184**(5): p. 2321-8.

57. Cook-Mills, J.M., M.E. Marchese, and H. Abdala-Valencia, *Vascular cell adhesion molecule-1 expression and signaling during disease: regulation by reactive oxygen species and antioxidants.* Antioxid Redox Signal, 2011. **15**(6): p. 1607-38.

58. Kilger, G., et al., *Differential regulation of alpha 4 integrin-dependent binding to domains 1 and 4 of vascular cell adhesion molecule-1.* J Biol Chem, 1995. **270**(11): p. 5979-84.

59. Alon, R. and M.L. Dustin, *Force as a facilitator of integrin conformational changes during leukocyte arrest on blood vessels and antigen-presenting cells.* Immunity, 2007. **26**(1): p. 17-27.

60. Li, S., et al., *The role of the dynamics of focal adhesion kinase in the mechanotaxis of endothelial cells.* Proceedings of the National Academy of Sciences, 2002. **99**(6): p. 3546-3551.

61. Hsu, S., et al., *Effects of shear stress on endothelial cell haptotaxis on micropatterned surfaces.* Biochem Biophys Res Commun, 2005. **337**(1): p. 401-9.

62. Woolf, E., et al., *Lymph node chemokines promote sustained T lymphocyte motility without triggering stable integrin adhesiveness in the absence of shear forces.* Nat Immunol, 2007. **8**(10): p. 1076-85.

63. Chen, C., et al., *High Affinity Very Late Antigen-4 Subsets Expressed on T Cells Are Mandatory for Spontaneous Adhesion Strengthening But Not for Rolling on VCAM-1 in Shear Flow.* The Journal of Immunology, 1999. **162**(2): p. 1084-1095.

64. Salas, A., et al., *Transition From Rolling to Firm Adhesion Is Regulated by the Conformation of the I Domain of the Integrin Lymphocyte Function-associated Antigen-1*. Journal of Biological Chemistry, 2002. **277**(52): p. 50255-50262.

65. Alon, R. and K. Ley, *Cells on the run: shear-regulated integrin activation in leukocyte rolling and arrest on endothelial cells.* Curr Opin Cell Biol, 2008. **20**(5): p. 525-32.

66. Valignat, M.P., et al., *T lymphocytes orient against the direction of fluid flow during LFA-1-mediated migration.* Biophys J, 2013. **104**(2): p. 322-31.

67. Steiner, O., et al., *Differential Roles for Endothelial ICAM-1, ICAM-2, and VCAM-1 in Shear-Resistant T Cell Arrest, Polarization, and Directed Crawling on Blood–Brain Barrier Endothelium.* The Journal of Immunology, 2010. **185**(8): p. 4846-4855.

68. Cinamon, G., et al., *Novel chemokine functions in lymphocyte migration through vascular endothelium under shear flow*. Journal of Leukocyte Biology, 2001. **69**(6): p. 860-866.

69. Cinamon, G., V. Shinder, and R. Alon, *Shear forces promote lymphocyte migration across vascular endothelium bearing apical chemokines.* Nat Immunol, 2001. **2**(6): p. 515-22.

70. O'Flynn, K., et al., *Different pathways of human T-cell activation revealed by PHA-P and PHA-M.* Immunology, 1986. **57**(1): p. 55-60.

71. Dustin, M.L. and T.A. Springer, *T-cell receptor cross-linking transiently stimulates adhesiveness through LFA-1.* Nature, 1989. **341**(6243): p. 619-24.

72. Shimizu, Y., et al., *Regulated expression and binding of three VLA (beta 1) integrin receptors on T cells.* Nature, 1990. **345**(6272): p. 250-3.

73. Takesono, A., et al., *Microtubules Regulate Migratory Polarity through Rho/ROCK Signaling in T Cells.* PLoS ONE, 2010. **5**(1): p. e8774.

74. Iden, S. and J.G. Collard, *Crosstalk between small GTPases and polarity proteins in cell polarization.* Nat Rev Mol Cell Biol, 2008. **9**(11): p. 846-859.

75. Weiger, M.C., et al., *Spontaneous phosphoinositide 3-kinase signaling dynamics drive spreading and random migration of fibroblasts.* Journal of Cell Science, 2009. **122**(3): p. 313-323.

76. Lämmermann, T., et al., *Cdc42-dependent leading edge coordination is essential for interstitial dendritic cell migration.* Blood, 2009. **113**(23): p. 5703-5710.

77. Chung, C.Y., S. Funamoto, and R.A. Firtel, *Signaling pathways controlling cell polarity and chemotaxis.* Trends in Biochemical Sciences, 2001. **26**(9): p. 557-566.

78. Haddad, E., et al., *The interaction between Cdc42 and WASP is required for SDF-1–induced T-lymphocyte chemotaxis.* Blood, 2001. **97**(1): p. 33-38.

79. Gallego, M.D., et al., *WIP and WASP play complementary roles in T cell homing and chemotaxis to SDF-1alpha.* Int Immunol, 2006. **18**(2): p. 221-32.

80. Snapper, S.B., et al., *WASP deficiency leads to global defects of directed leukocyte migration in vitro and in vivo.* Journal of Leukocyte Biology, 2005. **77**(6): p. 993-998.

81. Van Keymeulen, A., et al., *To stabilize neutrophil polarity, PIP3 and Cdc42 augment RhoA activity at the back as well as signals at the front.* The Journal of Cell Biology, 2006. **174**(3): p. 437-445.

82. Constantin, G., et al., *Chemokines Trigger Immediate β2 Integrin Affinity and Mobility Changes: Differential Regulation and Roles in Lymphocyte Arrest under Flow.* Immunity, 2000. **13**(6): p. 759-769.

83. Laudanna, C., J.J. Campbell, and E.C. Butcher, *Role of Rho in chemoattractant-activated leukocyte adhesion through integrins.* Science, 1996. **271**(5251): p. 981-3.

84. Krummel, M.F. and I. Macara, *Maintenance and modulation of T cell polarity.* Nat Immunol, 2006. **7**(11): p. 1143-9.

85. Lämmermann, T. and M. Sixt, *Mechanical modes of 'amoeboid' cell migration.* Current Opinion in Cell Biology, 2009. **21**(5): p. 636-644.

86. Wessels, D., et al., *PTEN plays a role in the suppression of lateral pseudopod formation during Dictyostelium motility and chemotaxis.* Journal of Cell Science, 2007. **120**(15): p. 2517-2531.

87. Hug, C., et al., *Capping protein levels influence actin assembly and cell motility in dictyostelium.* Cell, 1995. **81**(4): p. 591-600.

88. Svitkina, T.M., et al., *Analysis of the Actin–Myosin II System in Fish Epidermal Keratocytes: Mechanism of Cell Body Translocation.* The Journal of Cell Biology, 1997. **139**(2): p. 397-415.

89. Small, J.V., M. Herzog, and K. Anderson, *Actin filament organization in the fish keratocyte lamellipodium.* The Journal of Cell Biology, 1995. **129**(5): p. 1275-1286.

90. Henry, S.J., J.C. Crocker, and D.A. Hammer, *Ligand density elicits a phenotypic switch in human neutrophils.* Integrative Biology, 2014. **6**(3): p. 348-356.

91. Malawista, S.E. and A.d.B. Chevance, *Random locomotion and chemotaxis of human blood polymorphonuclear leukocytes (PMN) in the presence of EDTA: PMN in close quarters require neither leukocyte integrins nor external divalent cations.* Proceedings of the National Academy of Sciences, 1997. **94**(21): p. 11577-11582.

92. Ricart, B.G., et al., *Dendritic cells distinguish individual chemokine signals through CCR7 and CXCR4.* J Immunol, 2011. **186**(1): p. 53-61.

93. Renkawitz, J., et al., *Adaptive force transmission in amoeboid cell migration.* Nat Cell Biol, 2009. **11**(12): p. 1438-1443.

94. Quast, T., et al., *Cytohesin-1 controls the activation of RhoA and modulates integrin-dependent adhesion and migration of dendritic cells.* Blood, 2009. **113**(23): p. 5801-5810.

95. Ricart, Brendon G., et al., *Measuring Traction Forces of Motile Dendritic Cells on Micropost Arrays.* Biophysical Journal, 2011. **101**(11): p. 2620-2628.

96. Chambers, A.F., A.C. Groom, and I.C. MacDonald, *Dissemination and growth of cancer cells in metastatic sites.* Nat Rev Cancer, 2002. **2**(8): p. 563-72.

97. Luster, A.D., R. Alon, and U.H. von Andrian, *Immune cell migration in inflammation: present and future therapeutic targets.* Nat Immunol, 2005. **6**(12): p. 1182-90.

98. Lauffenburger, D.A. and J.J. Linderman, *Receptors: Modeling for Binding, Trafficking, and Signaling*. 1996, New York: Oxford University Press.

99. Berg, H.C., *Random Walks in Biology*. 1993: Princeton University Press.

100. Viswanathan, G.M., et al., *Necessary criterion for distinguishing true superdiffusion from correlated random walk processes.* Phys Rev E Stat Nonlin Soft Matter Phys, 2005. **72**(1 Pt 1): p. 011111.

101. Cahalan, M.D. and I. Parker, *Choreography of cell motility and interaction dynamics imaged by two-photon microscopy in lymphoid organs.* Annu Rev Immunol, 2008. **26**: p. 585-626.

102. Dieterich, P., et al., *Anomalous dynamics of cell migration.* Proc Natl Acad Sci U S A, 2008. **105**(2): p. 459-63.

103. Potdar, A.A., et al., *Human mammary epithelial cells exhibit a bimodal correlated random walk pattern.* PLoS One, 2010. **5**(3): p. e9636.

104. Takagi, H., et al., *Functional analysis of spontaneous cell movement under different physiological conditions.* PLoS One, 2008. **3**(7): p. e2648.

105. Harris, T.H., et al., *Generalized Levy walks and the role of chemokines in migration of effector CD8+ T cells.* Nature, 2012. **486**(7404): p. 545-548.

106. Boyer, D., et al., *Scale-free foraging by primates emerges from their interaction with a complex environment.* Proc Biol Sci, 2006. **273**(1595): p. 1743-50.

107. de Jager, M., et al., *Levy walks evolve through interaction between movement and environmental complexity.* Science, 2011. **332**(6037): p. 1551-3.

108. Humphries, N.E., et al., *Environmental context explains Levy and Brownian movement patterns of marine predators.* Nature, 2010. **465**(7301): p. 1066-9.

109. Miller, M.J., et al., *Two-Photon Imaging of Lymphocyte Motility and Antigen Response in Intact Lymph Node.* Science, 2002. **296**(5574): p. 1869-1873.

110. Zlotnik, A. and O. Yoshie, *Chemokines: A New Classification System and Their Role in Immunity.* Immunity, 2000. **12**(2): p. 121-127.

111. Ohl, L., et al., *Chemokines as organizers of primary and secondary lymphoid organs.* Seminars in Immunology, 2003. **15**(5): p. 249-255.

112. Murdoch, C. and A. Finn, *Chemokine receptors and their role in inflammation and infectious diseases.* Blood, 2000. **95**(10): p. 3032-3043.

113. Proudfoot, A.E.I., *Chemokine receptors: multifaceted therapeutic targets.* Nat Rev Immunol, 2002. **2**(2): p. 106-115.

114. Ma, Q., et al., *Impaired B-lymphopoiesis, myelopoiesis, and derailed cerebellar neuron migration in CXCR4- and SDF-1-deficient mice.* Proceedings of the National Academy of Sciences, 1998. **95**(16): p. 9448-9453.

115. Strieter, R.M., et al., *The Functional Role of the ELR Motif in CXC Chemokine-mediated Angiogenesis.* Journal of Biological Chemistry, 1995. **270**(45): p. 27348-27357.

116. Charo, I.F. and R.M. Ransohoff, *The Many Roles of Chemokines and Chemokine Receptors in Inflammation.* New England Journal of Medicine, 2006. **354**(6): p. 610-621.

117. Yoshida, R., et al., *Secondary Lymphoid-tissue Chemokine Is a Functional Ligand for the CC Chemokine Receptor CCR7.* Journal of Biological Chemistry, 1998. **273**(12): p. 7118-7122.

118. Meili, R. and R.A. Firtel, *Two Poles and a Compass.* Cell, 2003. **114**(2): p. 153-156.

119. Kohout, T.A., et al., *Differential Desensitization, Receptor Phosphorylation, β-Arrestin Recruitment, and ERK1/2 Activation by the Two Endogenous Ligands for the CC Chemokine Receptor 7.* Journal of Biological Chemistry, 2004. **279**(22): p. 23214-23222.

120. Byers, M.A., et al., *Arrestin 3 mediates endocytosis of CCR7 following ligation of CCL19 but not CCL21.* J Immunol, 2008. **181**(7): p. 4723-32.

121. Stein, J.V., et al., *CCR7-mediated physiological lymphocyte homing involves activation of a tyrosine kinase pathway.* Blood, 2003. **101**(1): p. 38-44.

122. Warnock, R.A., et al., *The Role of Chemokines in the Microenvironmental Control of T versus B Cell Arrest in Peyer's Patch High Endothelial Venules.* The Journal of Experimental Medicine, 2000. **191**(1): p. 77-88.

123. Ngo, V.N., H. Lucy Tang, and J.G. Cyster, *Epstein-Barr Virus–induced Molecule 1 Ligand Chemokine Is Expressed by Dendritic Cells in Lymphoid Tissues and Strongly Attracts Naive T Cells and Activated B Cells.* The Journal of Experimental Medicine, 1998. **188**(1): p. 181-191.

124. Mori, S., et al., *Mice lacking expression of the chemokines CCL21-ser and CCL19 (plt mice) demonstrate delayed but enhanced T cell immune responses.* J Exp Med, 2001. **193**(2): p. 207-18.

125. Lin, F. and E.C. Butcher, *T cell chemotaxis in a simple microfluidic device.* Lab Chip, 2006. **6**(11): p. 1462-9.

126. Nandagopal, S., D. Wu, and F. Lin, *Combinatorial guidance by CCR7 ligands for T lymphocytes migration in co-existing chemokine fields.* PLoS One, 2011. **6**(3): p. e18183.

127. Johnson, L.A. and D.G. Jackson, *Cell Traffic and the Lymphatic Endothelium.* Annals of the New York Academy of Sciences, 2008. **1131**(1): p. 119-133.

128. Green, N.M., *Avidin.* Adv Protein Chem, 1975. **29**: p. 85-133.

129. Campbell, J.J., et al., *Biology of chemokine and classical chemoattractant receptors: differential requirements for adhesion-triggering versus chemotactic responses in lymphoid cells.* J Cell Biol, 1996. **134**(1): p. 255-66.

130. Farrell, B.E., R.P. Daniele, and D.A. Lauffenburger, *Quantitative relationships between single-cell and cell-population model parameters for chemosensory migration responses of alveolar macrophages to C5a.* Cell Motil Cytoskeleton, 1990. **16**(4): p. 279-93.

131. Jannat, R.A., M. Dembo, and D.A. Hammer, *Traction forces of neutrophils migrating on compliant substrates.* Biophys J, 2011. **101**(3): p. 575-84.

132. Barkefors, I., et al., *Endothelial cell migration in stable gradients of vascular endothelial growth factor A and fibroblast growth factor 2: effects on chemotaxis and chemokinesis.* J Biol Chem, 2008. **283**(20): p. 13905-12.

133. Regehr, K.J., et al., *Biological implications of polydimethylsiloxane-based microfluidic cell culture.* Lab Chip, 2009. **9**(15): p. 2132-9.

134. Ye, H., Z. Gu, and D.H. Gracias, *Kinetics of Ultraviolet and Plasma Surface Modification of Poly(dimethylsiloxane) Probed by Sum Frequency Vibrational Spectroscopy.* Langmuir, 2006. **22**(4): p. 1863-1868.

135. Desai, R.A., N.M. Rodriguez, and C.S. Chen, *Chapter 1 - "Stamp-off" to Micropattern Sparse, Multicomponent Features*, in *Methods in Cell Biology*, P. Matthieu and T. Manuel, Editors. 2014, Academic Press. p. 3-16.

136. Rogers, J.A. and R.G. Nuzzo, *Recent progress in soft lithography.* Materials Today, 2005. **8**(2): p. 50-56.

137. Xia, Y. and G.M. Whitesides, *Soft Lithography.* Angewandte Chemie International Edition, 1998. **37**(5): p. 550-575.

138. Napoli, M., J.C.T. Eijkel, and S. Pennathur, *Nanofluidic technology for biomolecule applications: a critical review.* Lab on a Chip, 2010. **10**(8): p. 957-985.

139. Quake, S.R. and A. Scherer, *From Micro- to Nanofabrication with Soft Materials.* Science, 2000. **290**(5496): p. 1536-1540.

140. Chen, C.S., et al., *Geometric Control of Cell Life and Death.* Science, 1997. **276**(5317): p. 1425-1428.

141. Nelson, C.M., et al., *Tissue Geometry Determines Sites of Mammary Branching Morphogenesis in Organotypic Cultures.* Science, 2006. **314**(5797): p. 298-300.

142. Desai, R.A., et al., *Subcellular spatial segregation of integrin subtypes by patterned multicomponent surfaces.* Integr Biol (Camb), 2011. **3**(5): p. 560-7.

143. Rodriguez, N.M., et al., *Micropatterned Multicolor Dynamically Adhesive Substrates to Control Cell Adhesion and Multicellular Organization.* Langmuir, 2014. **30**(5): p. 1327-1335.

144. Folch, A. and M. Toner, *Microengineering of Cellular Interactions.* Annual Review of Biomedical Engineering, 2000. **2**(1): p. 227-256.

CHAPTER 3: T CELL HAPTOKINESIS AND CHEMOKINESIS ON MICROCONTACT PRINTED PDMS SUBSTRATES

Adapted from: Dominguez GA and DA Hammer. "Effect of adhesion and chemokine presentation on T-lymphocyte haptokinesis." **Integrative Biology.** 2014, 6 (9), 862 – 873.

ABSTRACT

Motility is critical for the function of T-lymphocytes. Motility in T-lymphocytes is driven by the occupancy of chemokine receptors by chemokines, and modulated by adhesive interactions. However, it is not well understood how the combination of adhesion and chemokine binding affects T-lymphocyte migration. We used microcontact printing on polymeric substrates to measure how T lymphocyte migration is quantitatively controlled by adhesion and chemokine ligation. Focusing only on random motion, we found that T-lymphocytes exhibit biphasic motility in response to the substrate concentration of either ICAM-1 or VCAM-1, and generally display more active motion on ICAM-1 surfaces. Furthermore, we examined how the combination of the homeostatic chemokines CCL19 and CCL21 contribute to motility. By themselves, CCL19 and CCL21, ligands for CCR7, elicit biphasic motility, but their combination synergistically increases CCR7 mediated chemokinesis on ICAM-1. By presenting CCL21 with ICAM-1 on the surface with soluble CCL19, we observed random motion that is greater than what is observed with soluble chemokines alone. These data suggest that ICAM-1 has a greater contribution to motility than VCAM-1 and that both adhesive interactions and chemokine ligation work in concert to control T-lymphocyte motility.

INTRODUCTION

Recruitment of T lymphocytes into lymphoid organs and peripheral tissues during immune surveillance and inflammation is critical for their function. T lymphocytes make use of the integrins Lymphocyte Function Associated Antigen-1 (LFA-1; αLβ2) and Very Late Antigen-4 (VLA-4; α4β1) in cell trafficking, TCR formation and maturation, cell-to-cell binding, and motility within secondary lymphoid organs (SLOs) and tissues [1-4].

Within SLOs, T lymphocytes are exposed to adhesion ligands and chemokines that coordinate interactions between T lymphocytes and antigen presenting cells [5-8]. *In vivo* it is thought that in order for T lymphocytes to reach their destination, migrating cells must sense a gradient of soluble or surface immobilized chemokine(s) released from a distant source providing them with a chemotactic cue for directed migration [6, 9]. Within the SLO, homeostatic chemokines such as CCL19 and CCL21 are thought to play a key role in controlling migration and regulating the dynamics of motility by binding to the CCR7 receptor. It has been shown *in vitro* that T cells undergo chemotaxis in response to CCL19 and CCL21 within microfluidic devices [10]. However, the role that adhesion molecules play in regulating the response to chemokines is under appreciated.

Although it is commonly thought that directional migration in chemokine gradients is needed for lymphocyte positioning in the SLOs, it is possible that chemokinesis plays a strong role in lymphocyte exploration within the SLOs. There is no convincing evidence for directional trafficking of T lymphocytes under steady-state conditions as observed within explanted lymph nodes, but adhesive ligands and chemokines expressed by fibroblastic reticular cells have been shown to guide migration within the lymph nodes to facilitate T-lymphocyte activation [10-16]. It has been shown *in vivo* that T cells are

capable of migrating at speeds up to 40 μm/min with frequent changes in direction [11]. At uniform concentrations, chemokines are capable of modulating cell speeds, and the observed random migration of T lymphocytes observed within lymph nodes may be due to a chemokinetic response to near-uniform levels of chemokines in the tissue [5, 17]. Additionally, binding of these chemokines to their G_i-protein-coupled receptor, CCR7, are capable of altering motility by modulating integrin activity through inside-out signaling pathways that indirectly modulate T cell homing to SLOs [5, 18, 19]. Recent work has elucidated the importance of how chemokines coordinate with adhesive ligands to support adhesion and migration, but the exact interplay between the two is still not fully understood [5, 20-22].

Presentation of the ligands Intracellular Adhesion Molecule-1 (ICAM-1) and Vascular Cell Adhesion Molecule-1 (VCAM-1) to their corresponding cognate receptors LFA-1 and VLA-4 in the absence of chemokine is capable of inducing polarization critical for adhesion and motility via reorganization of the actin and microtubule cytoskeletons [19, 23-25]. Studies have shown that CCL21 is capable of synergizing with adhesion ligands to increase adhesion, speed, and random motility *in vitro [5]*. However, to our knowledge, there has not been a quantitative analysis of the contributions of ICAM-1 and VCAM-1 on random motility in the absence of chemokines (haptokinesis) and the effect of varying chemokine concentrations (chemokinesis).

For this chapter, we measured the motility of primary human T lymphocytes on different densities of the cell adhesion molecules ICAM-1 and VCAM-1 on microcontact printed PDMS substrates. This technology allows for the precise control of the density and type of adhesion molecule present on the surface; for example, we recently used

microcontact printing to show how different densities of fibronectin can elicit a phenotypic switch in neutrophil motility [26]. Specifically, we investigated how the random motility of T lymphocytes is controlled by varying concentrations of adhesion ligands, first in the absence and then in the presence of chemokine. We found that T lymphocytes exhibit biphasic motility when either ICAM-1 or VCAM-1 is presented alone in the absence of chemokine, with an overall greater motility on ICAM-1 substrates than VCAM-1. Then, we measured the effects of CCL19 and CCL21 on the motility of T lymphocytes and how combinations of the two chemokines modulate their motility. We found that individually, CCL19 and CCL21 also elicit similar biphasic motility with a peak in the random motility coefficient near an intermediate concentration of chemokine, and when combined, synergize to increase random motility. Furthermore, this synergistic effect is maintained when CCL21 is presented on the surface with soluble CCL19 on ICAM-1 surfaces. These results provide insight to how adhesive ligands and chemokines control the random migration of T lymphocytes in the absence of chemokine gradients.

MATERIALS AND METHODS

Cell culture and reagents

Human blood was obtained via venipuncture from healthy adult donors and collected into sterile tubes containing sodium heparin (BD Biosciences, San Jose, CA). Samples were collected with University of Pennsylvania Institutional Review Board approval from consenting adult volunteers. Blood samples were carefully layered in a 1:1 ratio of whole blood to 1-Step™ Polymorphprep (Axis-Shield, Oslo, Norway). Vials were then centrifuged at 1500 rpm for 35 minutes and the mononuclear band was collected into a fresh vial. Figure 3.1 depicts resulting buffy coat after centrifugation and band isolated for culture. Cells were cultured in RPMI-1640 supplemented with 10% FBS and 1 μg/ml of phytohemagglutinin-M (PHA-M; Sigma-Aldrich, St. Louis, MO) overnight. After 24 hours, the lymphocyte suspension in the PHA medium was transferred into a new flask leaving behind adherent cells. After an additional 48 hours, the cells were then cultured in RPMI-1640 with 10% FBS and 1% penicillin-streptomycin supplemented with 20 ng/ml of interleukin-2 (IL-2; Roche, Mannheim, Germany). Cells were used for experimentation following an additional 72 hours in culture. Flow cytometry was employed to verify population of T-lymphocytes through identifying cells labeled with FITC conjugated anti-CD3+ (clone OKT3) (Affymetrix eBioscience, San Diego, CA) and population was determined to be 98.69% CD3+ (Figure 3.2). Other biological reagents included: protein A/G (Thermo Scientific, Rockford, IL), human ICAM-1/Fc and VCAM-1/Fc (R&D Systems, Minneapolis, MN), human IgG_1 (Abcam, Kendall Square, MA), human anti-α_L (clone 38) and human anti-β_2 (clone IB4) (Calbiochem, San Diego, CA), human anti-α_M (Clone M1/70.15.1) (Millipore, Temecula, CA), human anti-β_1 (clone Mab13) and rat

isotype IgG_2a (BD Pharmingen, San Jose, CA), human CCL19/CCL21 (PreproTech, Rocky Hill, NJ), Pluronics F127 (Sigma-Aldrich, St. Louis, MO), Alexa 568-labeled phalloidin and Alexa488-labeled mouse anti-α tubulin (Invitrogen, Grand Island, NY).

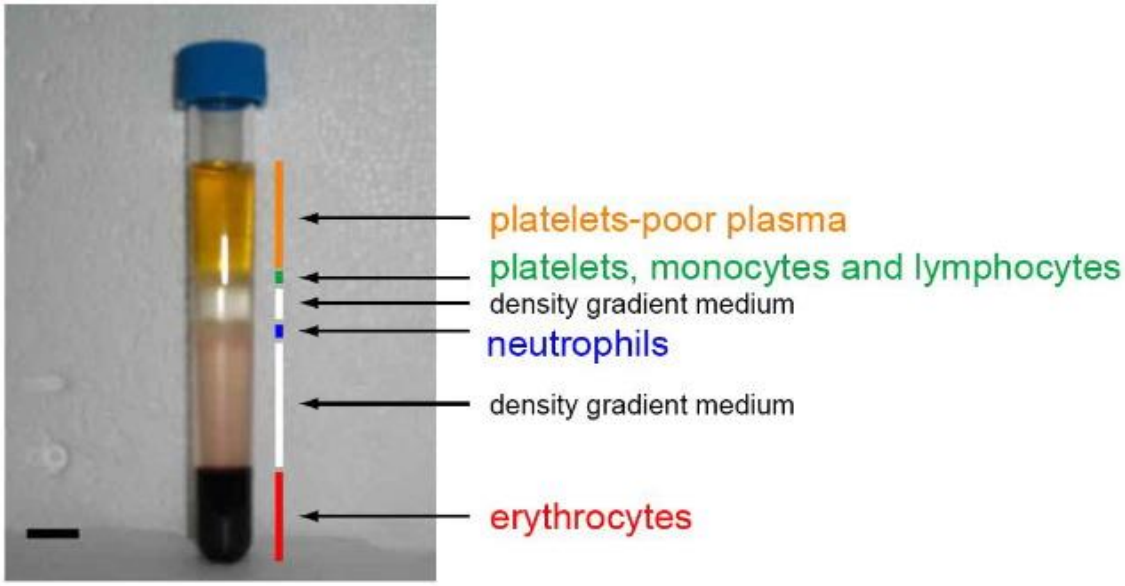

Figure 3.1. Separation of whole blood for cell isolation. Image of resulting buffy coat after centrifiguation of whole blood layered over 1-Step™ Polymorphprep. The layer containing platelets, monocytes, and lymphocytes was collected.

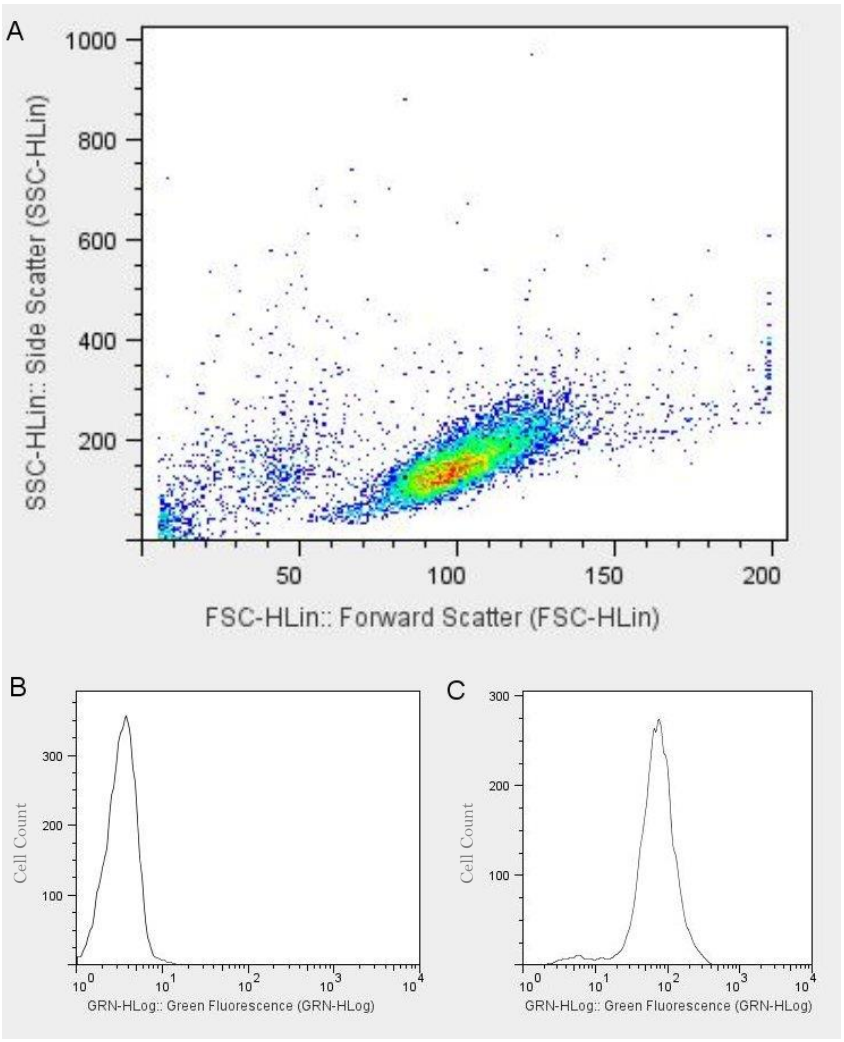

Figure 3.2. Flow cytometry results of T-lymphocytes to verify CD3+ population. (A) Plot of side scatter versus forward scatter of population of cells isolated from whole blood after 7 days of activation and culture. Heat map shows majority of cells to be mostly mononuclear indicating population of T-lymphocytes. (B) Isotype control and (C) anti-CD3 FITC antibody labeling showing high number of CD3+ positive cells in tested population after culturing. Population was determined to be 98.69% CD3+. These are representative plots from one of three separate experiments.

Substrate preparation

Poly(dimethylsiloxane) (PDMS) (Sylgard 184 Silicone Elastomer, Dow Corning, Midland, MI) coated coverslips were prepared from number one thickness glass coverslips (Fisher Scientific, Hampton, NH) of 25 mm diameter spin coated with degassed PDMS (10:1 base:cure by weight) and cured overnight at 65 ºC. PDMS-coated coverslips were affixed to the bottom of six-well tissue culture plates which has been laser-cut to generate a 22 mm diameter opening in the bottom of the wells. Coverslip bonding was performed using a small amount of PDMS (10:1 base:cure by weight) and baked at 65 ºC for 30 minutes for curing.

Protein printing and blocking

Flat stamps for printing were prepared by pouring degassed PDMS mixed at 10:1 base:cure by weight over an unpatterned silicon wafer. The polymer was cured for 2 hours or longer at 65 ºC. Stamps were trimmed, sonicated in 200 proof ethanol for 10 minutes, rinsed with dH_2O, and dried in a stream of $N_2(g)$. For motility studies, stamps were 1 cm^2 and were inked with 200 µl of 2 µg/ml of protein A/G in PBS for 2 hours at room temperature. The stamps were then thoroughly rinsed in H_2O and blown dry with a stream of N_2. In parallel, the six-well PDMS coverslip substrate was treated with ultraviolet ozone for 7 minutes (UVO Cleaner Model 342, Jelight Company, Irvine, CA) to render the surface hydrophilic. The stamp was then placed in conformal contact with the substrate for ~10 seconds and removed. A 0.2% (w/v) solution of Pluronics F127 was immediately adsorbed to the PDMS substrates for 30 minutes at room temperature to prevent protein adsorption to non-functionalized portions of the PDMS. The cell culture substrate was then rinsed with PBS 3X without dewetting the functionalized surface before deposition of

200 µl of either ICAM-1/Fc or VCAM-1/Fc in PBS for 2 hours at room temperature. The surfaces were then rinsed with PBS 3X without dewetting before incubation with cells. We tested whether saturation points of ICAM-1/Fc were different upon physisorption to glass or printed onto PDMS. Using Alexa Fluor-555 conjugated Protein A/G, we prepared substrates for adhesion that were either glass and blocked with 1% BSA in PBS or stamped onto PDMS and blocked with 0.2% F127 Pluronics. Figure 3.3 demonstrates that there is increased non-specific adhesion of T lymphocytes to glass substrates; PDMS substrates appear to have more uniformity in ligand deposition as indicated by a more uniform signal in fluorescence.

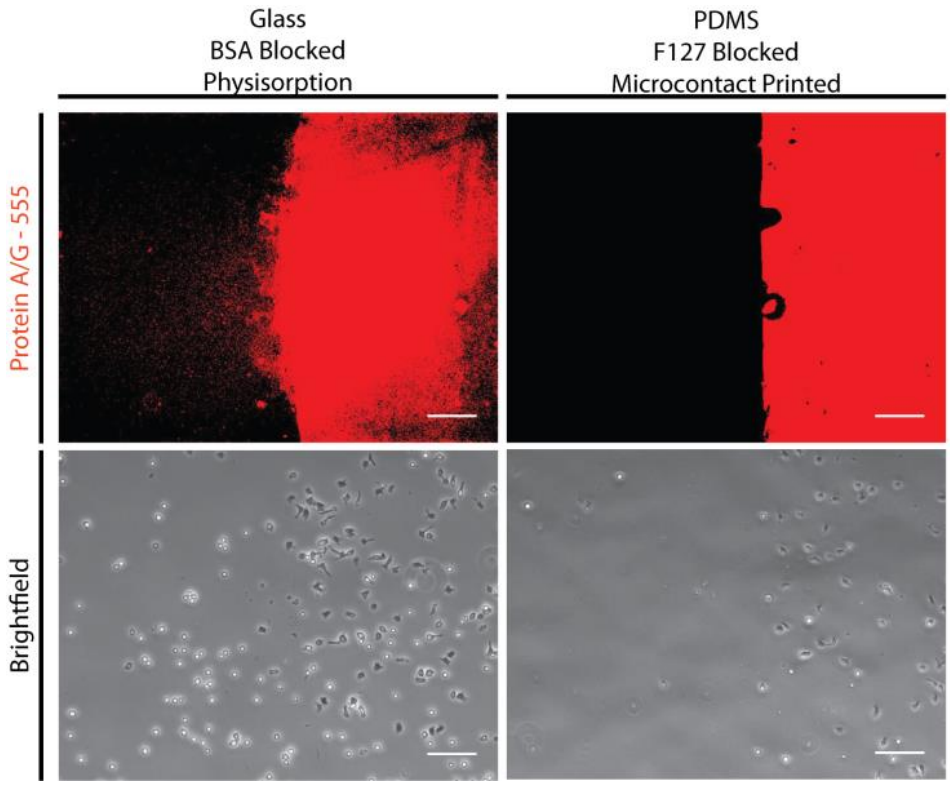

Figure 3.3. Physisorption and printing of fluorescent protein A/G. Scale bar = 100 µm; 10X magnification

ELISA to determine protein deposition on PDMS substrates

For substrate preparation, 45X50 mm glass coverslips (No. 1, Fisher Scientific Pittsburgh PA) were spin coated with PDMS and cured as described previously. Flat stamps were inked with Protein A/G solution as described previously followed by coverslip activation and printing. Coverslips (PDMS spin coated or glass) were then adhered via PDMS to the bottom of a 24 well plate whose bottoms had been cut out. 0.2% F-127 Pluronics solutions was deposited into each well for 30 minutes at room temperature. Each well was then rinsed with PBS 3X followed by deposition of 200 µl of ICAM-1/Fc protein solution into each well for 2 hours at room temperature. For the glass substrates, protein A/G was physisorbed to the surface for 2 hours at room temperature followed by surface blocking with 5% milk in PBS solution for 1 hour at room temperature. After wells were rinsed with PBS 3X, solutions of ICAM-1/Fc were deposited into each well for 2 hours at room temperature followed by rinses of PBS 3X. A dilution of 1:5000 of polyclonal anti-human ICAM1 antibody (Biotin) (ab7815, Abcam, Cambridge, MA) in PBS + 1% BSA and 200 µl was deposited into each well for one hour at room temperature. The plate was washed with PBS + 1% BSA 3X to remove excess primary antibody and 200 µl of 1:5000 HRP-avidin in PBS + 1% BSA was deposited into each well. The plate was then washed 3X with PBS + 1% BSA to remove excess secondary antibody followed by ensuring that the wells were completely dry.

400 µl of 1-Step™ Turbo TMB-ELISA reagent (Pierce Biotechnology), per well of a 24 well plate was added to each well, to visualize the amount of HRP on each substrate. The plate was incubated in the dark, at room temperature, for 15 minutes, to allow for the reaction to occur. The reagent will turn blue in the presence of HRP and the reaction is

quenched with the addition of 400 µl of 2N H_2SO_4. Quenching the reaction changes the color of the liquid in each well from blue to yellow. Finally, the ELISA was quantified by measuring the absorbance of the liquid in each well at 450 nm on the Tecan Infinite 200 PRO plate reader (Tecan Group Ltd., Switzerland) to determine the amount of HRP in each well. This colorimetric assay was then used to qualitatively asses the amount of ICAM-1/Fc present on each substrate and each conditions was done in triplicate on two separate occasions.

As shown in Figure 3.4, absorbance increases as the ICAM-1 concentration increases in solution indicating differences in protein presentation across the concentrations tested on both glass and PDMS substrates. All values are normalized by the background absorbance from the control wells with zero ICAM-1/Fc present. Since protein A/G is used and only capable of binding 6 Fc-chimera molecules at a time, we assume these results apply to surfaces with VCAM-1/Fc ligand as well [27].

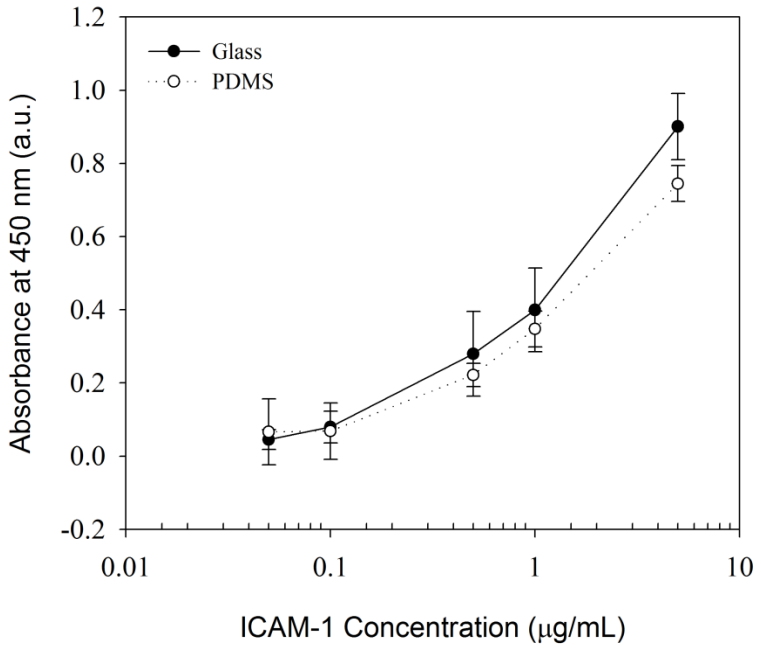

Figure 3.4. Results of an HRP ELISA for ICAM-1. Results show that varying bulk ICAM-1/Fc concentration incubated on protein A/G printed PDMS substrates results in varying concentration of protein adsorbed to the surface. Averages were calculated from replicates of three with error bars representing the standard error of the mean (s.e.m.).

Haptokinesis and chemokinesis assay

PDMS substrates were prepared as described above. For printed CCL21 studies, 20 nM of CCL21 was inked with Protein A/G followed by stamping onto PDMS substrates. Before use, all substrates were washed 3X with phosphate-buffered saline. Each well was plated at 5 x 10^5 cells/ml in serum-free RPMI-1640 supplemented with 0.1% BSA and 2 mg/ml glucose. The substrate was then placed in a 37°C humidified atmosphere containing 5% CO_2 in air incubator for 15 minutes to allow for cell attachment. The wells were then gently washed 3X with PBS to remove non-adherent cells followed by imaging in a 5% CO_2 and 37°C environment for at least 1 hour. Cells were placed into a motorized stage and observed using a Nikon Eclipse TE_{300} phase contrast microscope. A 10X objective was used to capture images during the course of the time lapse. For chemokinesis assays, a CCL19 and/or CCL21 chemokine solution was dispensed into each well before imaging and performed on ICAM-1 substrates at a concentration of 0.05 µg/ml. For surface presentation of CCL21, stamps were inked with 2 µg/ml of Protein A/G and 250 ng/ml of CCL21 and printed onto the PDMS substrates before blocking and application of the Fc protein solution.

Measurement of cell trajectories and mean-squared displacements

Cell movement was tracked using the ImageJ plugin Manual Tracking. ImageJ and the plugin are both freely available through the NIH website (http://rsbweb.nih.gov/ij/). The centroid of the cell was considered to represent the cell position. Time lapse microscopy was used and images were taken every 1.5 minutes. The result was a series of (x,y) positions with time for each cell. The net displacement during the ith 1.5 minute increment, D_i, was calculated by the difference of the position at the beginning and end of

that time step. The mean-squared displacement, $\langle D^2(t)\rangle$, over time was calculated using the method of non-overlapping intervals [28]. Speed, S, can be considered as the total path length over time and persistence time, P, is the time a cell remains moving without changing direction. S and P were obtained by fitting these to the persistent random walk equation (Dunn, 1983 $\langle D^2(t)\rangle = 2S^2\left[t - P\left(1 - e^{-t/P}\right)\right]$ where *t* is the time interval, using a non-linear least squares regression analysis [29, 30]. The mean-free path length (P_L) and random motility coefficient (μ) are then calculated as $P_L = PS$ and $\mu = \frac{1}{2}S^2P$ [31, 32].

Antibody Blocking

Functional blocking antibodies against the β_1 integrin subunit (clone Mab13), β_2 integrin subunit (clone IB4), α_L integrin subunit (clone 38), and IgG_2a isotype control (clone R35-95) were used at a final concentration of 50 μg/ml. 5 x 10^5 T-lymphocytes in 500 μl of running buffer were incubated for 30 minutes with the blocking antibodies at 37ºC and 5% CO_2. Cells were then plated and allowed to adhere for 15 minutes followed by rinsing with PBS 3X and subsequent imaging in media containing blocking antibody.

Immunofluorescence

Primary human T lymphocytes were plated on 5.0 μg/ml ICAM-1/Fc and VCAM-1/Fc surfaces with or without 250 ng/ml of stamped CCL21 at 5 x 10^5 cells/ml for 1 h in a 37°C humidified atmosphere containing 5% CO_2. The cells were then fixed with 4% paraformaldehyde in PBS for 7 minutes. Cells were permeabilized with 0.2% Triton X-100 for 5 minutes and blocked with 1% BSA in PBS for 30 minutes at room temperature. Cells were incubated with 1:200 Alexa 568-labeled phalloidin and Alexa 488-labeled mouse anti-α tubulin (Invitrogen) for 30 minutes at room temperature. Cells were mounted

in Fluoromount-G mounting medium (SouthernBiotech, Birmingham, Alabama) and examined by confocal microscopy (Leica SP5).

RESULTS AND DISCUSSION

Microcontact printing of Protein A/G and T lymphocyte adhesion

Protein A/G is a molecule produced through the fusion of the Fc-binding domains of Protein A and Protein G. Use of this molecule in conjunction with Fc-chimera ligands, such as ICAM-1/Fc and VCAM-1/Fc, has proven effective to immobilize chimeric proteins bearing the Fc domain [27]. We used microcontact printing of Protein A/G to prepare surfaces with controlled ratios of adhesion ligands linked to the Fc chimeras while keeping total protein concentration constant. This is achieved by varying the ratios of ICAM-1/Fc and VCAM-1/Fc molecules and human IgG_1. The steps for microcontact printing for our experimental system are illustrated in Figure 3.5.

Primary human T lymphocytes do not polarize and migrate on microcontact printed Protein A/G alone or on Protein A/G surfaces incubated with human IgG_1 as indicated by a rounded morphology (Fig. 3.6A). Figure 3.6B demonstrates the fidelity of microcontact printing and the binding selectivity of primary human T lymphocytes to ICAM-1/Fc surfaces.

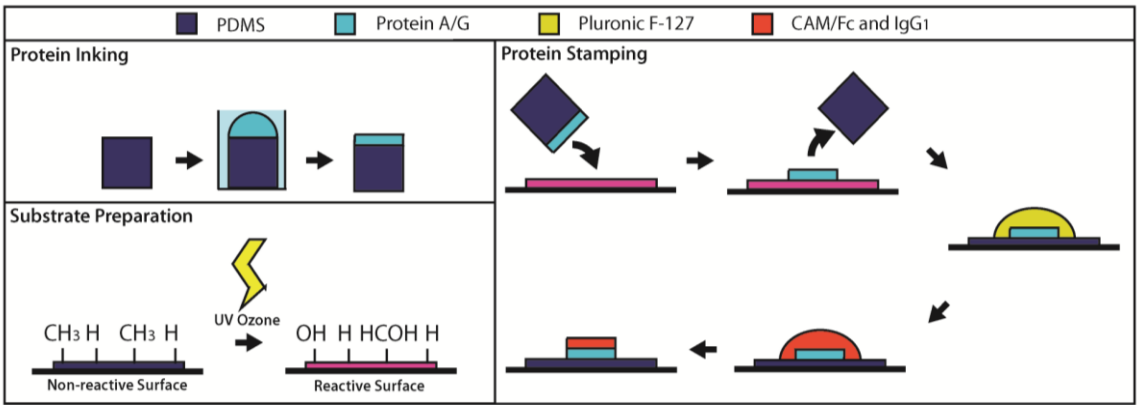

Figure 3.5. Microcontact printing of PDMS substrates. Illustration for microcontact printing of protein A/G followed by subsequent binding of either ICAM-1/Fc or VCAM-1/Fc with IgG_1.

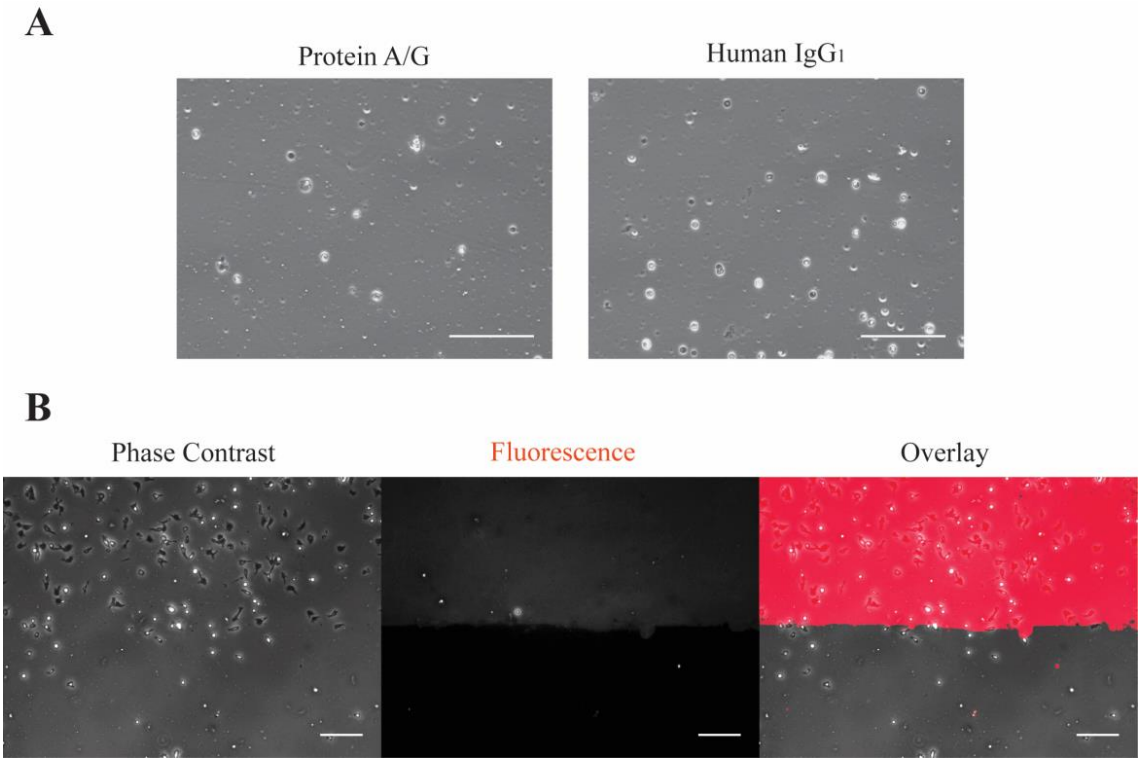

Figure 3.6. T lymphocytes adhere to microcontact printed PDMS substrates. (A) Phase contrast images showing rounded morphologies for T lymphocytes indicating no polarity and adhesion to Protein A/G or human IgG1 alone. Scale bars, 100 µm (B) Phase contrast, fluorescence, and overlay images showing the fidelity of microcontact printed protein A/G-Alex Fluor 555 conjugate on PDMS surfaces and binding selectivity of T lymphocytes to ICAM-1/Fc. Scale bars, 100 µm.

Either ICAM-1 and VCAM-1 alone trigger T lymphocyte haptokinesis

Primary human T lymphocytes adhere and migrate on PDMS surfaces printed with ICAM-1 and VCAM-1. We measured haptokinesis on these ligands by quantifying the mean-squared displacements over a range of ligand concentrations in the absence of chemokine. From the mean-squared displacements over time, we could determine the speed, persistence time, and random motility coefficient for each condition. T lymphocytes plated on ICAM-1 or VCAM-1 surfaces were tracked for 30 minutes. As illustrated by representative single-cell migration tracks (Fig. 3.7), T lymphocytes migrated substantial distances on both 0.5 and 5.0 μg/ml of ICAM-1 or VCAM-1 with no preferred direction. This remained true for all other concentrations of ligand tested.

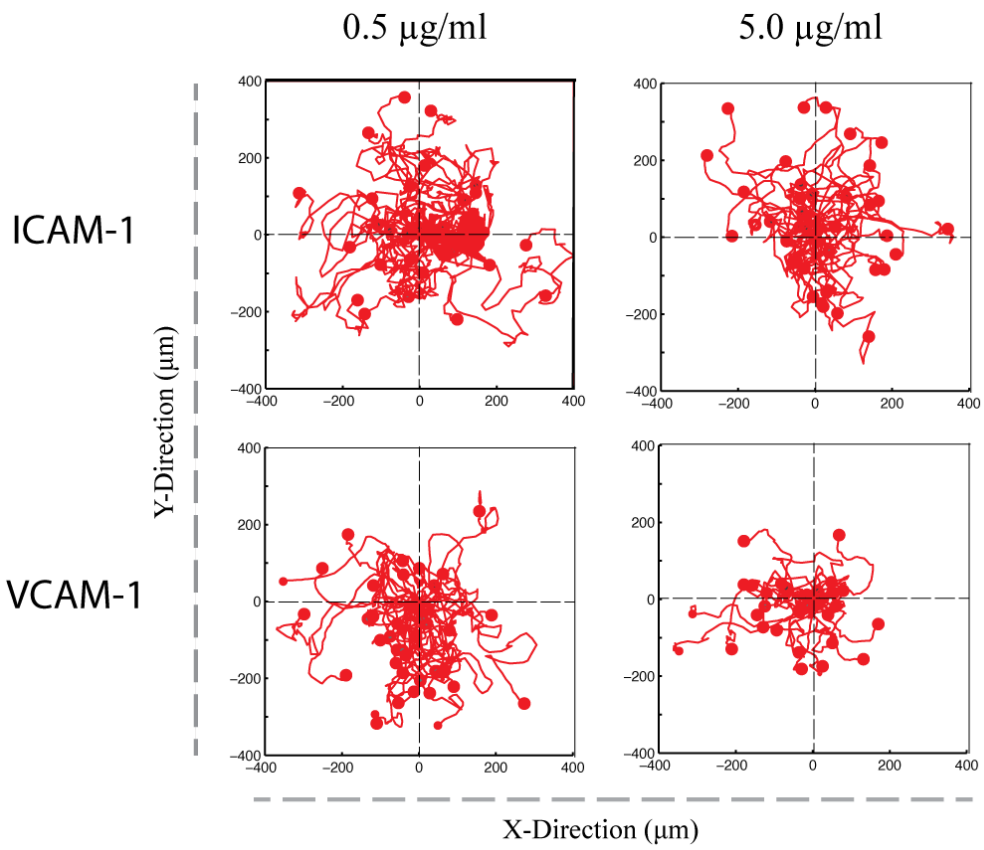

Figure 3.7. T lymphocytes are more migratory on ICAM-1 than VCAM-1. Representative single-cell migration tracks for T lymphocytes on 0.5 and 5.0 µg/ml of ICAM-1 and VCAM-1 showing no preferred direction in migration.

It is known that through LFA-1 ($\alpha_L\beta_2$) and VLA-4 ($\alpha_4\beta_1$) integrin interactions T lymphocytes are capable of migrating on ICAM-1 and VCAM-1 surfaces, respectively; we verified this through functional integrin blocking (Fig. 3.8, A and B). Blocking of the α_L and β_2 integrin chains resulted in a significant decrease in cell adhesion on ICAM-1 relative to the positive control without antibody present ($p < 0.01$) (Fig. 3.8C). By targeting the β_1 integrin, a significant decrease in cell adhesion on VCAM-1 relative to the positive control without antibody present was observed ($p < 0.01$) (Fig. 3.8C). These data led us to attribute the observed ICAM-1 and VCAM-1-induced adhesion and resulting motility to the specific ligation of $\alpha_L\beta_2$ and $\alpha_4\beta_1$ with their cognate ligands on these microcontact printed surfaces.

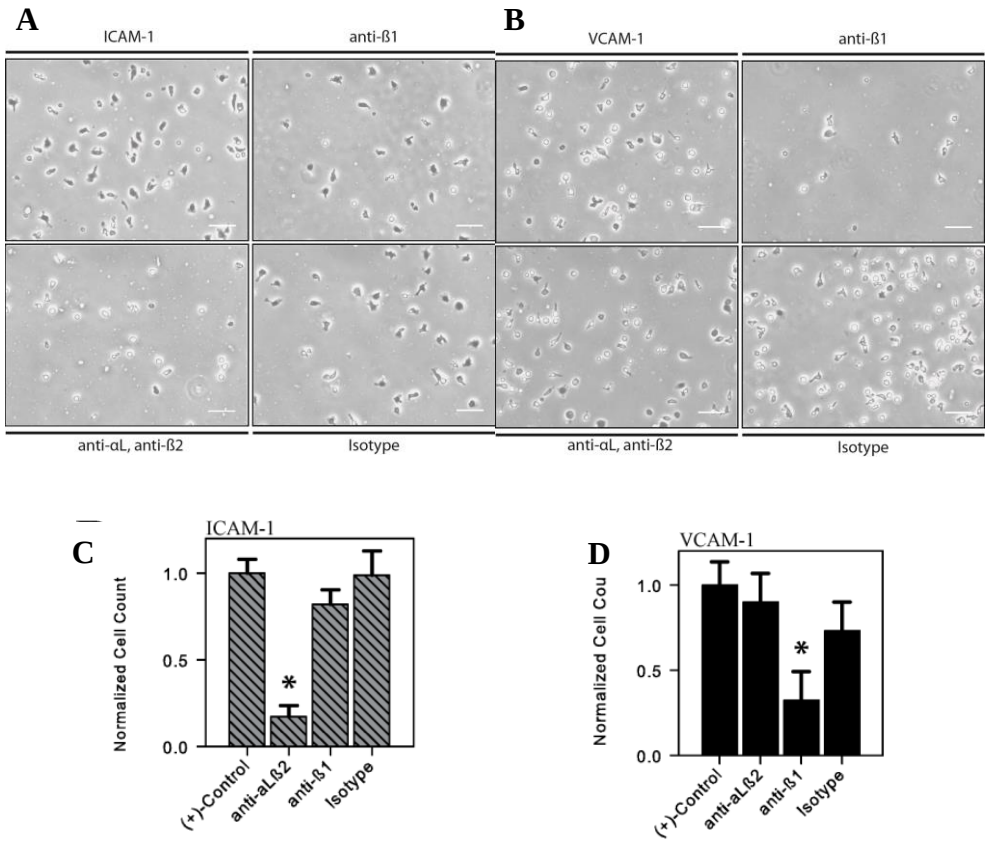

Figure 3.8. Antibody blocking against LFA-1 and VLA-4 reveal discrete integrin/ligand interactions on printed PDMS surfaces. (A) Phase contrast images of T lymphocytes blocked against $\beta_1$or $\alpha_L\beta_2$ integrins on ICAM-1 surfaces. (B) Phase contrast images of T lymphocytes blocked against $\beta_1$or $\alpha_L\beta_2$ integrins on VCAM-1 surfaces. Quantification of antibody blocking against (C) $\alpha_L\beta_2$ and (D) β_1 integrins show decreased cell adhesion to ICAM-1 and VCAM-1 substrates, respectively; *$p < 0.05$, compared to isotype; one-sample t test, error bars represent standard error of the mean (s.e.m.).

Using the mean-squared displacements (MSD), we found that migrating T lymphocytes on ICAM-1 surfaces traveled greater distances than on VCAM-1 surfaces as suggested by larger MSDs with increasing time for all concentrations (Fig. 3.9, A and B). This demonstrates that the dynamics of T lymphocyte motility on ICAM-1 and VCAM-1 are distinct. The use of random walk theories is common to quantify mammalian cell migration. The MSDs of migration can be scaled as $x^2(t) \propto t^{\alpha}$ during $0 < t < 90$ minutes where fitting can be used to determine the exponent α to classify the type of motion for each type and concentration of ligand. Random or Brownian motion is observed for the value of $\alpha = 1$ and ballistic motion is observed for $\alpha = 2$, while values between the two are categorized as superdiffusive motion. Cells migrating on ICAM-1 surfaces display an average α over all concentrations of 1.57, indicating that T lymphocytes on ICAM-1 migrate superdiffusively through LFA-1 mediated interactions. Similarly on VCAM-1, T lymphocytes display superdiffusive motion with an average α of 1.38 (Fig. 3.9C). Table 3.1 shows all values of fitted α's for all concentrations of ligand tested. This data is consistent with the recent observation that neither effector CD8+ T cells *in vivo* nor neutrophils on microcontact printed fibronectin PDMS surfaces display pure diffusive motion [26, 33].

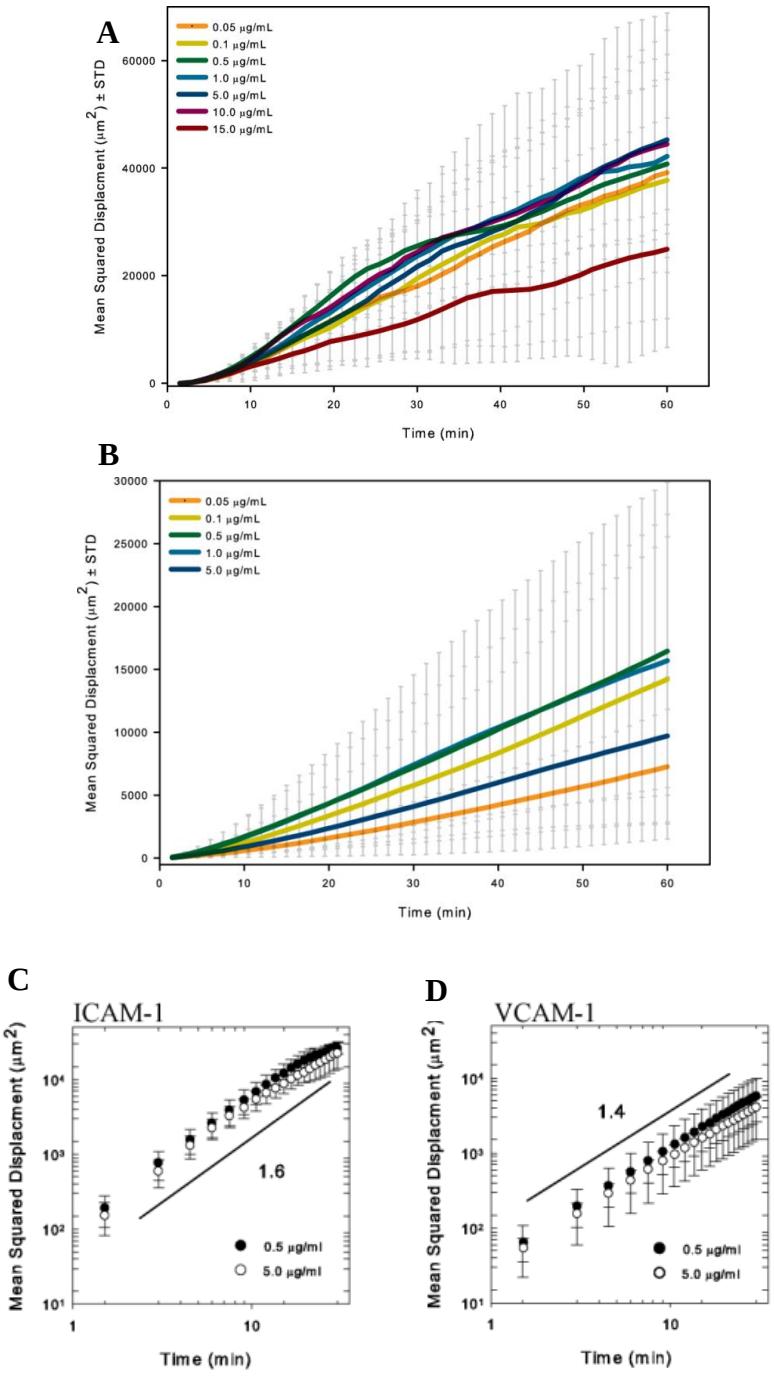

Figure 3.9. The mean-squared displacements versus time are linear on ICAM-1 and VCAM-1. (A) MSD versus time showing linear trends on all concentrations of ICAM-1 tested. (B) MSD versus time showing linear trends on all concentrations of VCAM-1 tested. MSD can be scaled as $x^2(t) \propto t^{\alpha}$ indicating that T lymphocytes acquire displacement superdiffusively ($\alpha > 1$) on representative concentrations of (C) ICAM-1 and (D) VCAM-1 surfaces. Numbers on line represent approximate values of α over all concentrations of ligand tested.

ICAM-1 (μg/mL)	Average α ± STD	VCAM-1 (μg/mL)	Average α ± STD
0.05	1.40 ± 0.15	0.05	0.98 ± 0.12
0.1	1.36 ± 0.15	0.1	1.34 ± 0.13
0.5	1.11 ± 0.04	0.5	1.29 ± 0.11
1.0	1.34 ± 0.34	1.0	1.29 ± 0.08
1.5	1.25 ± 0.05	1.5	1.24 ± 0.16
5.0	1.21 ± 0.13	5.0	1.24 ± 0.18

Table 3.1. Average fitted α ± standard deviation on ICAM-1 and VCAM-1 surfaces. Values of fitted α's indicate superdiffusive for almost all concentration conditions on ICAM-1 and VCAM-1 surfaces.

By scaling the mean squared displacements to t^{α} and plotting them as slopes over time, we see that all T lymphocyte motility lies between a slope of 1 (pure diffusion motion) and a slope of 2 (pure ballistic motion) lying in the superdiffusive region (Fig. 3.10). This is the first indication, to our knowledge, that T lymphocytes exhibit superdiffusive motion on ICAM-1 and VCAM-1 ligands *in vitro*.

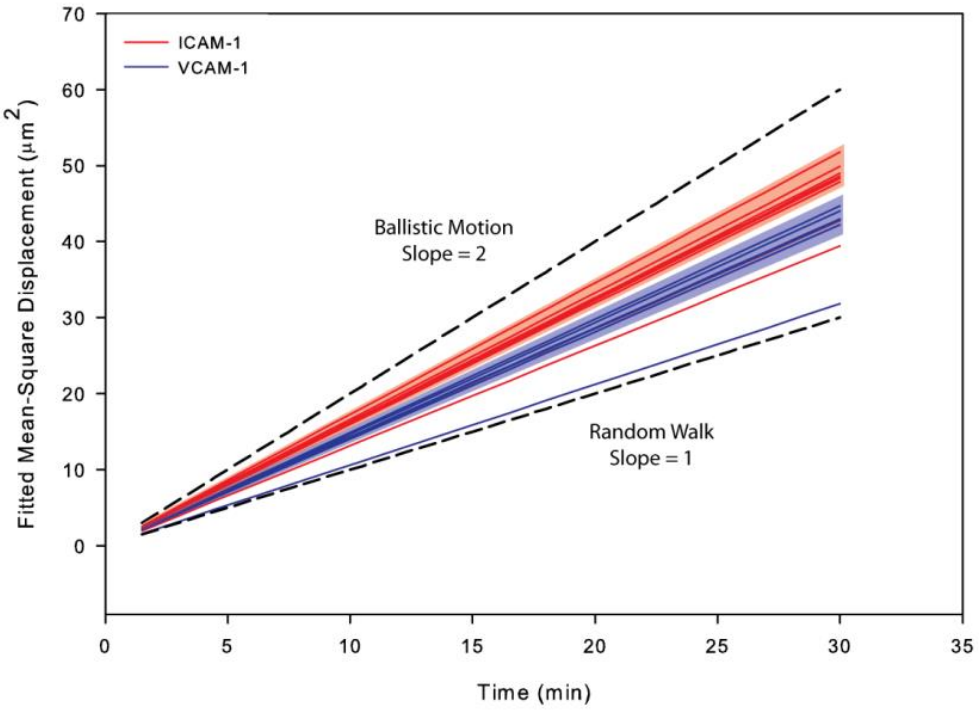

Figure 3.10. Fitted mean-squared displacements versus time on ICAM-1 and VCAM-1 surfaces. The slopes of lines indicate the α's determined by scaling the MSD previously to t^{α}. Red lines are values on ICAM-1 surfaces and blue lines are values on VCAM-1 surfaces. Slopes of the lines fall between values of 1 (pure diffusive motion) and 2 (pure ballistic motion).

To further characterize the motility of T cells on ICAM-1 and VCAM-1 surfaces, we used the experimental mean-squared displacements of each cell population with the persistent random walk model to fit for speed and persistence time. T lymphocytes were shown to have larger cell speeds on varying concentrations of ICAM-1 when compared to VCAM-1 (Fig. 3.11A); migrating T lymphocytes had average peak speeds (S) of 11.9 ± 1.12 μm/min and 4.3 ± 0.83 μm/min on 1.0 μg/ml of ICAM-1 and VCAM-1, respectively. These values correspond to observations of speed as seen previously *in vivo* and *in vitro* by other groups [9, 13, 14, 34, 35]. Persistence times (P) ranged from 1.9 ± 0.3 to 5.1 ± 0.7 minutes on ICAM-1 and 4.5 ± 0.7 to 8.9 ± 0.6 minutes on VCAM-1 (Fig. 3.11B). In our system, higher cell speeds were observed on ICAM-1 compared to VCAM-1 ($S_{ICAM-1} > S_{VCAM-1}$) while generally cells were more persistent on VCAM-1 than ICAM-1 ($P_{ICAM-1} < P_{VCAM-1}$). Previous empirical observations have showed that speed and persistence times are inversely correlated across a variety of cells types with high speeds correlating to short persistence times and vice versa [36]. By plotting the speeds and persistence times across all concentrations of ICAM-1 and VCAM-1, we observed that this inverse correlation holds true for primary human T lymphocytes with a coefficient of determination (R^2) of 0.7699 (Fig. 3.11C). Overall, on ICAM-1 surfaces, T- lymphocytes have higher speeds with lower persistence times ($\uparrow S_{ICAM-1}$, $\downarrow P_{ICAM-1}$) and on VCAM-1 surfaces, T lymphocytes have lower speeds with higher persistence times ($\downarrow S_{VCAM-1}$, $\uparrow P_{VCAM-1}$). These data suggests that each ligand stimulates different adhesion signaling pathways.

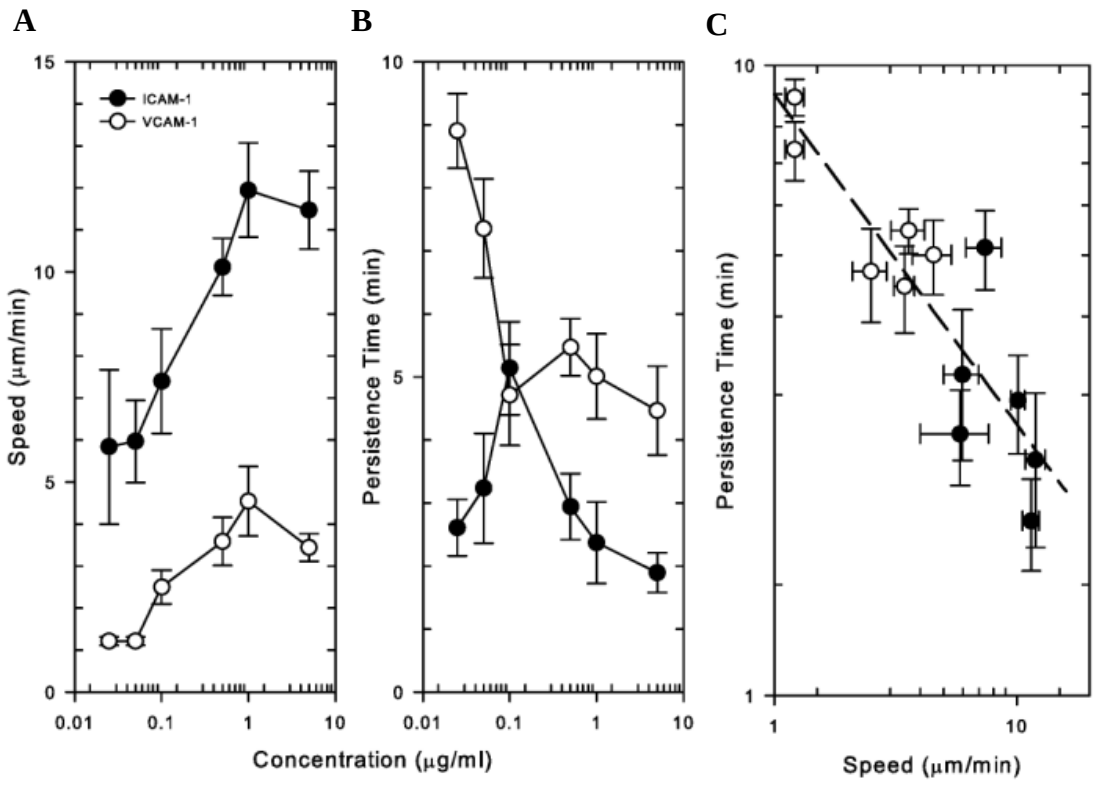

Figure 3.11. T lymphocytes elicit biphasic responses in speed and an inverse correlation with persistence time on ICAM-1 and VCAM-1. T lymphocyte (A) speeds and (B) persistence times determined from using the persistent random walk model; cells have faster speeds and shorter persistence times on ICAM-1 with lower speeds and longer persistence times on VCAM-1. (C) Across all concentrations of ligand an inverse correlation is maintained between persistence time and cell speed. The error bars represent the standard error of the mean (s.e.m.).

The random motility coefficient (μ) is a metric that is commonly used to quantify migration in response to ligands or cytokines in a population of cells and is the product of the average cell speed (S) and mean-free path length (SP) divided by the dimensionality of the system; therefore, it depends on the square of the speed and the first power of the persistence time. Figure 3.12 demonstrates that the random motility coefficient increases with increasing concentration of either ligand before reaching a maximum and then decreases; in other words, the behavior is biphasic. On ICAM-1, the highest random motility coefficient ($\mu_{ICAM\text{-}1}$) is 160 μm^2/min, observed over a range of ICAM-1 concentrations between 0.5 to 10.0 μg/ml. T lymphocytes display a maximum $\mu_{VCAM\text{-}1}$ of 103 ± 16.1 μm^2/min at 0.5 μg/ml VCAM-1. The biphasic response of random motility with ligand density has been observed in other systems, and is often explained by the ratio of cell-substratum adhesiveness to cell contractility that would promote the highest level of motility [37-39]. Overall, we found that cells exhibit greater motility on ICAM-1 than VCAM-1 ($\mu_{ICAM\text{-}1} > \mu_{VCAM\text{-}1}$) for all concentrations tested.

Our data demonstrates that primary human T lymphocytes adhere and migrate differently on ICAM-1 and VCAM-1 microcontact printed PDMS substrates. It is known that T lymphocytes are capable of robust migration on ICAM-1 surfaces in the absence of chemokine predominantly driven by outside-in signaling triggering full LFA-1 activation [40, 41]. VLA-4, on the other hand, has been classically known to require chemokine engagement to achieve full integrin activation and induce cell polarization; this may explain why we observed decreased motility on VCAM-1 in the absence of chemokine albeit the cells were previously activated. In Hyun *et al.*, cells were similarly isolated and activated in the same manner as we did yet they did not observe competent cell migration

on VCAM-1 surfaces alone in the absence of chemokine [42]. Furthermore, experiments conducted in Stachowiak *et al.* showed that unactivated (or naïve) murine T-lymphocytes are not motile on adhesive ligand alone (ICAM-1, VCAM-1, fibronectin) and require chemokine to exhibit robust migration [5]. In the next section, we further expand upon the requirements of chemokine engagement to induce polarization and migration of human T-lymphocytes on ICAM-1 and VCAM-1 surfaces.

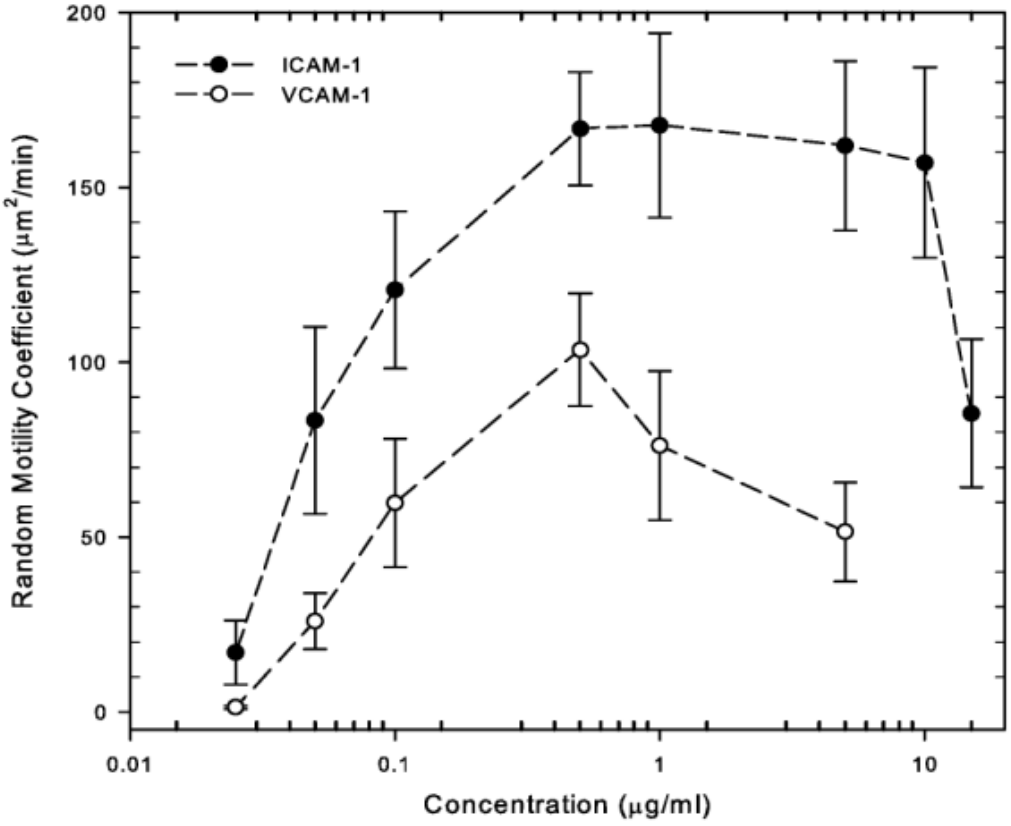

Figure 3.12. Response in the random motility coefficient for all ligand concentrations on ICAM-1 and VCAM-1 surfaces is biphasic. Comparison of the random motility coefficients (μ) show biphasic motility as a function of ligand concentration with ICAM-1 (peak $\mu_{ICAM\text{-}1} = 172.77 \pm 45.45\ \mu m^2/min$) promoting increased haptokinesis than VCAM-1 (peak $\mu_{VCAM\text{-}1} = 103.58 \pm 16.06\ \mu m^2/min$). The error bars represent the standard error of the mean (s.e.m.).

Phenotypes of motility on the two ligands

Cell polarization and motility require the dynamic rearrangement of the actin and microtubule cytoskeletons through signaling pathways involving the Rho family GTPases [43-45]. For T lymphocytes, lamellipodium extension requires Rac-induced actin polymerization while uropod detachment is mediated through Rho-ROCK signaling and actomyosin contractility [40, 46, 47]. Studies have also demonstrated that chemokines regulate integrin adhesive activity by modulating avidity and affinity and induce distinct polarized cell morphology [48-50].

In order to investigate the mechanisms of motility of T lymphocytes on ICAM-1 and VCAM-1, we plated cells on 5.0 μg/ml of either ICAM-1 or VCAM-1. We found no difference in cell area between ICAM-1 (189.6 ± 36.3 μm^2; n = 281) and VCAM-1 (173.4 ± 55.9 μm^2; n = 127), (Fig. 3.13A). After plating T lymphocytes on 5.0 μg/ml of ICAM-1 and VCAM-1, we fixed and permeabilized the cells, and fluorescently labeled their actin and microtubule cytoskeletons. Based upon our observations, we observed the following T lymphocyte phenotypes (Fig. 3.13C):

- Polarized, Motile – cells which migrated several cell diameters with a polarized morphology involving a clearly identifiable lamellipod, cell body, and uropod;
- Polarized, Tethered – lymphocytes with a polarized morphology but tethered and unable to move;
- Non-polarized, Motile – migrating several cell diameters with protrusions but lacking a clear polarized morphology;
- Non-polarized, Non-motile – spherical cells which do not have protrusions and are not migrating.

ICAM-1 surfaces induce increased lamellipod formation and greater cell adhesion when compared to VCAM-1 surfaces (Fig. 3.13B, left column). There are higher percentages of polarized and motile T lymphocytes on ICAM-1 than VCAM-1 surfaces (37% versus 12%; Fig. 3.13D and 3.13E). Also, ICAM-1 surfaces have fewer non-polarized and non-motile lymphocytes compared to VCAM-1 surfaces (23% versus 69%).

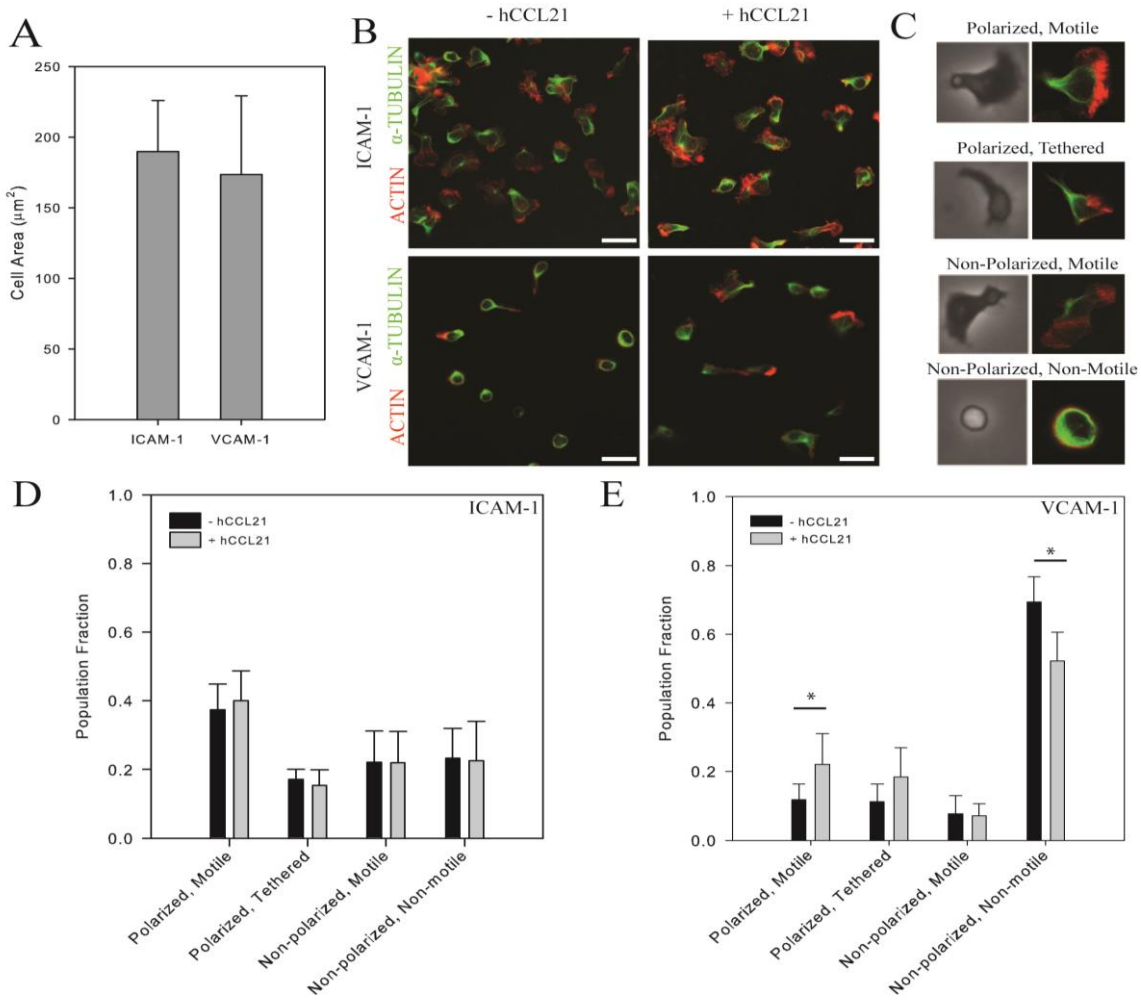

Figure 3.13. T lymphocytes are more polarized on ICAM-1 than VCAM-1. (A) Measurements found no difference in cell area for ICAM-1 (189.6 ± 36.3 μm^2; n = 281) versus VCAM-1 (173.4 ± 55.9 μm^2; n = 127) (B) Fluorescence images showing T lymphocytes on either ICAM-1 or VCAM-1 with or without hCCL21 on the surface. T lymphocytes visibly exhibit greater polarity (lamellipod, cell body, and uropod) on ICAM-1 surfaces with or without hCCL21 (top row) than compared to VCAM-1 surfaces (bottom row). Cells were stained with Alexa568 phalloidin (red) and Alexa488 anti-α-tubulin antibody (green). Scale bars, 10 μm. (C) Phase contrast and fluorescence images of the four classifications for T lymphocyte migration: polarized and motile, polarized and tethered, non-polarized and motile, and non-polarized and non-motile. (D) T lymphocytes were classified based upon their migratory phenotype on ICAM-1 (n = 281) with or without hCCL21. Around 37% of cells plated exhibited a polarized, motile phenotype. There was no observable differences with the addition of hCCL21 (n = 127). (E) On VCAM-1 (n = 244) surfaces, cells are less polarized and motile (12% of cells) and the addition of hCCL21 (n = 267 for VCAM-1 increases the number of polarized, motile lymphocytes while decreasing the number of non-polarized, non-motile cells on VCAM-1; *$p < 0.05$, compared to no CCL21; one-sample t test.

Effect of chemokines on T-lymphocyte motility

It is known that chemokines are capable of modulating T lymphocyte migration by promoting integrin activation and Rho GTPase signaling and synergize with adhesion ligands to alter adhesion, polarity, and motility [5]. The chemokine CCL21 is known to adhere to surfaces and affect leukocyte motion [22, 51, 52]. We investigated whether printing the chemokine CCL21 would increase the number of polarized and motile lymphocytes in tandem with either ICAM-1 or VCAM-1. We found that hCCL21 does not significantly change lamellipod formation of T lymphocytes on ICAM-1 ($n = 244$; Fig. 3.13B, top row) while it increases lamellipod formation on VCAM-1 surfaces ($n = 267$; Fig. 3.13B, bottom row). The fraction of polarized and motile lymphocytes on ICAM-1 with or without hCCL21 did not change (37% versus 40%; Fig. 3.13D). However, hCCL21 increased the fraction of polarized and migratory cells significantly on VCAM-1 surfaces (12% versus 22%) leading to a decrease in the percentage of non-polarized and non-motile cells (69% versus 52%; Fig. 3.13E) ($p < 0.05$).

Our data demonstrates that T lymphocytes are capable of spontaneous adhesion and migration to ICAM-1 and VCAM-1 surfaces in the absence of chemokine. We also demonstrated that by the addition of CCL21 to the surface, T lymphocytes significantly increase cell polarity and migration on VCAM-1 but not on ICAM-1 surfaces.

CCL19 and CCL21 individually induce T lymphocyte chemokinesis that is dependent on ICAM-1 concentration

The chemokines CCL19 and CCL21 bind to the CCR7 receptor and are capable of driving chemokinesis and chemotaxis [53-56]. Previous studies have predominantly used

transwell assays to demonstrate chemokinesis and chemotaxis, but these three dimensional assays provided limited ability to directly observe cells [20, 21, 57]. After having determined the effect of ligand composition and densities on the motility of primary human T lymphocytes, we investigated how soluble CCL19 (sCCL19) and CCL21 (sCCL21) drive CCR7-mediated chemokinesis on ICAM-1 microcontact printed PDMS surfaces and, specifically, how ligand concentration plays a role in the cell's ability to respond to chemokine concentration. We designated ICAM-1 concentrations of 5.0 µg/ml as *high* and 0.05 µg/ml as *low*; these two concentrations support spontaneous and robust T lymphocyte migration, as shown above. We measured the random motility coefficient for a range of CCL19 and CCL21 chemokine concentrations on both *high* and *low* concentrations of ICAM-1. We observed no significant differences in the random motility coefficients as a function of chemokine concentration on the *high* ICAM-1 surface with random motility coefficients (μ_{HIGH}) ranging between 164 ± 14.4 to 226 ± 40.6 μm^2/min (Fig. 3.14A). We have shown that T lymphocytes are capable of sustained motility on ICAM-1 alone without the need for chemokines, leading us to believe that sustained signaling through LFA-1/ICAM-1 interactions at this high ligand concentration was overwhelming the signals that resulted from CCR7 receptor engagement (outside-in versus inside-out signaling). On the *low* ICAM-1 surface, we observed a biphasic response in motility to chemokine concentrations. Statistically significant peaks in the random motility coefficients (μ_{LOW}) were observed at 20 nM for both sCCL19 (114.83 ± 4.76 μm^2/min) and sCCL21 (109.37 ± 8.77 μm^2/min) when compared to the random motility coefficient observed on *low* ICAM-1 alone ($p < 0.05$; Fig. 3.14A; Fig. 3.15). Empirical observations in other cell systems, such as in murine dendritic cells, have estimated the K_D of the CCR7 receptor to

be near 10 nM, which is close to the value of 20 nM that corresponds to our observed peaks in the random motility coefficients for both CCR7 ligands [58, 59]. Furthermore, Fig. 3.14B shows that T cell persistence times and speeds change with the addition of chemokines while still maintaining an inverse correlation as seen in the absence of chemokine. Almost all chemokine concentrations led to decreased speeds with increased persistence times except at our maximum motility coefficient seen at sCCL21 and sCCL19 = 20 nM which had increased speeds and shorter persistence times (Fig. 3.14B; right panel).

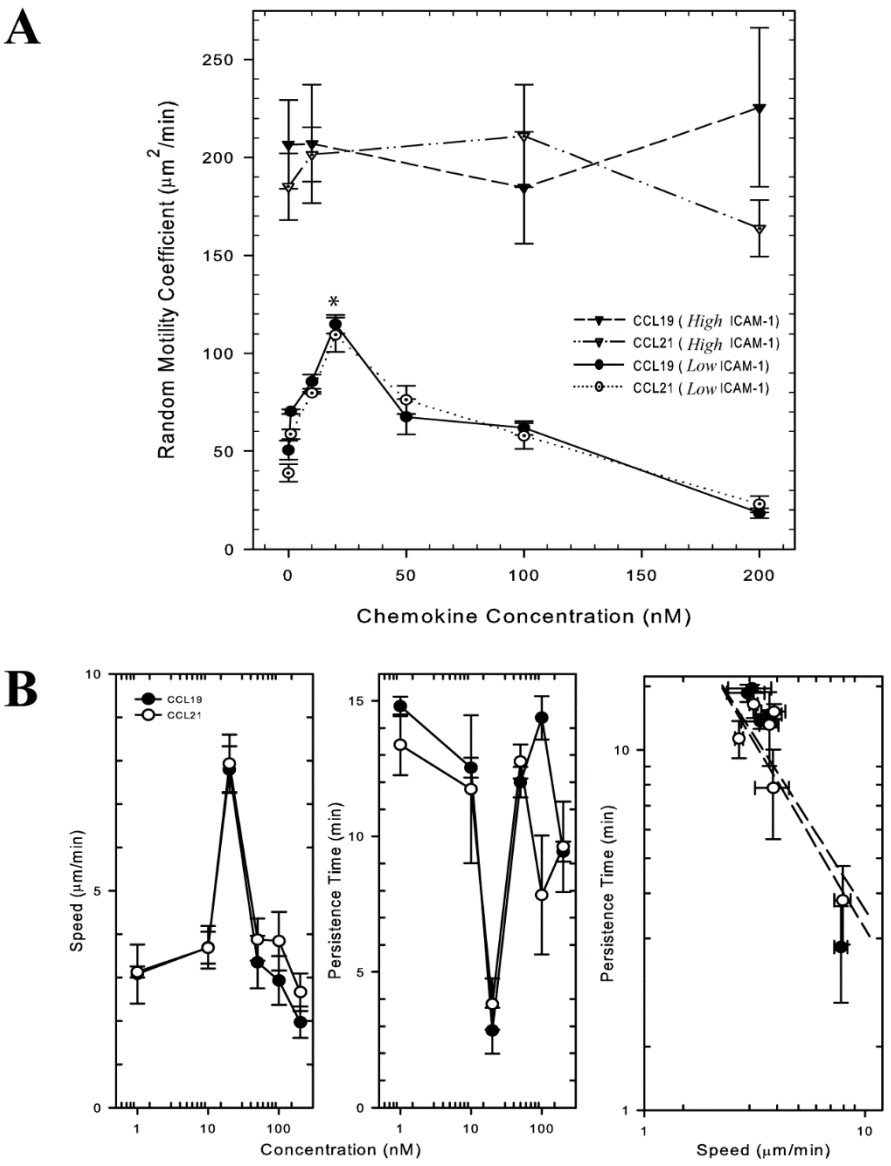

Figure 3.14. sCCL19 and sCCL21 individually induce chemokinesis on *low* ICAM-1 surfaces. (A) Comparison of the random motility coefficients (μ) for sCCL19 and sCCL21 show biphasic motility on *low* but not *high* ICAM-1 surfaces. Peak in chemokinesis observed at 20 nM (μ_{CCL19} = 174.13 ± 4.76 μm²/min and μ_{CCL21} = 146.52 ± 8.77 μm²/min); *$p < 0.05$, compared to all concentrations; one-sample t test. (B) T lymphocyte speeds and persistence times during chemokinesis for sCCL19 and sCCL21 (left two panels); cells maintain near same speeds and persistence times for each concentration of chemokine. The right graph shows that across all concentrations of chemokine an inverse correlation is maintained between persistence time and cell speed with an increased speed and decreased persistence time for 20 nM. The error bars represent the standard error of the mean (s.e.m.).

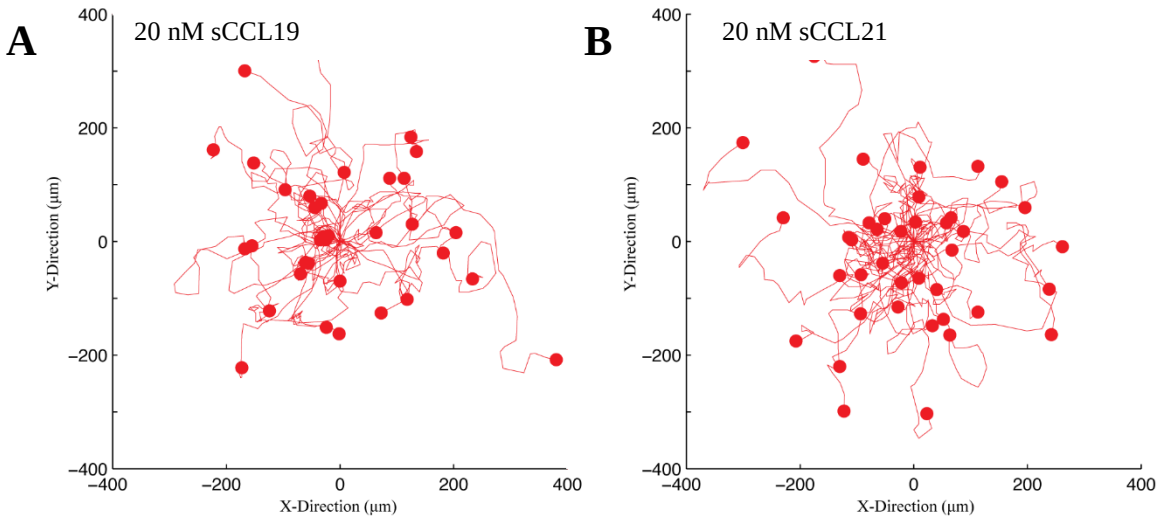

Figure 3.15. Cell traces for sCCL19 and sCCL21 chemokinesis. Single cell migration tracks showing random motility at (A) 20 nM CCL19 and (B) 20 nM CCL21 with no preferred direction in migration.

Combinatorial chemokine signaling on ICAM-1 surfaces increases chemokinesis

We have demonstrated that varying ligand concentration (haptokinesis) and chemokine concentration (chemokinesis) can affect T lymphocyte motility. We next examined how T lymphocyte motility can be modulated by combining soluble CCL19 and CCL21 together, which both bind to the CCR7 receptor. Previous studies have shown that these ligands elicit different responses upon binding to CCR7 owing to receptor internalization and desensitization and signal attenuation [55, 60-62]. It has also been shown that murine dendritic cells and human T lymphocytes are capable of differential responses during chemotaxis to gradients of CCL19 and CCL21 [10, 59]. It is thought that within the lymph node, T lymphocytes encounter antigen presenting cells, such as dendritic cells, through random, autonomous motility within chemokine fields [11]. This led us to believe that by exposing primary human T lymphocytes to varying uniform fields of both sCCL19 and sCCL21, we would observe a difference in motility than what was seen with sCCL19 or sCCL21 alone. Interestingly, we found that the chemokines act together to increase motility greater than what was observed with the chemokines individually. A peak in motility was observed when T lymphocytes were exposed to 1 nM of both sCCL19 and sCCL21 with a random motility coefficient of 203.00 ± 11.45 μm^2/min (Fig. 3.16, Fig. 3.17B). For all equivalent concentrations of chemokines tested, the effect is superadditive producing random motility coefficients that are greater than the sum of the values observed individually with each chemokine except for the 20 nM condition. Our previous data has shown that for 100 nM and 200 nM of sCCL19 and sCCL21 individually, the motility coefficients are much lower than the maximum observed random motility coefficients found at 20 nM for each chemokine. Surprisingly, when 100 nM sCCL19 and 100 nM

sCCL21 were combined, the random motility coefficient increased significantly implying a synergistic effect (172.87 ± 16.12 μm^2/min). Furthermore, this effect was also observed when 200 nM sCCL19 and 200 nM sCCL21 were combined (146.23 ± 36.45 μm^2/min). The combination of both 20 nM of sCCL19 and sCCL21 produced no significant changes in the motility coefficient when compared to that of the chemokines individually, with a random motility coefficient of 129.28 ± 4.82 μm^2/min. We then tested the effects of combining a high concentration of one chemokine with another that is near where observed peaks with chemokines alone. For cells exposed to 20 nM of sCCL19 and 200 nM of sCCL21, we observed a random motility coefficient that is between what was observed on the two surfaces alone, 148.71 ± 12.41 μm^2/min. Furthermore, when we exposed cells to 200 nM of sCCL19 and 20 nM of sCCL21, we again observed an intermediate random motility coefficient equal to 114.30 ± 11.92 μm^2/min. Table 3.2 lists all random motility coefficients for all combined chemokinesis values tested.

It is known that CCL19 and CCL21 elicit different responses upon CCR7 engagement, and the synergy we observed in our combined chemokinesis experiments is most likely a direct result of this. The CCR7 receptor is recycled upon chemokine binding with CCL19 eliciting rapid internalization when compared to CCL21; furthermore, once internalized, CCL19 is targeted for degradation while CCL21 is not [60-62]. We suspect that larger quantities of free CCL21 is capable of binding to CCR7 since it is not targeted for degradation. This would lead to increased unbound CCR7 on the cell surface that can then be engaged to promote increased chemokinesis through CCL21 engagement. To test this hypothesis, we could employ using a CCR7-GFP construct to quantify internalization upon simultaneous engagement of CCL19 and CCL21 in our experimental system.

Furthermore, we could verify whether the CCR7 receptor co-localizes with endosomes for recycling or lysosomes for degradation and how the concentration of each chemokine dictates this. These data would provide further insight into how T lymphocytes respond to combinatorial chemokine signaling and the effect on their motility in conditions possibly similar to what is seen in SLOs.

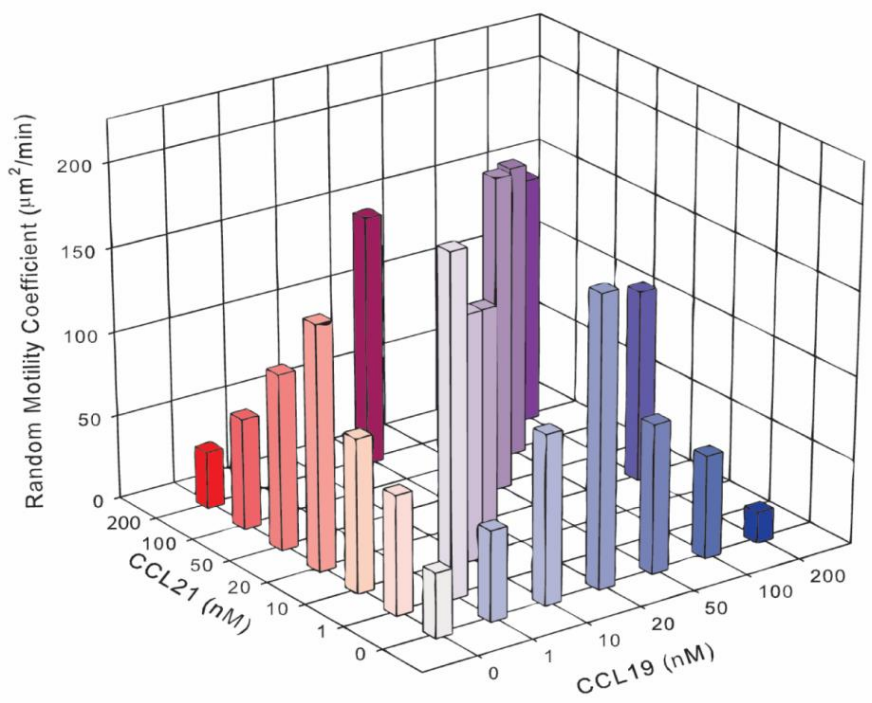

Figure. 3.16. sCCL19 and sCCL21 synergize for combinatorial chemokinesis on *low* ICAM-1 surfaces. Combined chemokinesis of sCCL19 and sCCL21 show that motility is increased to levels greater than what is observed with each chemokine individually. Peak in chemokinesis observed at 1 nM sCCL19 and sCCL21 (μ = 203.00 ± 11.45 μm^2/min). Each average value is calculated from at least three independent experiments.

CCL19 (nM)	CCL21 (nM)	μ (μm^2/min)	SEM
1	1	203.00	11.45
10	10	146.98	19.82
20	20	129.28	4.82
50	50	186.42	13.21
100	100	172.87	16.12
200	200	146.23	36.45
20	200	148.71	12.41
200	20	114.30	11.92

Table 3.2. Random motility coefficient values for combined chemokinesis with sCCL19 and sCCL21 on *low* ICAM-1 surfaces. Values of the random motility coefficients for all chemokine variations tested. SEM = standard error of the mean.

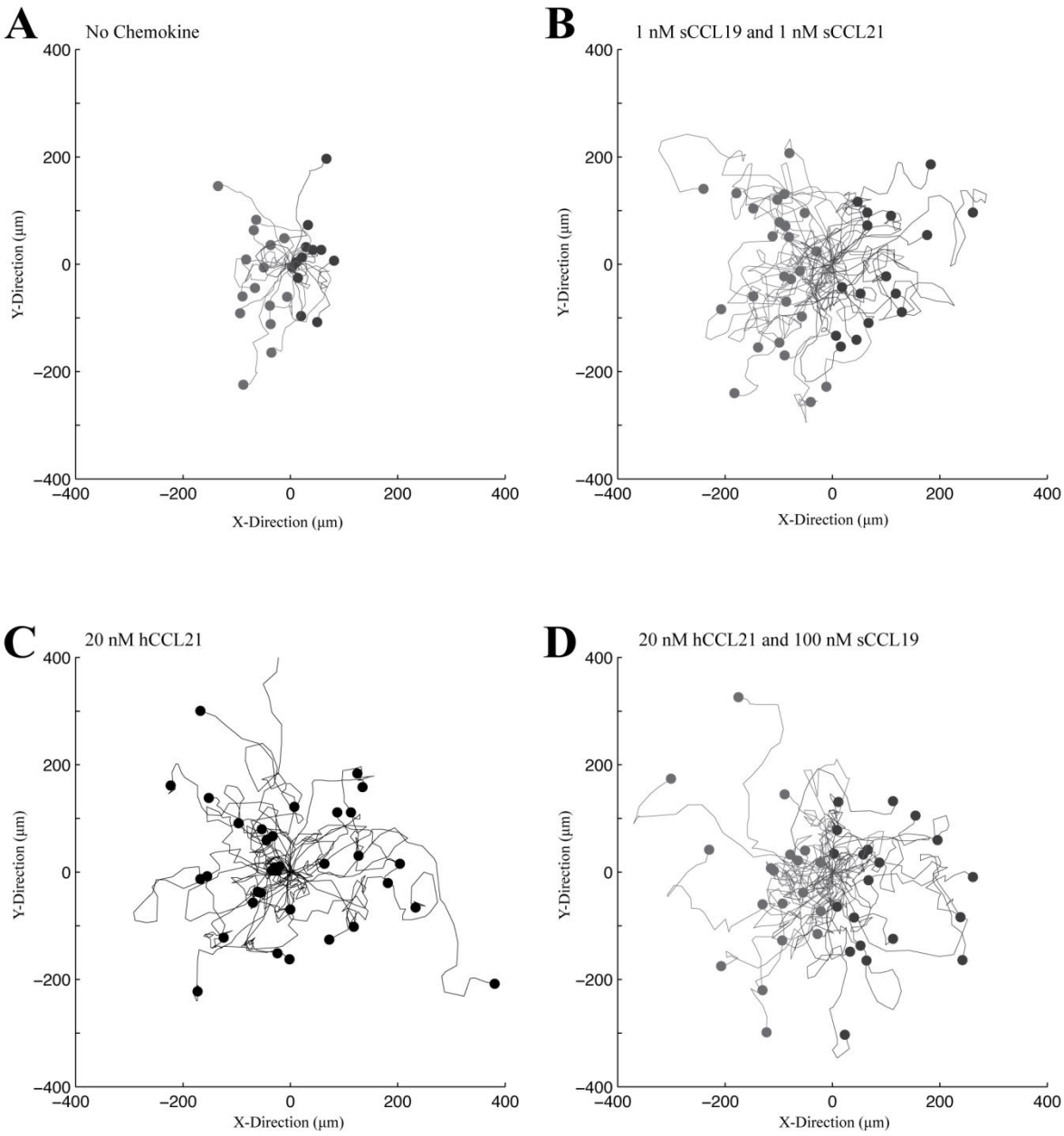

Figure. 3.17. Single cell traces for combinatorial chemokinesis. Single cell migration tracks showing random motility on (A) 0.05 μg/ml of ICAM-1 alone (B) 1nM soluble CCL19 and 1 nM soluble CCL21 (C) 20 nM of printed CCL21 and (D) 20 nM of printed CCL21 with 100 nM soluble CCL19 with no preferred direction in migration.

Printed CCL21 and soluble CCL19 promote robust chemokinesis on ICAM-1 surfaces

We have demonstrated that soluble CCL19 and CCL21 can lead to combinatorial chemokine signaling with enhanced levels of motility. It is well understood that CCL21 is capable of triggering integrin-dependent adhesion of peripheral blood T lymphocytes under shear flow *in vitro*, and is displayed to flowing lymphocytes at the surface of high endothelial venules (HEVs) and within the T cell zones of the SLOs [63, 64]. CCL19, on the other hand, is not presented on a surface in large enough quantities but rather expressed in soluble form to act upon their common receptor, CCR7 [6, 65]. Furthermore, it is not well understood why two chemokine ligands capable of binding the same receptor are expressed in the same regions, but it can be thought that one, CCL21, promotes T lymphocyte binding to the HEVs while soluble CCL19, in concert with CCL21, is needed for recruitment of T lymphocytes to the T cell zones of the SLOs. To further understand the contribution of ligand presentation to T lymphocyte motility, we performed chemokinesis experiments that mimic the expression pattern of these chemokines *in vitro* by exposing primary human T lymphocytes to microcontact printed CCL21 (hCCL21) along with varying concentrations of soluble CCL19 (sCCL19) on *low* ICAM-1 surfaces.

We observed with the addition of varying sCCL19 concentrations to ICAM-1 with hCCL21 there were no significant differences in speed with values ranging between 8.57 ± 0.55 to 10.27 ± 0.41 μm/min (Figure 3.18A; left panel). For persistence times, there was no significant differences with varying sCCL19 concentrations but a peak was observed at 100 nM with a P of 7.02 ± 2.43 minutes (Figure 3.18A; middle panel). This value is essentially half of what was observed at 100 nM sCCL19 on *low* ICAM-1 without hCCL21.

The previous observed inverse correlation between speed and persistence time was lost with the addition of sCCL19 to hCCL21; the speed remains constant while persistence times shift (Figure 3.18A; right panel). However, these speeds do correlate to our previous observations at 20 nM of sCCL19 and sCCL21 alone.

The addition of hCCL21 to *low* ICAM-1 surfaces in the absence of sCCL19 more than doubles the random motility coefficient of cells compared to values observed on *low* ICAM-1 alone (195.55 ± 14.1 versus 83.37 ± 26.7 μm^2/min; Fig. 3.17A, Fig. 3.17C). When sCCL19 concentrations were varied, a peak in motility was observed at 100 nM of sCCL19 with a random motility coefficient value of 275.63 ± 31.3 μm^2/min (Figure 3.18B; $p < 0.05$). This is the largest random motility coefficient recorded in all sets of experiments indicating the importance of the difference in presentation patterns for CCL19 and CCL21. Due to CCL19 and CCL21 both being constitutively expressed by stromal cells within the T cell zones and CCL21 expressed by the HEVs, these data may represent what is seen physiologically and further indicates possible requirements for T lymphocyte recruitment.

By printing CCL21, we have shown that T lymphocytes are capable of robust migration on ICAM-1 with high speeds, and with the addition of 100 nM sCCL19, T lymphocytes have an increased persistence time which may assist in increased directional migration required for recruitment to the SLOs.

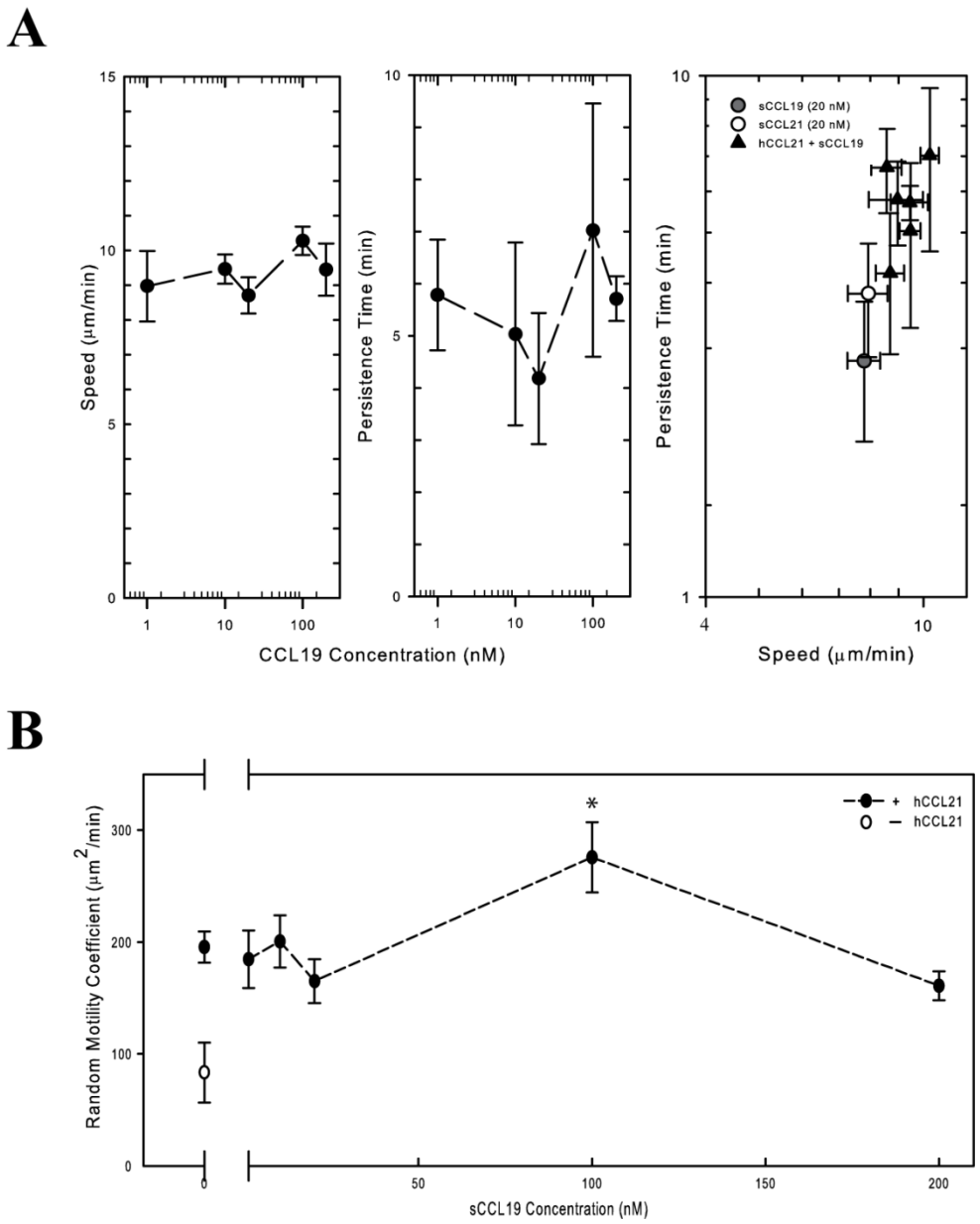

Figure. 3.18. hCCL21 and sCCL19 induce chemokinesis on *low* ICAM-1 surfaces. (A) T lymphocyte speeds and persistence times on hCCL21 and varying sCCL19 concentrations (left two panels); speed remains constant with a peak in persistence time at 100 nM sCCL19. The right graph indicates a loss of the inverse correlation between speed and persistence time. (B) Peak in hCCL21 and sCL19 chemokinesis at 100 nM sCCL19 with the highest observed $\mu = 275.63 \pm 31.3\ \mu m^2/min$; *$p < 0.05$, compared to no CCL21; one-sample t test The error bars represent the standard error of the mean ± (s.e.m.).

CONCLUSIONS

In this chapter, we measured the migration of primary human T lymphocytes on ICAM-1 and VCAM-1 microcontact printed PDMS surfaces. Our results show that ligand composition and concentration are essential in controlling spontaneous and robust T lymphocyte motility by modulating their speed, persistence time, and thus their random motility. These haptokinesis studies also demonstrated that through non-Brownian motion T lymphocytes are more active on ICAM-1 than VCAM-1 surfaces. From chemokinesis studies on *low* ICAM-1 surfaces, we have demonstrated that chemokine signaling elicits biphasic motility with peaks in the random motility coefficient near 20 nM for both of the CCR7 ligands CCL19 and CCL21 and is dependent on ligand concentration. By combining both soluble CCL19 and CCL21, T lymphocyte motility was increased to levels above what was observed by each chemokine individually through synergistic effects. We also demonstrated that by microcontact printing CCL21, we can double the motility of T lymphocytes on ICAM-1, and with the addition of soluble CCL19, we can further increase motility to levels that are higher than exposure to both soluble CCL19 and CCL21, combined or individually. These data provides insight into the dynamic behavior of T lymphocytes and the roles of ligand, chemokines, and combinatorial signaling in an effort for controlling motility to and within the SLOs. Furthermore, our finding that the motility of T lymphocytes is not diffusive is consistent with measurements of made of the migration of murine CD8+ T lymphocytes *in vivo* which undergo Levy walks in response to CXCL10; this is believed to enhance the ability of T lymphocytes to encounter rare targets with more efficiency than Brownian motion walkers [33].

Our work in this chapter follows upon work from the Irvine laboratory on the motility of murine T lymphocytes on surfaces coated with ICAM-1, VCAM-1, and fibronectin. In contrast to what we showed here on microcontact printed surfaces, they did not observe significant random motility on any adhesive ligand by itself [5]. We attribute this difference to the exquisite control over non-specific interactions that can be achieved on microcontact printed surfaces. However, consistent with what was shown here, the chemokine CCL21 enhanced motion, and that enhancement was dependent on the presence of an adhesive ligand. They did not investigate the effects of printing hCCL21 on surfaces, quantify the random motility coefficient under any conditions, or identify the synergy of motility from two different chemokine molecules [5]. As we previously showed with neutrophils, our ability to print molecules on substrates allows us to identify modes of motility that cannot be observed on traditional surfaces [26].

REFERENCES

1. Springer, T.A., *Traffic signals for lymphocyte recirculation and leukocyte emigration: the multistep paradigm.* Cell, 1994. **76**(2): p. 301-14.
2. Butcher, E.C. and L.J. Picker, *Lymphocyte homing and homeostasis.* Science, 1996. **272**(5258): p. 60-6.
3. von Andrian, U.H. and C.R. Mackay, *T-cell Function and Migration: Two Sides of the Same Coin.* N Engl J Med, 2000. **343**(14): p. 1020-34.
4. Rose, D.M., J. Han, and M.H. Ginsberg, *Alpha4 integrins and the Immune Response.* Immunol Rev, 2002. **186**: p. 118-24.
5. Stachowiak, A.N., et al., *Homeostatic lymphoid chemokines synergize with adhesion ligands to trigger T and B lymphocyte chemokinesis.* J Immunol, 2006. **177**(4): p. 2340-8.
6. Cyster, J.G., *Chemokines, Sphingosine-1-Phosphate, and Cell Migration in Secondary Lymphoid Organs.* Annual Review of Immunology, 2005. **23**(1): p. 127-159.
7. Forster, R., A.C. Davalos-Misslitz, and A. Rot, *CCR7 and its ligands: balancing immunity and tolerance.* Nat Rev Immunol, 2008. **8**(5): p. 362-71.
8. Kaiser, A., et al., *CC chemokine ligand 19 secreted by mature dendritic cells increases naive T cell scanning behavior and their response to rare cognate antigen.* J Immunol, 2005. **175**(4): p. 2349-56.
9. Sumen, C., et al., *Intravital microscopy: visualizing immunity in context.* Immunity, 2004. **21**(3): p. 315-29.

10. Lin, F. and E.C. Butcher, *T cell chemotaxis in a simple microfluidic device.* Lab Chip, 2006. **6**(11): p. 1462-9.

11. Miller, M.J., et al., *Autonomous T cell trafficking examined in vivo with intravital two-photon microscopy.* Proc Natl Acad Sci U S A, 2003. **100**(5): p. 2604-9.

12. Miller, M.J., et al., *T cell repertoire scanning is promoted by dynamic dendritic cell behavior and random T cell motility in the lymph node.* Proceedings of the National Academy of Sciences of the United States of America, 2004. **101**(4): p. 998-1003.

13. Bousso, P. and E.A. Robey, *Dynamic Behavior of T Cells and Thymocytes in Lymphoid Organs as Revealed by Two-Photon Microscopy.* Immunity, 2004. **21**(3): p. 349-355.

14. Miller, M.J., et al., *Two-Photon Imaging of Lymphocyte Motility and Antigen Response in Intact Lymph Node.* Science, 2002. **296**(5574): p. 1869-1873.

15. Nandagopal, S., D. Wu, and F. Lin, *Combinatorial guidance by CCR7 ligands for T lymphocytes migration in co-existing chemokine fields.* PLoS One, 2011. **6**(3): p. e18183.

16. Bajenoff, M., et al., *Stromal cell networks regulate lymphocyte entry, migration, and territoriality in lymph nodes.* Immunity, 2006. **25**(6): p. 989-1001.

17. Luther, S.A., et al., *Differing Activities of Homeostatic Chemokines CCL19, CCL21, and CXCL12 in Lymphocyte and Dendritic Cell Recruitment and Lymphoid Neogenesis.* The Journal of Immunology, 2002. **169**(1): p. 424-433.

18. Shimonaka, M., et al., *Rap1 translates chemokine signals to integrin activation, cell polarization, and motility across vascular endothelium under flow.* J Cell Biol, 2003. **161**(2): p. 417-27.

19. Hyun, Y.-M., C. Lefort, and M. Kim, *Leukocyte integrins and their ligand interactions.* Immunologic Research, 2009. **45**(2-3): p. 195-208.

20. Yoshida, R., et al., *EBI1-ligand chemokine (ELC) attracts a broad spectrum of lymphocytes: activated T cells strongly up-regulate CCR7 and efficiently migrate toward ELC.* International Immunology, 1998. **10**(7): p. 901-910.

21. Campbell, J.J., et al., *6-C-kine (SLC), a Lymphocyte Adhesion-triggering Chemokine Expressed by High Endothelium, Is an Agonist for the MIP-3β Receptor CCR7.* The Journal of Cell Biology, 1998. **141**(4): p. 1053-1059.

22. Woolf, E., et al., *Lymph node chemokines promote sustained T lymphocyte motility without triggering stable integrin adhesiveness in the absence of shear forces.* Nat Immunol, 2007. **8**(10): p. 1076-85.

23. Luster, A.D., R. Alon, and U.H. von Andrian, *Immune cell migration in inflammation: present and future therapeutic targets.* Nat Immunol, 2005. **6**(12): p. 1182-90.

24. Valignat, M.P., et al., *T lymphocytes orient against the direction of fluid flow during LFA-1-mediated migration.* Biophys J, 2013. **104**(2): p. 322-31.

25. Cinamon, G., V. Shinder, and R. Alon, *Shear forces promote lymphocyte migration across vascular endothelium bearing apical chemokines.* Nat Immunol, 2001. **2**(6): p. 515-22.

26. Henry, S.J., J.C. Crocker, and D.A. Hammer, *Ligand density elicits a phenotypic switch in human neutrophils.* Integrative Biology, 2014. **6**(3): p. 348-356.

27. Eliasson, M., et al., *Chimeric IgG-binding receptors engineered from staphylococcal protein A and streptococcal protein G.* Journal of Biological Chemistry, 1988. **263**(9): p. 4323-4327.

28. Dickinson, R.B. and R.T. Tranquillo, *A stochastic model for adhesion-mediated cell random motility and haptotaxis.* Journal of Mathematical Biology, 1993. **31**(6): p. 7.

29. Othmer, H.G., S.R. Dunbar, and W. Alt, *Models of dispersal in biological systems.* Journal of Mathematical Biology, 1988. **26**(3): p. 263.

30. Dunn, G.A., *Characterising a kinesis response: time averaged measures of cell speed and directional persistence.* Agents and Actions Supplements, 1983. **12**: p. 19.

31. Stokes, C.L., D.A. Lauffenburger, and S.K. Williams, *Migration of individual microvessel endothelial cells: stochastic model and parameter measurement.* J Cell Sci, 1991. **99 (Pt 2)**: p. 419-30.

32. Ford, R.M. and D.A. Lauffenburger, *Measurement of bacterial random motility and chemotaxis coefficients: II. Application of single-cell-based mathematical model.* Biotechnology and Bioengineering, 1991. **37**(7): p. 661-672.

33. Harris, T.H., et al., *Generalized Levy walks and the role of chemokines in migration of effector CD8+ T cells.* Nature, 2012. **486**(7404): p. 545-548.

34. Wei, S.H., et al., *A stochastic view of lymphocyte motility and trafficking within the lymph node.* Immunol Rev, 2003. **195**: p. 136-59.

35. Svensson, L., et al., *Calpain 2 controls turnover of LFA-1 adhesions on migrating T lymphocytes.* PLoS One, 2010. **5**(11): p. e15090.

36. Lauffenburger, D.A. and J.J. Linderman, *Receptors: Modeling for Binding, Trafficking, and Signaling*. 1996, New York: Oxford University Press.

37. Palecek, S.P., Loftus, J.C., Ginsberg, M.H., Lauffenburger, D.A., and A.F. Horwitz, *Integrin-ligand binding properties govern cell migration speed through cell-substratum adhesiveness.* Nature, 1997. **385**(6616): p. 537-540.

38. DiMilla, P.A., K. Barbee, and D.A. Lauffenburger, *Mathematical model for the effects of adhesion and mechanics on cell migration speed.* Biophys J, 1991. **60**(1): p. 15-37.

39. DiMilla, P.A., et al., *Maximal migration of human smooth muscle cells on fibronectin and type IV collagen occurs at an intermediate attachment strength.* J Cell Biol, 1993. **122**(3): p. 729-37.

40. Smith, A., et al., *LFA-1-induced T cell migration on ICAM-1 involves regulation of MLCK-mediated attachment and ROCK-dependent detachment.* J Cell Sci, 2003. **116**(Pt 15): p. 3123-33.

41. Evans, R., et al., *The integrin LFA-1 signals through ZAP-70 to regulate expression of high-affinity LFA-1 on T lymphocytes.* Blood, 2011. **117**(12): p. 3331-3342.

42. Hyun, Y.M., et al., *Activated integrin VLA-4 localizes to the lamellipodia and mediates T cell migration on VCAM-1.* J Immunol, 2009. **183**(1): p. 359-69.

43. Wittmann, T. and C.M. Waterman-Storer, *Cell motility: can Rho GTPases and microtubules point the way?* Journal of Cell Science, 2001. **114**(21): p. 3795-3803.

44. Ridley, A.J., et al., *Cell Migration: Integrating Signals from Front to Back.* Science, 2003. **302**(5651): p. 1704-1709.

45. Raftopoulou, M. and A. Hall, *Cell migration: Rho GTPases lead the way.* Developmental Biology, 2004. **265**(1): p. 23-32.

46. Krummel, M.F. and I. Macara, *Maintenance and modulation of T cell polarity.* Nat Immunol, 2006. **7**(11): p. 1143-1149.

47. Lee, J.-H., et al., *Roles of p-ERM and Rho–ROCK signaling in lymphocyte polarity and uropod formation.* The Journal of Cell Biology, 2004. **167**(2): p. 327-337.

48. van Kooyk, Y. and C.G. Figdor, *Avidity regulation of integrins: the driving force in leukocyte adhesion.* Current Opinion in Cell Biology, 2000. **12**(5): p. 542-547.

49. Constantin, G., et al., *Chemokines Trigger Immediate β2 Integrin Affinity and Mobility Changes: Differential Regulation and Roles in Lymphocyte Arrest under Flow.* Immunity, 2000. **13**(6): p. 759-769.

50. del Pozo, M.A., et al., *Chemokines regulate cellular polarization and adhesion receptor redistribution during lymphocyte interaction with endothelium and extracellular matrix. Involvement of cAMP signaling pathway.* The Journal of Cell Biology, 1995. **131**(2): p. 495-508.

51. Weber, M., et al., *Interstitial Dendritic Cell Guidance by Haptotactic Chemokine Gradients.* Science, 2013. **339**(6117): p. 328-332.

52. Schumann, K., et al., *Immobilized Chemokine Fields and Soluble Chemokine Gradients Cooperatively Shape Migration Patterns of Dendritic Cells.* Immunity, 2010. **32**(5): p. 703-713.

53. Worbs, T., et al., *CCR7 ligands stimulate the intranodal motility of T lymphocytes in vivo.* J Exp Med, 2007. **204**(3): p. 489-95.

54. Okada, T. and J.G. Cyster, *CC chemokine receptor 7 contributes to Gi-dependent T cell motility in the lymph node.* J Immunol, 2007. **178**(5): p. 2973-8.

55. Britschgi, M.R., et al., *Dynamic modulation of CCR7 expression and function on naive T lymphocytes in vivo.* J Immunol, 2008. **181**(11): p. 7681-8.

56. Forster, R., et al., *CCR7 coordinates the primary immune response by establishing functional microenvironments in secondary lymphoid organs.* Cell, 1999. **99**(1): p. 23-33.

57. Frow, E.K., J. Reckless, and D.J. Grainger, *Tools for anti-inflammatory drug design: In vitro models of leukocyte migration.* Medicinal Research Reviews, 2004. **24**(3): p. 276-298.

58. Yoshida, R., et al., *Secondary Lymphoid-tissue Chemokine Is a Functional Ligand for the CC Chemokine Receptor CCR7.* Journal of Biological Chemistry, 1998. **273**(12): p. 7118-7122.

59. Ricart, B.G., et al., *Dendritic cells distinguish individual chemokine signals through CCR7 and CXCR4.* J Immunol, 2011. **186**(1): p. 53-61.

60. Bardi, G., et al., *The T cell chemokine receptor CCR7 is internalized on stimulation with ELC, but not with SLC.* Eur J Immunol, 2001. **31**(11): p. 3291-7.

61. Byers, M.A., et al., *Arrestin 3 mediates endocytosis of CCR7 following ligation of CCL19 but not CCL21.* J Immunol, 2008. **181**(7): p. 4723-32.

62. Otero, C., M. Groettrup, and D.F. Legler, *Opposite fate of endocytosed CCR7 and its ligands: recycling versus degradation.* J Immunol, 2006. **177**(4): p. 2314-23.

63. Stein, J.V., et al., *CCR7-mediated physiological lymphocyte homing involves activation of a tyrosine kinase pathway.* Blood, 2003. **101**(1): p. 38-44.

64. Warnock, R.A., et al., *The Role of Chemokines in the Microenvironmental Control of T versus B Cell Arrest in Peyer's Patch High Endothelial Venules.* The Journal of Experimental Medicine, 2000. **191**(1): p. 77-88.

65. Ngo, V.N., H. Lucy Tang, and J.G. Cyster, *Epstein-Barr Virus–induced Molecule 1 Ligand Chemokine Is Expressed by Dendritic Cells in Lymphoid Tissues and Strongly Attracts Naive T Cells and Activated B Cells.* The Journal of Experimental Medicine, 1998. **188**(1): p. 181-191.

CHAPTER 4: LFA-1 and VLA-4 MEDIATED MIGRATION UNDER SHEAR FLOW

Adapted from: Dominguez GA, Anderson NR, and DA Hammer. "The direction of migration of T-lymphocytes under flow depends upon which adhesion receptors are engaged." **Intergrative Biology.** *Under revision.*

NR Anderson contributed to the integrin profiling via flow cytometry.

ABSTRACT

T-lymphocyte migration is important for homing, cell trafficking, and immune surveillance. T-lymphocytes express lymphocyte function-associated antigen-1 (LFA-1; $\alpha_L\beta_2$) and very late antigen-4 (VLA-4; $\alpha_4\beta_1$), which bind to their cognate ligands, intercellular adhesion molecule-1 (ICAM-1) and vascular cell adhesion molecule-1 (VCAM-1). These adhesive interactions provide T-lymphocytes with the ability to withstand hemodynamic shear forces to facilitate adhesion and migration along the blood endothelium. Recently, work has been shown that T-lymphocytes will crawl upstream against the direction of flow on surfaces functionalized with ICAM-1. Here, we have investigated whether the identity of the receptor and the magnitude of its engagement affects the direction of T-lymphocyte migration under flow. We used microcontact printed ICAM-1 and VCAM-1 PDMS surfaces on which density and type of adhesion molecule can be tightly controlled and non-specific adhesion adequately blocked. Using a laminar flow chamber, we demonstrate that T-lymphocytes migrate either upstream or downstream dependent upon ligand type, ligand concentration and shear rate. We found that T-lymphocytes migrate upstream on ICAM-1 but downstream on VCAM-1 surfaces – a behavior unique to T-lymphocytes. By varying concentrations of ICAM-1 and VCAM-1,

we observe directed migration under flow that is dependent upon the type and concentration of ligand. At high shear rates (800 s^{-1}), T-lymphocytes favor upstream migration when any ICAM-1 is present, even in the presence of substantial VCAM-1. These results indicate that T-lymphocytes exhibit two different modes of motility – upstream or downstream – depending on ligand composition and the shear rate.

INTRODUCTION

For efficient homing, T-lymphocytes must withstand the hemodynamic forces caused by fluid flow to effectively adhere and migrate along the endothelium [1, 2]. T-lymphocytes express the integrins lymphocyte function-associated antigen-1 (LFA-1; $\alpha_L\beta_2$) and very late antigen-4 (VLA-4; $\alpha_4\beta_1$), which bind to the ligands intercellular adhesion molecule-1 (ICAM-1) and vascular cell adhesion molecule-1 (VCAM-1), respectively. These integrins are known to be crucial for cell activation and to facilitate interactions with other leukocytes in order to elicit effector functions [3-5]. LFA-1 and VLA-4 are also required for firm adhesion to the blood endothelium under shear flow to permit migration into lymph nodes or inflamed tissues [6-8].

Previous work has shown the rather fascinating phenomenon that murine T-lymphocytes crawl efficiently *against* the direction of flow on immobilized ICAM-1 and ICAM-2 surfaces while undergoing recurrent downstream arrest on VCAM-1 [9]. Valignat et al. demonstrated that both freshly isolated and effector human T-lymphocytes increase their upstream migration against flow as shear rate increases on ICAM-1 surfaces [10]. Furthermore, T-lymphocytes undergo adhesion strengthening on ICAM-1 surfaces upon spontaneous LFA-1-mediated adhesion under shear flow that is dependent upon calcium/calmodulin signaling and the assembly of the actin cytoskeleton [11].

Often, multiple integrins are engaged, and a question that has not been fully addressed is how the engagement of multiple integrins controls T-lymphocyte motility under shear flow [12-15]. It is known that chemokine engagement leads to increased integrin activation through heterologous modulation (inside-out signaling) [16-18]; on the other hand, homologous modulation, when one integrin binds its specific ligand activating

a signaling pathway that then activates a different integrin, can also occur. For example, VCAM-1 engagement of VLA-4 is known to regulate β_2-dependent adhesion under flow on ICAM-1 surfaces [5, 19, 20]. Previous studies have also shown a synergistic response in adhesion strengthening and resistance to shear upon plating human T-lymphocytes on surfaces that have been co-immbolized with ICAM-1 and VCAM-1 [19]. However, it is not well understood how the simultaneous engagement of LFA-1 and VLA-4 with their cognate ligands controls the directional migration of T-lymphocytes under fluid flow, which is especially interesting given the dichotomous response of T-lymphocytes on each ligand alone.

In Chapter 3, we demonstrated that human primary T-lymphocytes are capable of spontaneous and robust migration under static conditions on microcontact printed ICAM-1 and VCAM-1 PDMS surfaces, but it is not well understood how the application of shear modulates this behavior. Here, we used the same surfaces, presenting ICAM-1 and VCAM-1 in a controllable ratio, to measure how ligand presentation affects directional migration under fluid flow. We quantified T-lymphocyte migration under shear flow using a parallel plate laminar flow assay [10, 11, 21-23]. We show that under conditions of shear flow, T-lymphocytes can crawl either upstream or downstream, and the motility is dependent upon ligand concentration, type, and shear rate, over a range of physiological shear rates mimicking conditions encountered in the postcapillary venules where leukocyte extravasation predominantly takes place [24, 25]. Furthermore, we show that presentation of both ICAM-1 and VCAM-1 at different densities orients T-lymphocyte migration either upstream or downstream of fluid flow at low shear rates while at high shear rates preferential migration is observed upstream provided there is any ICAM-1 present. These

results suggest that β_2 integrins play a dominant role in dictating the direction of migration under fluid flow. Our current observations correspond well to the previous studies showing that VCAM-1 mediated motility exhibits lower migration speeds and, overall, less motility than on ICAM-1 surfaces and provides new insight into their behavior on surfaces containing both ligands under shear flow [26].

MATERIALS AND METHODs

Cell Culture and Reagents

Human blood was obtained via venipuncture from healthy adult donors and collected into sterile tubes containing sodium heparin (BD Biosciences, San Jose, CA). These experiments involved human T-lymphocytes which were obtained by fractionation of whole blood. Whole blood was obtained by phlebotomy, in compliance with relevant laws and institutional guidelines for the University of Pennsylvania. The institutional review board (IRB) of the University of Pennsylvania reviewed and approved the protocols. Donations were made voluntarily and in all cases, informed consent was obtained. Blood samples were carefully layered in a 1:1 ratio of whole blood to 1-Step Polymorphprep (Axis-Shield, Oslo, Norway). Vials were then centrifuged at 1500 rpm for 35 minutes and the mononuclear band was collected into a fresh vial. Cells were cultured in RPMI-1640 supplemented with 10% FBS and 1 μg/ml of phytohemagglutinin (PHA-M; Sigma-Aldrich, St. Louis, MO) overnight. After 24 hours, the lymphocyte suspension in the PHA medium was transferred into a new flask leaving behind adherent cells. After an additional 48 hours, the cells were then cultured in RPMI-1640 with 10% FBS and 1% penicillin-streptomycin supplemented with 20 ng/ml of interleukin-2 (IL-2; Roche, Mannheim, Germany). Cells were used for experimentation following an additional 72 hours in culture. Other biological reagents included: protein A/G (Thermo Scientific, Rockford, IL), human ICAM-1/Fc and VCAM-1/Fc (R&D Systems, Minneapolis, MN), human IgG_1 (Abcam, Kendall Square, MA), human anti-β_2 (clone IB4) (Calbiochem, San Diego, CA), human anti-β_1 (clone Mab13) and rat isotype IgG_2a (BD Pharmingen, San Jose, CA), and Pluronics F127 (Sigma-Aldrich, St. Louis, MO). Fluorescent conjugates of

anti-α_L (clone HI111), anti-α_M (clone ICRF44), anti- α_4 (clone 9F10), anti- β_1 (clone TS2/16), and anti- β_2 (clone 6.7) as well as the isotype controls were obtained from eBioscience (San Diego, CA).

Substrate preparation

Poly(dimethylsiloxane) (PDMS) (Sylgard 184 Silicone Elastomer, Dow Corning, Midland, MI) coated slides were prepared from 1 mm thick precleaned microscope slides (Fisher Scientific, Hampton, NH) with 25 X 75 mm dimensions spin coated with degassed PDMS (10:1 base:cure by weight) and cured overnight at 65 ºC.

Protein printing and blocking

Flat stamps for printing were prepared by pouring degassed PDMS mixed at 10:1 base:cure by weight over an unpatterned silicon wafer. The polymer was cured for 2 hours or longer at 65 ºC. Stamps were trimmed, sonicated in 200 proof ethanol for 10 minutes, rinsed with dH_2O, and dried in a stream of N_2(g). For motility studies, stamps were 1 cm^2 and were inked with 200 µl of 2 µg/ml of protein A/G in PBS for 2 hours at room temperature. The stamps were then thoroughly rinsed in H_2O and blown dry with a stream of N_2. In parallel, the PDMS spincoated microscope slide was treated with ultraviolet ozone for 7 minutes (UVO Cleaner Model 342, Jelight Company, Irvine, CA) to render the surface hydrophilic. The stamp was then placed in conformal contact with the substrate for ~10 seconds and removed. A 0.2% (w/v) solution of Pluronics F127 was immediately adsorbed to the PDMS substrates for 30 minutes at room temperature to prevent protein adsorption to non-functionalized portions of the PDMS. The cell culture substrate was then rinsed with PBS 3X without dewetting the functionalized surface before deposition of 200 µl of either ICAM-1/Fc, VCAM-1/Fc, or ICAM-1/Fc and VCAM-1/Fc in PBS for 2

hours at room temperature. Ligand concentrations of the substrates were controlled by varying ratios of ICAM-1/Fc and VCAM-1/Fc to human IgG_1. For all experiments (unless otherwise noted), effective total protein concentration remained constant at 10.0 μg/ml. Lack of unspecific T-lymphocyte interactions with the PDMS substrates was tested in control experiments using protein A/G surfaces blocked with 0.2% Pluronics or protein A/G overlaid with a saturating concentration of human IgG_1.

Flow Cytometry

Cells were prepared at 5 X 10^6 cells/ml in 1 ml total volume of flow cytometry buffer (5% FBS in PBS). 100 μl of cells were incubated with 5 μl of either FITC anti-α_L (clone HI111), FITC anti-α_M (clone ICRF44), PE anti- α_4 (clone 9F10), FITC anti- β_1 (clone TS2/16), and FITC anti- β_2 (clone 6.7) as well as the isotype controls for 30 minutes at 4ºC. Cells were then washed 3X with flow cytometry buffer via centrifugation at 1500 rpm for 5 minutes each. Cells were then resuspended into a final volume of 750 μl of flow cytometry buffer. Cells were analyzed using a BD FACSCalibur (Franklin Lakes, NJ) instrument followed by data processing using FlowJo (Ashland, OR).

Flow Chamber Assembly and Assay

A parallel-plate flow chamber (GlycoTech, Gaithersburg, MD) was used with the prepared PDMS substrate. The channel template was cut from 0.01-inch-thick Duralastic sheeting (Allied Biomedical, Goose Creek, SC). For each flow experiment, the template was placed over the prepared PDMS coated slide. The template and slide were placed in the bottom well of the flow chamber, and the top was secured with screws. The chamber was assembled under water to minimize the introduction of air. It was then mounted on the microscope in a 5% CO_2 and 37°C environment for 10 minutes to allow for

equilibration. Before introduction of T-lymphocytes, the chamber was flushed with running media consisting of RPMI-1640 supplemented with 0.1% BSA and 2 mg/ml glucose. A volume of 1.5 ml containing 1 X 10^6 cells in running media was introduced into the chamber and cells were allowed to attach for 15 minutes. Fluid flow was initiated using a syringe pump (11 Plus, Harvard Apparatus, Holliston, MA) and volumetric flow rates were adjusted accordingly to correspond to desired shear rates. Shear rate was calculated using $\tau_w = \frac{6\mu Q}{h^2 w}$ where μ is the fluid viscosity, Q is the volumetric flow rate, h is the channel height and w is the channel width. For this chamber, h = 0.023 cm, w = 0.1 cm. Images were captured every minute on a motorized stage and observed using a Nikon Eclipse TE_{300} phase contrast microscope. Images were captured using a 10X objective. Migrating cells had a polarized morphology consisting of a lamellipod at the front and a uropod at the rear; spherical and non-adherent cells were either washed away upon application of flow or demonstrated no motility and were not included in analysis.

Antibody Blocking

Functional blocking antibodies against the β_1 integrin subunit (clone Mab13), β_2 integrin subunit (clone IB4), and IgG_2a isotype control (clone R35-95) were used at a final concentration of 50 µg/ml. 1.5 X 10^6 T-lymphocytes in 500 µl of running media were incubated for 30 minutes with antibodies at 37C and 5% CO_2. Cells were then injected into flow chamber apparatus and allowed to adhere in the absence of flow for 15 minutes. Running buffer consisted of RPMI-1640 supplemented with 0.01% BSA, 2 mg/ml glucose, and 1/10 final antibody blocking concentration. Cells were exposed to flow for 30 minutes before quantification of speed and MI.

Measurement of Cell Trajectories, Speed, and Migration Index

Cell movement was tracked using the ImageJ plugin Manual Tracking. ImageJ and the plugin are both freely available through the NIH website (http://rsbweb.nih.gov/ij/). The centroid of the cell was considered to represent the cell position. Time lapse microscopy was used and images were taken every minute. The result was a series of (x_i,y_i) positions with time for each cell. The net displacement during the ith 1.0 minute increment, D_i, was calculated by the difference of the position at the beginning and end of that time step. The sum of total displacements ($D_{i,accum}$) was used to calculate the cell speed over the entire experimental time course of 30 minutes. The migration index (MI) was defined as the ratio of the difference between the initial and final x-displacement to total displacement where $MI = \frac{x_{i,end} - x_{i,initial}}{D_{i,accum}}$. Values of the migration index near +1, indicate that cells migrate in a straight trajectory against the direction of flow while values near -1, indicate a preference of migration in a straight trajectory along the direction of flow. When the MI is near 0, there is no preferred direction in migration indicating random motility.

Surface quantification

Protein A/G stamped surfaces were prepared as described above. Fluorescently labeled human IgG_1 was prepared using 1 mg of human IgG_1 and the Alexa Fluor® 555 Protein Labeling Kit (Life Technologies, Grand Island, NY). Concentration and degree of labeling of the sample was calculated as described in the provided procedure. Solutions of fluorescently labeled and unlabeled human IgG_1 were mixed together in varying combinations and deposited onto stamped protein A/G surfaces for 2 hours. Surfaces were then rinsed with PBS 3X without dewetting the functionalized surface before mounting on the microscope. A 20X objective was used to image.. Pixel intensities were calculated using ImageJ by averaging over four distinct areas in the field of view across a minimum

of four different locations on each surface. A solution of unlabeled human IgG_1 was used as a control.

Immunofluorescence

Parallel flow chamber assays were performed as described above. Upon completion of experiments, the cells were fixed with 4% paraformaldehyde in PBS for 7 minutes that was flowed through at the experimental shear rate. The substrate was removed from the flow chamber apparatus and then permeabilized with 0.2% Triton X-100 for 5 minutes and blocked with 1% BSA in PBS for 30 minutes at room temperature. Cells were incubated with 1:200 Alexa Fluor 568-labeled phalloidin and Alexa Fluor 488-labeled mouse anti-α tubulin (Invitrogen) for 30 minutes at room temperature. Cells were mounted in Fluoromount-G mounting medium (SouthernBiotech, Birmingham, Alabama) and examined by confocal microscopy (Leica SP5).

Data analysis

Data are presented as mean ± SEM. Statistical significance was computed using one-way ANOVA and pairwise comparisons were performed with the student t test. Values of *p* are indicated in the figures or figure legends.

RESULTS AND DISCUSSION

Microcontact printing of Protein A/G and Surface Quantification

We verified the relative composition of our surfaces using fluorescently tagged human IgG_1 molecules that bind to microcontact printed protein A/G. Briefly, Alexa Fluor-555 tagged IgG_1 (IgG_1-555) was mixed with unlabeled human IgG_1 in different ratios to maintain a total protein solution concentration of 20 μg/ml. Figure 1A-F shows the fluorescence intensities of surfaces with increasing concentrations of IgG_1-555. By quantifying the pixel intensities for each condition, we found a linear correlation (R^2 = 0.991) between IgG_1-555 concentration and pixel intensity (Fig. 4.1G). These data allows us to conclude that as we increase ligand concentration within solution, we are proportionately increasing the amount of ligand on our surfaces, up to a solution concentration of 20 μg/ml IgG_1. This range of concentrations cover what was used to prepare our surfaces.

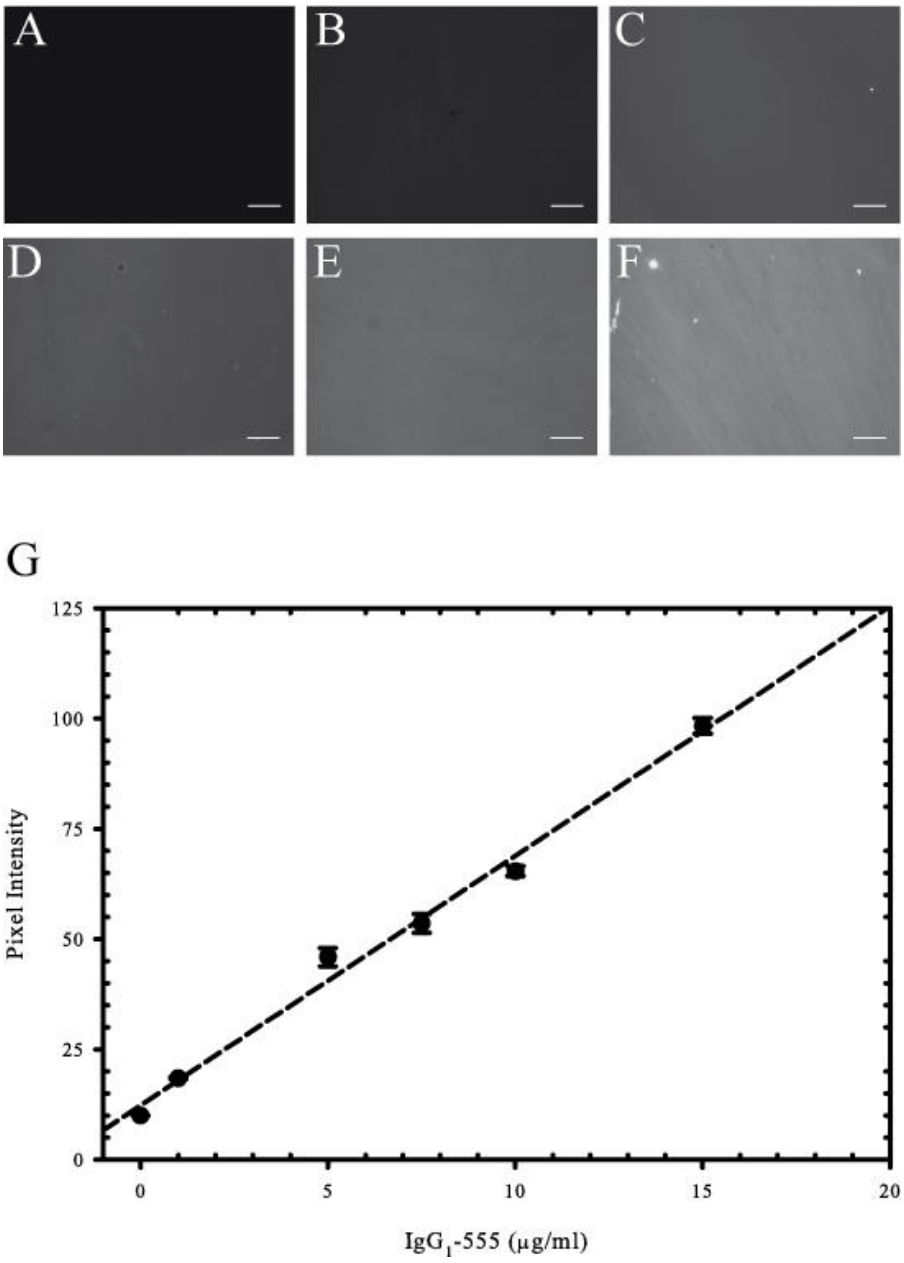

Figure 4.1. Increasing solution concentrations of Fc-containing ligand correlates to increasing surface ligand concentrations. Fluorescent images of surfaces prepared with increasing concentrations of Alexa Fluor-555 tagged human IgG_1 (IgG_1-555). Solution concentrations of IgG_1-555 depicted are as follows: A) 0 μg/ml, B) 1 μg/ml, C) 5 μg/ml, D) 7.5 μg/ml, E) 10 μg/ml, and F) 15 μg/ml. G) The pixel intensities were calculated for each concentration and plotted. Data reveals a linear correlation between soluble IgG1-555 concentration and fluorescent signal present on the surface (R^2 = 0.991). Data are mean ± SE. Scale bar = 50 μm.

ICAM-1, but not VCAM-1, supports T-lymphocyte migration against the direction of flow as a function of shear rate

Intraluminal crawling under shear flow is required for T-lymphocyte extravasation and is dependent upon engagement of integrins to support adhesion and migration [27]. Recently, Valignat *et al.* showed that primary human T-lymphocytes crawl against fluid flow in a shear dependent manner on ICAM-1 surfaces [10]. In this study, we extend upon this recent work and report upon the effect of substrate chemistry on the directionality of primary human T-lymphocyte migration under fluid flow. T-lymphocytes express the integrin heterodimers VLA-4 and LFA-1, and we employed flow cytometry to confirm the expression of α_L, α_4, β_1, and β_2 on primary human T-lymphocytes (Fig. 4.2). We also verified that our cells do not express the MAC-1 integrin heterodimer ($\alpha_M\beta_2$) which is capable of binding to ICAM-1, allowing us to conclude that the interactions observed on ICAM-1 are solely due to LFA-1 engagement.

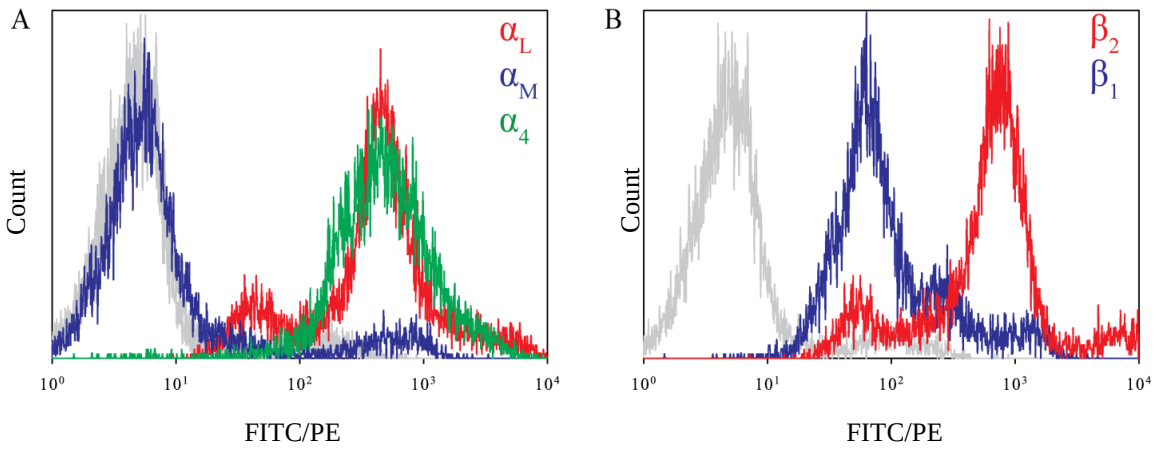

Figure 4.2. Expression of LFA-1, VLA-4, and MAC-1 on primary human T-lymphocytes. (A) The expression levels of the three integrin α subunits α_L (red), α_M (blue), and α_4 (green). (B) The expression levels of the two integrin beta subunits β_2 (red) and β_1 (blue). All negative controls are depicted in gray. Plots represent one set of data from three separate experiments.

Through the use of a parallel flow chamber, we quantified cell motility under fluid flow on substrates with different adhesive ligands in the absence of chemokine. The motility of cells at different shear rates was measured on surfaces prepared by incubating either 5 µg/ml of ICAM-1 or VCAM-1 onto surfaces stamped with protein A/G. After injection and a resting time of 15 minutes to allow for adhesion, cells were exposed to shear rates of 100, 200, 400, or 800 s^{-1}. As illustrated by representative cell traces (Fig. 4.3. A and F), T-lymphocytes migrated substantial distances under static conditions on ICAM-1 or VCAM-1 surfaces, and upon application of flow, directional responses were observed. Blue traces indicate cells that traveled upstream in fluid flow while red traces indicate cells that traveled downstream. At a low shear rate of 100 s^{-1}, cells on ICAM-1 surfaces showed a slight preference for migrating upstream, and with increasing shear rates, cells on ICAM-1 surfaces showed an increasing preference to migrate upstream (Fig. 3, B-E). In contrast, cells on VCAM-1 surfaces preferred to migrate downstream with little to no migration upstream at any shear rate (Fig. 4.3, G-J). To quantify the directional motion, we calculated the migration index (MI) for all cells, defined as the ratio of total x-displacement to total overall displacement, with positive values indicating motion upstream and negative values indicating motion downstream. Under static conditions, the MIs for cells on ICAM-1 and VCAM-1 were near 0, indicating random migration with no preference in direction. Upon exposure to flow, cells on ICAM-1 migrated upstream with increasing MIs as a function of increasing shear rate with values ranging from 0.21 to 0.38 (Fig. 4.3K). On VCAM-1 substrates, migration was downstream with MIs having no dependence on shear rate with values between -0.69 and -0.77 (Fig. 4.3K). Furthermore, T-lymphocytes exposed to surfaces of protein A/G alone did not adhere allowing us to assume that the observed

directional migration on ICAM-1 and VCAM-1 surfaces is specifically due to the ligation of adhesion receptors, and not due to non-specific interactions.

As shear rates increased, we observed a decrease in migration speed on both ligands (Fig. 3L). We observe higher migration speeds on ICAM-1 than VCAM-1 under flow, which corresponds to previous observations under static conditions [26]. On ICAM-1 surfaces, a significant decrease in speed was seen at larger shear rates (400 s^{-1} and 800 s^{-1}) compared to under static conditions. The peak speed was observed at 100 s^{-1} (11.47 ± 0.93 μm/min) with the lowest speed observed at 800 s^{-1} (7.97 ± 0.30 μm/min). For VCAM-1 surfaces, application of 100 s^{-1} of fluid flow doubled the migration speed (5.93 ± 0.52 μm/min) compared to what was observed under static conditions (3.44 ± 0.33 μm/min). Furthermore, when shear rates were increased further on VCAM-1 substrates, the migration speeds decreased with increasing shear rate with the lowest speed being observed at 800 s^{-1} (4.08 ± 0.33 μm/min).

The integrins LFA-1 and VLA-4 are known to be mechanoresponsive to force, leading to increased activation and adhesion stabilization [2, 11, 21, 23, 28]. We expect that as shear rate is increased the integrin-ligand bonds strengthen to promote adhesion and migration. Overall, increasing shear rates led to an increase in the orientation of migration upstream of fluid flow on ICAM-1 surfaces but not VCAM-1 surfaces. These unique responses are likely caused by the inherent differences between these two integrins and their roles physiologically. The integrin LFA-1 binds to ICAM-1 and is required for firm adhesion and extravasation under fluid flow after transient adhesion events and chemokine exposure. Therefore, it appears that LFA-1/ICAM-1 interactions secure adhesion and promote lamellipodial extension upstream. VLA-4, on the other hand, is capable of

supporting both tethering and rolling (in the absence of other adhesion ligands) through engagements with VCAM-1 and is required for capture of T-lymphocytes from fluid flow. Furthermore, after chemokine exposure, VLA-4 increases its affinity to promote firm adhesion and, along with LFA-1, mediates migration along the blood endothelium supporting diapedesis through the endothelium [4, 27, 29, 30]. Although VLA-4 participates in transient as well as firm adhesion events, we hypothesize that this integrin facilitates weaker adhesions compared to LFA-1 and cannot stabilize upstream interactions. Under flow, VLA-4 most likely supports a passive form of adhesion that can support downstream migration and prevent T-lymphocytes from being swept away but not facilitate migration upstream. This has been proposed in other cell types, such as neutrophils, and is hypothesized to be due to lack of a mechanosensing mechanism through this receptor [10, 31].

An alternate hypothesis for T-lymphocytes migrating either upstream or downstream of flow may lie in the integrin expression patterns and their specific interactions with cytoskeletal proteins. Integrin molecules and cytoskeletal linker proteins support bidirectional transmission of force by linking the extracellular matrix (ECM) and the actin cytoskeleton [32, 33]. Application of force is known to strengthen this linkage preventing slippage between the actin cytoskeleton and integrin molecules allowing them to sustain much larger forces [34-36]. Talin, a cytoskeletal linker protein, is known to associate with high affinity conformation states of LFA-1 and VLA-4 on migrating T-lymphocytes [37-39]. These higher affinity forms of VLA-4 are expressed at the leading edge while the higher affinity forms of LFA-1 are expressed in the mid-cell to rear regions of migrating T-lymphocytes [14, 38]. Recent traction force microscopy (TFM) studies

have shown that actomyosin contraction occurs in the rear region of neutrophils thus generating the traction stresses required for cell translocation and motility [31, 40]. The activated LFA-1 found in the mid-cell to rear regions of a migrating T-lymphocyte might support the traction necessary for the actomyosin contractility in the rear to generate the upstream migration against shear. VLA-4, on the hand, may not generate enough traction - given its localization at the front of cell - to support upstream motion but rather permits the more passive form that is dictated by the fluid flow. We would expect to observe large traction stresses generated on ICAM-1 in the rear while more forces would be found in the front on VCAM-1. Furthermore, unlike previous studies, we observed decreased speeds with increasing shear rate on both ICAM-1 and VCAM-1 surfaces [10]. A possible explanation for the increased speed of upstream migration is the increase in the modulation of integrin-ligand affinity that leads to greater adhesive interactions [41, 42].

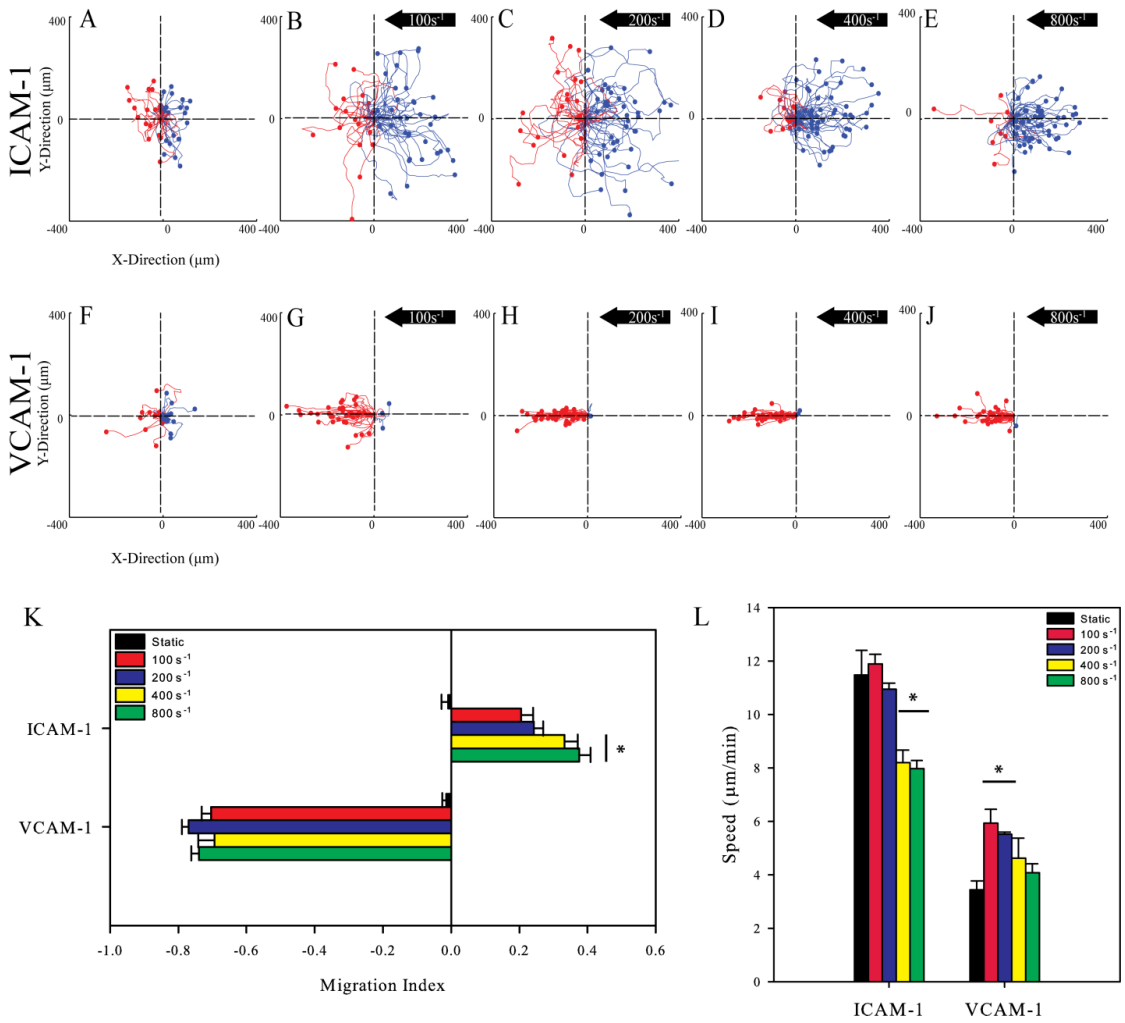

Figure 4.3. T-lymphocytes crawl against the direction of flow on immobilized ICAM-1 but not on VCAM-1 to an extent that depends on shear rate. A-E) Cell traces of T-lymphocytes under shear flow (right to left) on ICAM-1 (5.0 μg/ml) and F-J) VCAM-1 (5.0 μg/ml) coated PDMS surfaces under varying shear rates. The traces depicted under flow are for one representative experiment in each group. Blue traces indicate cells that traveled upstream of flow while red traces indicate cells that traveled downstream. Black arrow indicates direction of shear flow for all conditions. Traces are in μm. K) The direction of T-lymphocytes under shear flow as expressed as the migration index (MI). A positive MI indicates migration against the flow (upstream) while a negative MI indicates migration in the direction of flow (downstream). T-lymphocytes on ICAM-1 migrate upstream to an increasing extent with increasing shear rate while cells on VCAM-1 migrate downstream. The MI was calculated from T-lymphocyte tracks from three independent experiments. *$p < 0.05$. L) T-lymphocytes on ICAM-1 migrate faster than cells on VCAM-1 and is decreased at higher shear rates. Migration speeds were calculated from three independent experiments each. *$p < 0.05$.

Downstream migration of T-lymphocytes is dependent upon VCAM-1 concentration

We have previously demonstrated that the concentration of ICAM-1 and VCAM-1 controls cell speed and the random motility of primary human T-lymphocytes [26]. We investigated whether this is also true under shear flow. We exposed cells to shear rates of 100 s^{-1} and 800 s^{-1} on ICAM-1 surfaces coated with 0.5, 1.0, 5.0, and 10.0 μg/ml of ICAM-1 Fc chimera. Representative cell traces shows that T-lymphocytes preferred to migrate upstream on ICAM-1 for both shear rates (Fig. 4.4, A-D, E-H). We calculated the migration index for each condition to ascertain whether ligand concentration affects the directionality of migration along with shear rate. At a shear rate of 100 s^{-1}, the MIs ranged between 0.14 to 0.21, and upon application of 800 s^{-1}, these values increased significantly and ranged from 0.33 to 0.46 (Fig. 4.4I) with no dependence on ligand concentration for both shear conditions. For the lower concentrations of 0.5 and 1.0 μg/ml of ICAM-1, there were no differences in the speed of T-lymphocytes between shear rates of 100 s^{-1} and 800 s^{-1} (Fig. 4.4J). On surfaces prepared with concentrations of 5.0 and 10.0 μg/ml of ligand, speeds significantly decreased when shear rate increased from 100 s^{-1} to 800 s^{-1}.

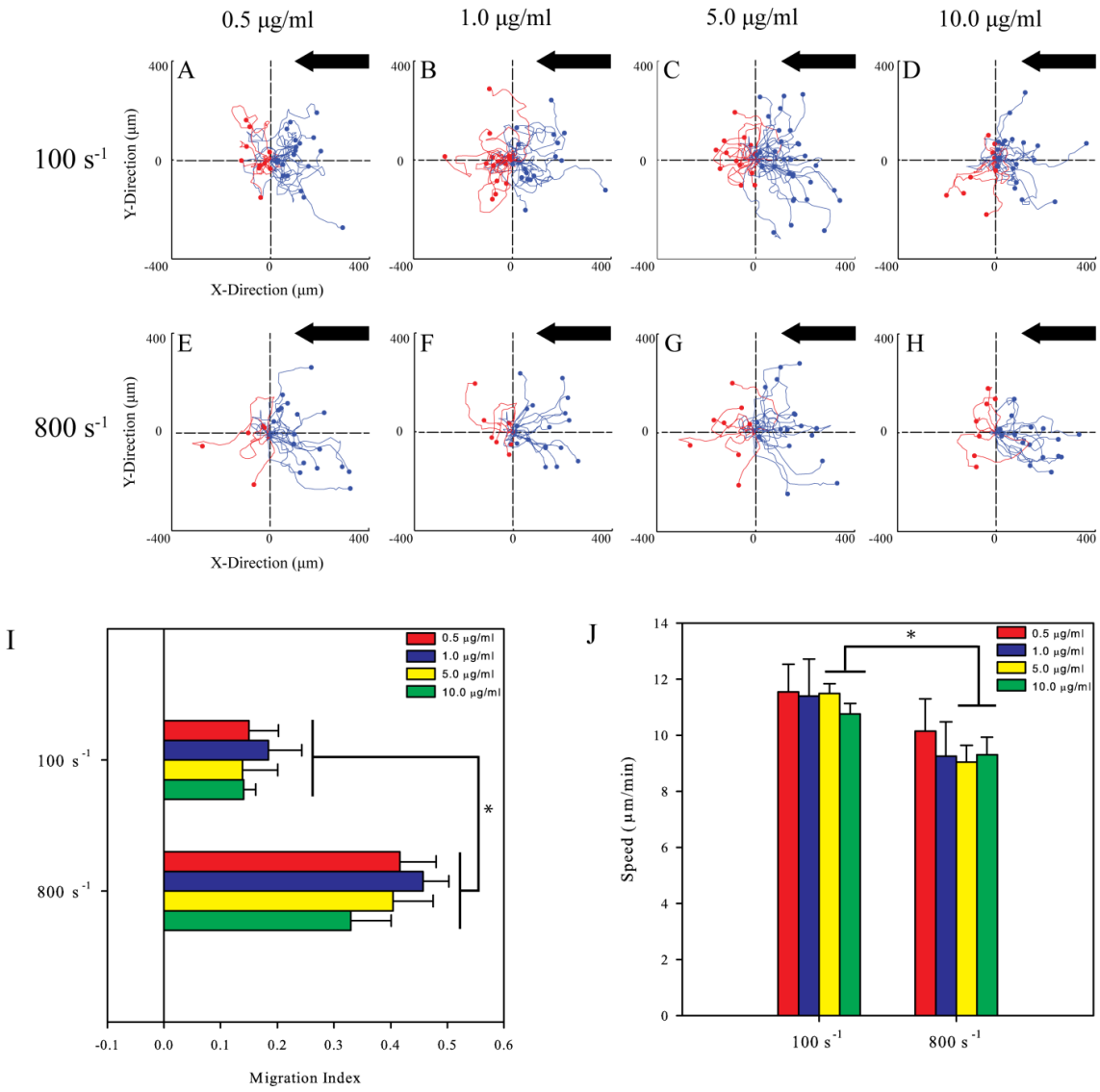

Figure 4.4. T-lymphocytes crawl upstream on different concentrations of immobilized ICAM-1. A-D). Cell traces of T-lymphocytes crawling at a shear rate of 100 s^{-1} on varying concentrations of ICAM-1 PDMS surfaces. E-H) Cell traces of T-lymphocytes under 800 s^{-1} of shear flow on varying concentrations of ICAM-1 PDMS surfaces. Black arrow indicates direction of shear flow for all conditions. The traces depicted under flow are for one representative experiment under the stated conditions. I) The direction of T-lymphocyte migration under shear flow expressed as the migration index (MI). T-lymphocytes on ICAM-1 surfaces migrate upstream and directionality depends on shear rate. The MI was calculated from T-lymphocyte tracks from three independent experiments. *$p < 0.05$. J) T-lymphocytes on varying concentrations of ICAM-1 migrate with the same speed at each shear rate tested . Migrations speeds were calculated from three independent experiments each. *$p < 0.05$

We also measured the motility of T-lymphocytes on VCAM-1 surfaces prepared at 0.5, 1.0, 5.0, and 10.0 μg/ml of the VCAM-1 Fc chimera. The representative cell traces show that at shear rates of 100 s^{-1} (Fig. 5, A-D) and 800 s^{-1} (Fig. 5, E-H) cells crawl downstream for all VCAM-1 concentrations. Unlike ICAM-1 surfaces, the MIs for cells on VCAM-1 surfaces strongly depend upon ligand concentration. Under 100 s^{-1} of flow, the MIs became more negative as VCAM-1 concentration increased, ranging from -0.33 (at 0.5 μg/ml) to -0.83 (at 10 μg/ml) (Fig. 5I). At a shear rate of 800 s^{-1}, the effect of ligand density is more moderate with the two lower concentrations having similar MIs (-.75 and -.77) and the two larger concentrations having significantly larger values (-.88 and -.91). On VCAM-1 surfaces exposed to a shear rate of 100 s^{-1}, crawling speeds ranged between 5.93 to 6.43 μm/min and were largely independent of ligand concentrations. However, at a shear rate of 800 s^{-1}, cells exhibited lower migration speeds at lower ligand concentrations that doubled on surfaces made with higher ligand concentrations (3.12 versus 6.26 μm/min; Fig. 5J). Overall, upon varying ligand concentration, we observed increased upstream migration on ICAM-1 surfaces that is dependent upon shear rate not ligand density. On the other hand, cells migrating on increasing VCAM-1 concentrations showed increased downstream migration as ligand density increased but only during exposure to 100 s^{-1} of fluid flow.

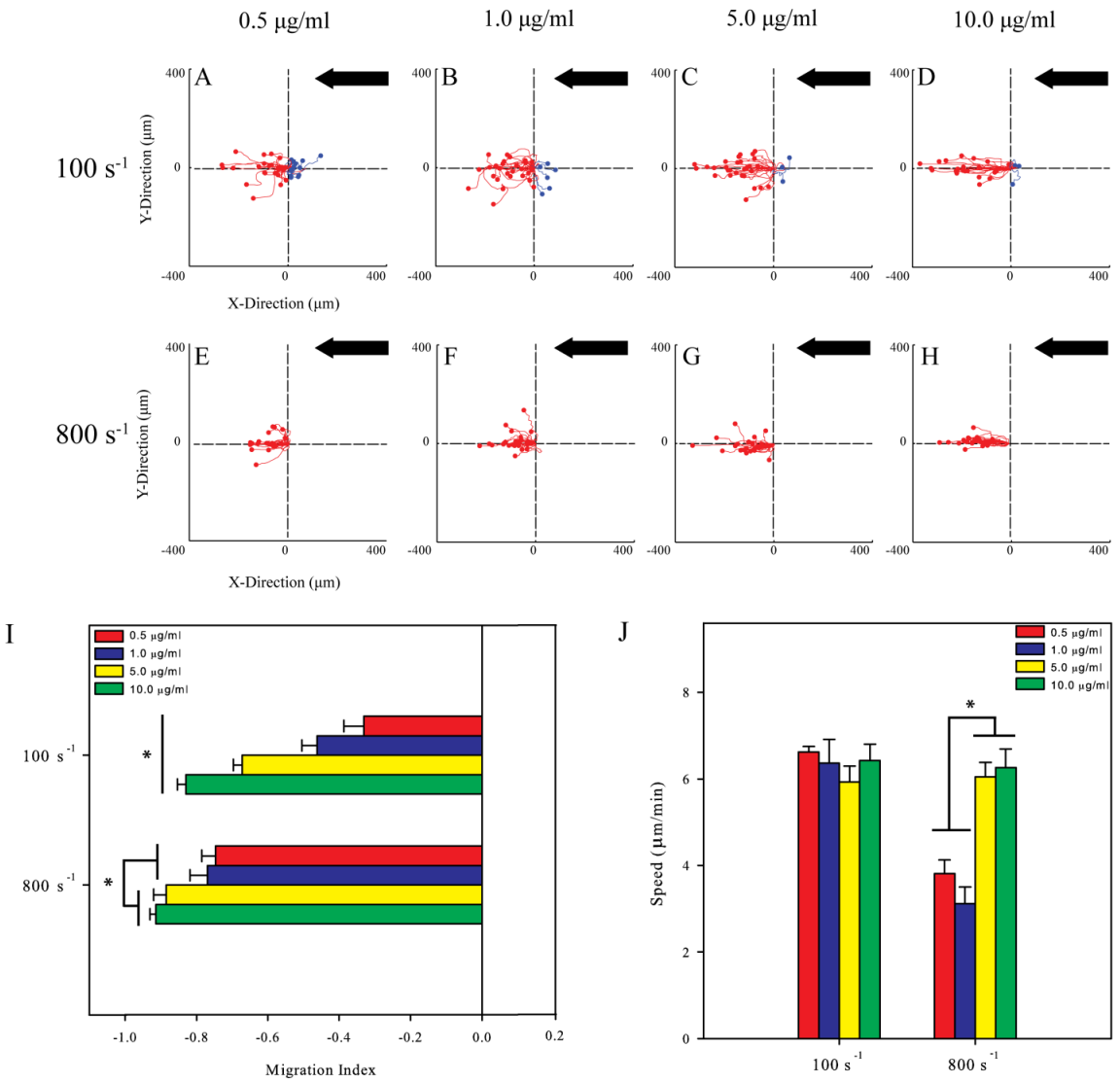

Figure 4.5. The migration index of T-lymphocytes crawling in the direction of flow increases with concentration of immobilized VCAM-1. A-D) Cell traces of T-lymphocytes at a shear rate of 100 s^{-1} on different concentrations of ICAM-1 on PDMS surfaces. E-H) Cell traces of T-lymphocytes at a shear rate of 800 s^{-1} on varying concentrations of ICAM-1 PDMS surfaces. The traces depicted under flow are for one representative experiment in each group. Black arrow indicates direction of shear flow for all conditions. I) The direction of T-lymphocytes under shear flow expressed as the migration index (MI). T-lymphocytes on VCAM-1 migrate downstream and the migration index is dependent upon ligand concentration. The MI was calculated from T-lymphocyte tracks from three independent experiments. *$p < 0.05$. J) T-lymphocytes on varying concentrations of VCAM-1 migrate with the same speed at a shear rate of 100 s^{-1} but increases speed on higher concentrations of VCAM-1 at a shear rate of 800 s^{-1}. Migrations speeds were calculated from three independent experiments each. *$p < 0.05$.

Directional migration of T-lymphocytes under fluid flow can be controlled through combinations of ICAM-1 and VCAM-1 under shear flow

Under homeostatic conditions, endothelial cells express basal levels of ICAM-1 and VCAM-1, and upon activation by inflammatory stimuli, expression of these molecules is upregulated to facilitate increased cell arrest and migration [43]. It has also been shown on murine endothelial cells that baseline expression levels of ICAM-1 are greater than VCAM-1, and upon stimulation via known inflammatory stimuli, upregulation of these adhesive ligands varies depending upon the tissue [44]. This motivated us to create surfaces that present both ICAM-1 and VCAM-1 together at various densities to elucidate how simultaneous ligation of LFA-1 and VLA-4 controls migration under fluid flow. Upon presentation of both adhesion molecules, we expected to observe motility that was intermediate between the behaviors of each ligand alone. Because VCAM-1 engagement can regulate β_2-dependent adhesion on ICAM-1 surfaces, crosstalk between the two signaling pathways downstream of receptor engagement presents an additional layer of complexity in the regulation of T-lymphocyte motility [5, 19, 20, 45]. T-lymphocytes were plated on surfaces where the ratio of ICAM-1 and VCAM-1 was varied by changing the ratios of ICAM-1 and VCAM-1 within solution while maintaining a constant total protein concentration of 10 μg/ml. For example, by mixing 3 μg/ml of ICAM-1 and 7 μg/ml of VCAM-1, equaling to a total protein concentration of 10 μg/ml, a surface called $I_3 + V_7$ was created; this surface was 30% ICAM-1 and 70% VCAM-1. On all surfaces, we measured the direction of migration either upstream or downstream as a function of the ratios of ICAM-1 and VCAM-1 present on the surface (Fig. 4.6). At a shear rate of 100 s^{-1}, we observed directional responses that were dependent upon the concentrations of both

ligands with preferred upstream migration on surfaces with higher concentrations of ICAM-1 and preferred downstream migration on surfaces with higher concentrations of VCAM-1. This behavior is consistent with the hypothesis that the phenotype of adhesion is consistent with the concentration of ligand. The magnitude of the migration index for each condition on combined surfaces is less than what is observed for each ligand individually, again consistent with an intermediate response. Upon exposure to 800 s^{-1}, the presence of any ICAM-1 oriented the motion of cells upstream even when large amounts of VCAM-1 were present. At this shear rate, only surfaces made purely of VCAM-1 (V_{10}) favored downstream migration.

On the other hand, upon application of 800 s^{-1} of fluid flow, we observe only upstream migration if any ICAM-1 is present, independent of the concentration of VCAM-1 present on the surface. It is known that adhesion strengthening occurs upon plating human T-lymphocytes on co-immbolized ICAM-1 and VCAM-1 surfaces [19]. Together, these observations lead us to believe that under conditions of high shear, T-lymphocytes utilize LFA-1-ICAM-1 engagements over VLA-4-VCAM-1 engagements to resist detachment due to shear stress. These interactions stabilize adhesions supporting upstream migration when presented with both adhesion ligands. This shear resistance is hypothesized to occur as a result of outside-in integrin signaling triggered upon application of shear stress across the body of the cell that is translated into applied tension across the ligated integrin bonds thus increasing integrin activation.

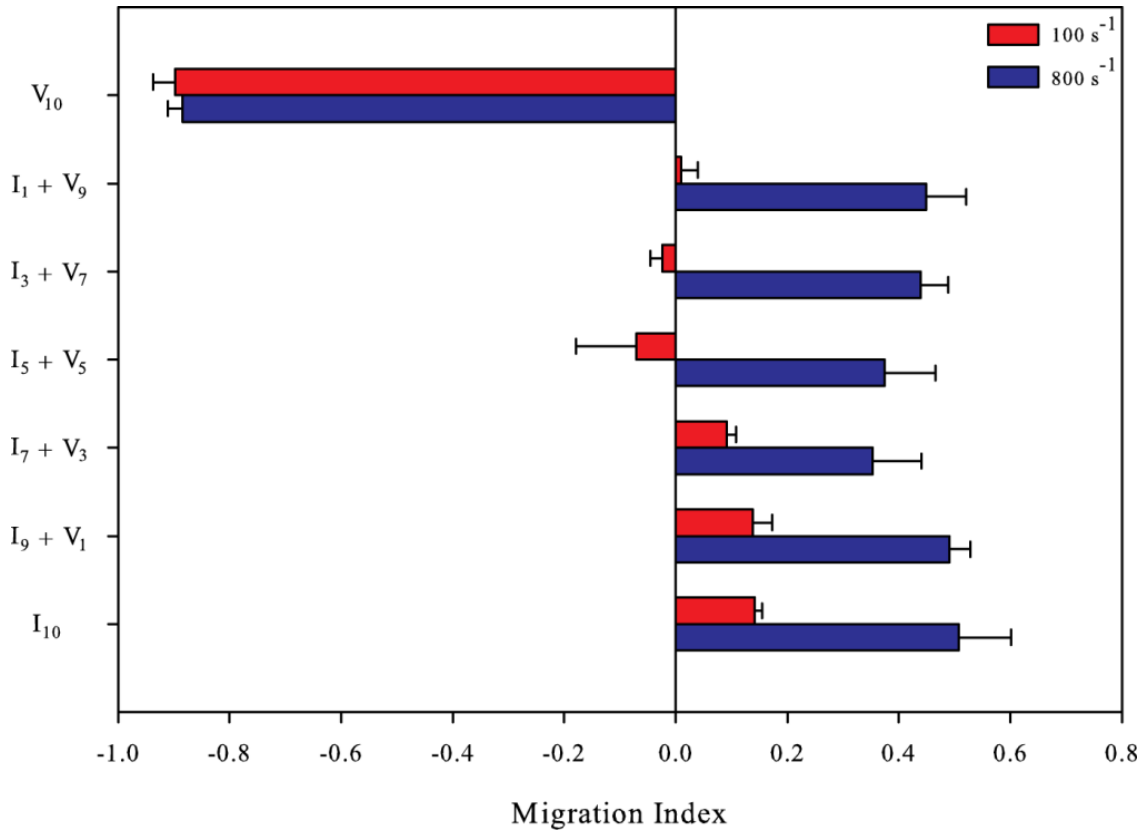

Figure 4.6. T-lymphocytes elicit different responses on surfaces made with both immobilized ICAM-1 + VCAM-1 that are dependent upon shear rate. (Abbreviations: I - ICAM-1; V - VCAM-1; 10 - 10 μg/ml; 7 - 7 μg/ml; 5 - 5 μg/ml; 3 - 3 μg/ml; 1 – 1 μg/ml) The direction of T-lymphocytes under shear flow expressed as the migration index (MI) under 100 s^{-1} (red bars) and 800 s^{-1} (blue bars). The total protein concentration was fixed at 10 μg/ml and the ratios of ICAM-1 to VCAM-1 were varied. Directional migration is dictated by ligand concentration at a shear rate of 100 s^{-1}, with a substantial amount of ICAM-1 necessary for upstream migration. However, the presence of any ICAM-1 supports upstream migration at a shear rate of 800 s^{-1}. The MI was calculated from T-lymphocyte tracks from three independent experiments.

T-lymphocyte resistance to shear flow is mediated through LFA-1-ICAM-1 interactions

Antibodies were used to block either the β_2 or β_1 integrin subunits and cells were plated on surfaces of 5 μg/ml ICAM-1, 5 μg/ml VCAM-1, and 2.5 μg/ml ICAM-1 + 2.5 μg/ml VCAM-1. Upon blocking against the β_2 integrin subunit on surfaces comprised of ICAM-1 alone, no cell adhesion was observed under flow meaning that the MI could not be calculated (Fig. 4.7A). The same was observed on surfaces made from VCAM-1 surfaces when the β_1 integrin subunit was blocked. When T-lymphocytes were blocked against the β_2 integrin and exposed to a surface of combined ICAM-1 and VCAM-1 ligand, we observed downstream migration of cells with fluid flow mimicking the behavior of cells on surfaces of VCAM-1 alone. Conversely, upon blocking against the β_1 integrin, the MI was positive, indicating upstream migration - a result that was similar to what was observed on surfaces containing ICAM-1 alone. These results show that the motility observed on ICAM-1 and VCAM-1 surfaces under fluid flow are due to the specific interactions of the ligand-integrin pairs.

Next, we qualitatively assessed the adhesion strength of T-lymphocytes to printed surfaces of ICAM-1, VCAM-1, or ICAM-1 + VCAM-1, deduced by exposing cells to increasing shear rates which were increased every 5 minutes for a period of 40 minutes. Cells were initially injected and allowed to adhere under static conditions for 15 minutes on surfaces of 5 μg/ml of ICAM-1, VCAM-1, or a combined surface of the two before exposure to shear. Fluid flow was then increased incrementally from 100 s^{-1} to 2000 s^{-1} and the number of cells that remained bound from those that originally settled on the surface was determined. Upon initial application of fluid flow at a shear rate of 100 s^{-1},

approximately 20 – 30% of the cells were detached, presumably due to little or no adhesion to any of the three ligand conditions (Fig. 4.7B). For cells on ICAM-1, increasing the shear rate further did not decrease the number of remaining bound cells significantly (76 versus 73%). However, for cells on VCAM-1 surfaces, the number of bound cells significantly decreased as a function increasing shear rate from 68% to 41% bound. For surfaces on which both ICAM-1 and VCAM-1 were combined, there was no significant decrease in number of cells bound with increasing shear rates, similar to what was found on ICAM-1 surfaces.

Flow cytometry revealed that there are larger quantities of the β_2 integrin than β_1 present on the cell surface; by having more LFA-1 available to bind, smaller quantities of ICAM-1 may be capable of supporting upstream motion on the combined surfaces even in the presence of much larger quantities of VCAM-1. Also, if there is a larger number of activated LFA-1 versus VLA-4, this could explain why we observe more upstream motion on combined surfaces of the two ligands especially at high shear rates. This further supports our previous hypothesis that LFA-1 is supporting the majority of the traction allowing the cell to resist shear flow and migrate upstream. If there are more activated LFA-1 molecules than VLA-4 present on the surface, then greater traction can be produced. Through a shear flow cell detachment assay we demonstrated that cells on surfaces of ICAM-1 or combined ICAM-1 and VCAM-1 have greater resistance to shear stress than on surfaces of VCAM-1 alone. This further supports our claim that LFA-1-ICAM-1-mediated interactions are necessary for robust upstream migration and dominate under high shear on surfaces that present both adhesive ligands. This may also explain why T lymphocytes migrate more on ICAM-1 than VCAM-1 as seen in Chapter 3; if there is more

β_2 than β_1 integrin, then possibly more motility can be supported on ICAM-1 surfaces than compared to VCAM-1 given that there is more receptor to bind its cognate ligand.

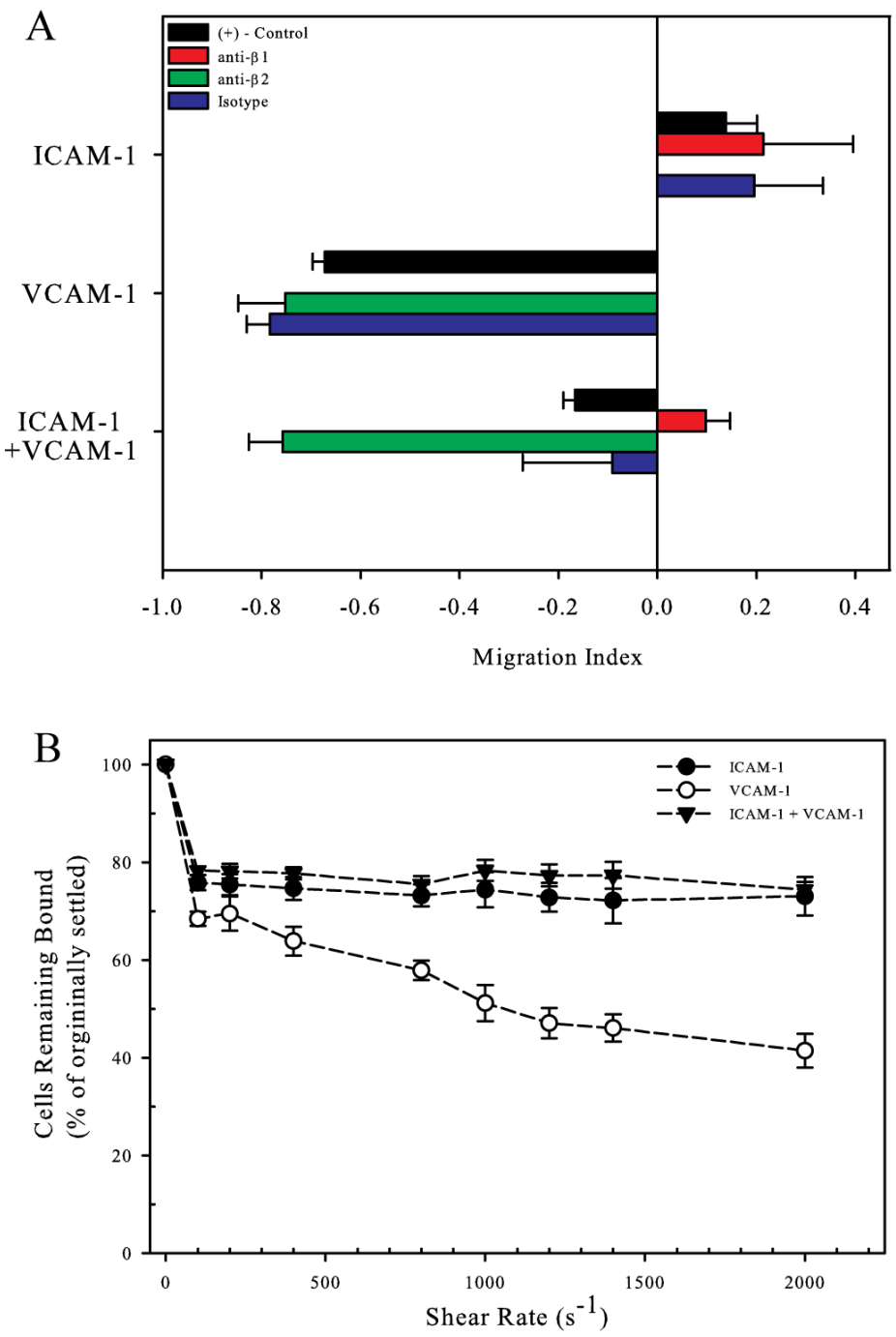

Figure 4.7. T-lymphocytes resist shear detachment through the β_2 integrin. A) T-lymphocytes pretreated with blocking antibodies against the β_1 (red bar) or β_2 (green bar) integrin subunits and were exposed to ICAM-1, VCAM-1, or ICAM-1 + VCAM-1 surfaces under 100 s^{-1} of fluid flow and the MI was determined. Data are mean ±SE B) T-lymphocytes were exposed to increasing shear rates and the percent of cells remaining bound after 5 minutes of exposure was calculated. Shear rate was increased every 5 minutes starting at 100 s^{-1} and ending at 2000 s^{-1}.

Migration on ICAM-1 or VCAM-1 is robust and reversible but not on combined ligand surfaces

We investigated whether the directional responses of T-lymphocytes on ICAM-1, VCAM-1, and ICAM-1 + VCAM-1 surfaces under high shear rates were reversible. We allowed cells to migrate in periodic square waves of shear rate, alternating between no flow and a shear rate of 800 s^{-1}, in increments of 10 minutes for a total time of 90 minutes. This technique is similar to that employed recently by Valignat *et al* [10]. At shear rates of 800 s^{-1}, cells on ICAM-1 migrate upstream (MI ~ 0.4) while cells on VCAM-1 migrate downstream (MI ~ -0.6) (Fig. 4.8A). Furthermore, upon application of alternating periods of no flow and shear rates of 800 s^{-1}, the direction of migration is reversible with a return to a MI to nearly zero (random migration) demonstrating no memory of being exposed to shear flow. However, for cells on the combined ligand surface ($I_5 + V_5$), this behavior was not reversible; the MI remained positive during all periods of flow and even when the flow was removed. The exception was the absence of flow in the initial 10 minutes (Fig. 4.8A), when the cell had not been previously exposed to flow. During these periods of alternating shear flow, we found no change in cell speed in the presence or absence of flow (Fig. 4.8B). However, the average cell speeds on ICAM-1 alone during the time course of the experiment were always greater than those observed on VCAM-1 alone. Furthermore, cell speeds on surfaces with the combination of VCAM-1 and ICAM-1 remained between the speeds observed for ICAM-1 and VCAM-1 independently.

T-lymphocyte upstream migration on ICAM-1 surfaces has been previously shown to be robust and reversible with cells migrating upstream upon application of flow and returning to random motion once it is removed [10]. We showed that motility is reversible

on surfaces of VCAM-1 with downstream migration seen under fluid flow and random migration upon removal. On surfaces with ICAM-1 and VCAM-1 together, the directionality of motility is not reversible with T-lymphocytes maintaining upstream motion during periods of no flow. This suggests upstream motion is driven by signaling, not physical effects such as forces from shear stresses. This implies that memory occurs upon the removal of flow and this memory of signaling requires simultaneous ligation of both LFA-1 and VLA-4 since it is not observed upon ligation of each integrin receptor individually. An interesting question to ask is how long does this directional persistence last in the absence of flow and if it is dependent upon how long the cells are exposed to flow itself before its removal. By exposing cells to flow for longer periods of time (greater than our tested time interval of 10 minutes), we could determine how long this persistence of migration upstream occurs upon removal of fluid flow.

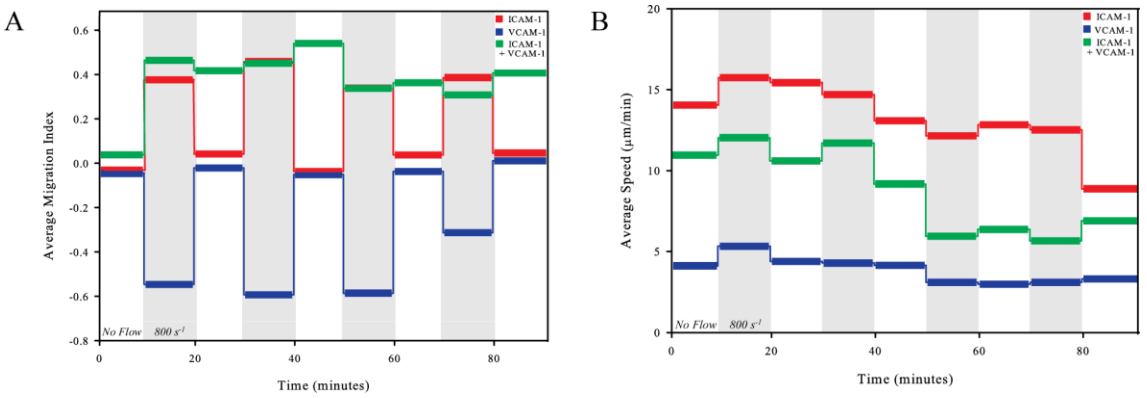

Figure 4.8. T-lymphocytes exhibit reversible directional responses to periodic shear flow on ICAM-1 and VCAM-1 but not on combined surfaces. A) and B) T-lymphocytes were exposed to periodic square waves of duration of 10 min and between shear rates of 0 s^{-1} and 800 s^{-1} (shaded region) on 5 μg/ml ICAM-1, 5 μg/ml VCAM-1, and 2.5 μg/ml each of both ICAM-1 and VCAM-1. The average MI and average speed over the 10 minute time interval were measured.

Shear flow leads to rearrangement of the T-lymphocyte cytoskeleton

To further investigate the mechanisms of motility of T-lymphocytes, we exposed cells to shear flow on surfaces of 5 μg/ml of ICAM-1, VCAM-1, or combinations of the two followed by cell fixation, permeabilization, and fluorescent labeling of the actin and microtubule cytoskeletons. It has been previously shown that T-lymphocytes polarize on ICAM-1 and VCAM-1 surfaces alone in the absence of chemokine with an actin-rich lamellipod and an uropod containing the microtubule organizing center (MTOC) [26]. In the absence of flow for all three substrates, we observe distinct cytoskeletal polarity with actin predominantly located in the lamellipod and microtubules originating from the (MTOC) behind the nucleus (Fig. 4.9A a-c, 4.9B a-c, 4.9C a-c). Upon the introduction of shear flow, we observe loss of cytoskeletal polarity with increasing co-localization of actin and tubulin on all three substrates; at both 100 s^{-1} and 800 s^{-1} shear rates, we observe this rearrangement of cytoskeletal proteins (Fig. 4.9A d-i, 4.9B d-i, 4.9C d-i).

It has been speculated that shear stress may trigger signals or changes within the cytoskeletal machinery in T-lymphocytes. T-lymphocyte polarity and motility is highly dependent upon the arrangement of the actin and microtubule cytoskeletons through signaling pathways involving the Rho family GTPases [46-48]. Upon fluorescent labeling of the cytoskeletal proteins after exposing cells to shear flow, we observed increased co-localization of these cytoskeletal proteins, and the absence of a clearly defined lamellipod. We hypothesize that this increased co-localization of actin and tubulin occurs in order to withstand extracellular forces required to resist deformation caused by the shear stress. The cellular cytoskeleton is known to be involved with several signaling pathways thus possibly providing the signals required for adaptation to a new mechanical environment

[49]. This has been well established in other cells types, such as endothelial cells, which are capable of rearranging their cytoskeletons in response to fluid shear forces [50, 51].

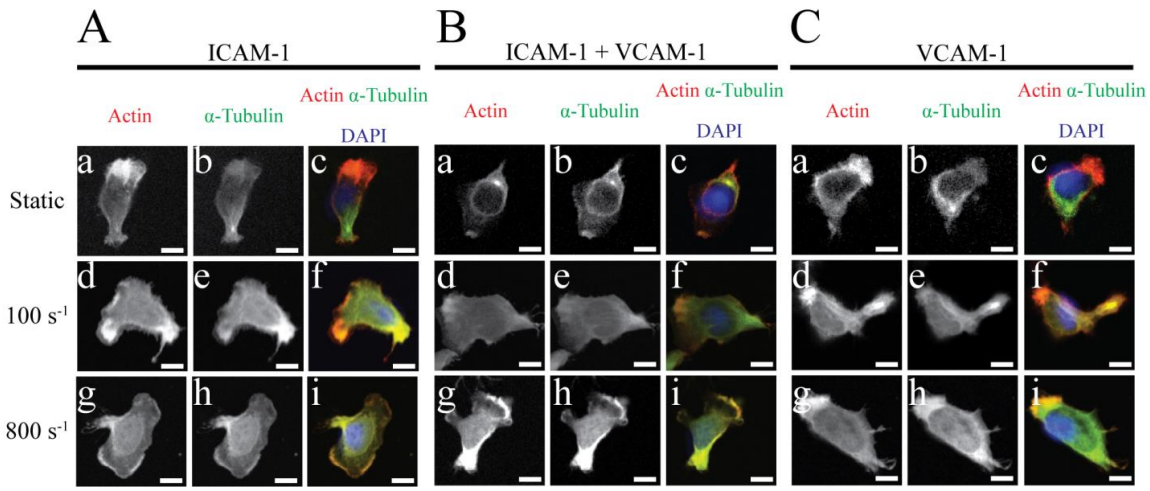

Figure 4.9. T-lymphocytes undergo cytoskeletal rearrangement upon application of shear flow during migration. A) Fluorescent images of migrating T-lymphocytes on 5 μg/ml ICAM-1 under static (a-c), 100 s^{-1} (d-f), and 800 s^{-1} (g-i) shear rates. B) Fluorescent images of migrating T-lymphocytes on 2.5 μg/ml ICAM-1 and 2.5 μg/ml VCAM-1 under static (a-c), 100 s^{-1} (d-f), and 800 s^{-1} (g-i) shear rates. C) Fluorescent images of migrating T-lymphocytes on 5 μg/ml VCAM-1 under static (a-c), 100 s^{-1} (d-f), and 800 s^{-1} (g-i) shear rates. The direction of flow is from right to left. Scale bar = 5 μm.

CONCLUSIONS

In this chapter, we measured the motility of human T-lymphocytes on surfaces comprised of ICAM-1, VCAM-1, or combinations of the two under varying shear rates. Confirming previous studies, we observed upstream migration against fluid flow on ICAM-1 surfaces. We further investigated the effects of varying ligand concentrations and shear rates not only on ICAM-1 surfaces but also VCAM-1, as well as combinations of the two at various densities. For cells on ICAM-1, upstream migration is not dependent upon ligand concentration but rather shear rate, with increasing shear rates resulting in an increase in the preferred upstream migration. Contrary to the findings by Valignat et al., we found that migration speed decreases with increasing shear rate likely contributed to the increased strengthening of LFA-1-ICAM-1 interactions as a result of fluid flow [10]. Steiner et al. also showed that T-lymphocytes do not crawl on VCAM-1 surfaces but rather undergo recurrent arrest with an absence in cell polarization. We found the opposite - cells polarized and migrated downstream and were found to be dependent upon ligand density and, to a lesser extent, shear rate. We then studied the effects of simultaneous engagement of both LFA-1 and VLA-4 on T-lymphocyte migration under fluid flow. At low shear rates, we observed directed migration either upstream or downstream that is dependent upon the concentration of ICAM-1 and VCAM-1 present demonstrating synergy between engagement of the LFA-1 and VLA-4 integrin receptors. In contrast, exposure to high shear rates caused a switch in motility that favors LFA-1-mediated migration over VLA-4-mediated migration with an overall preference for upstream migration. Through a shear flow detachment assay, we suggest that LFA-1 interactions lead to stronger adhesions thus providing the resistance for T-lymphocytes under fluid shear flow to support robust

upstream migration. Furthermore, we show that the actin and tubulin cytoskeletons undergo rearrangement upon the application of shear flow perhaps in order to increase the cell tension required for migration under shear flow as well as to maintain structural integrity. Together, these data suggests that the modes of T-lymphocyte motility are governed not only by the presence of adhesive ligand but also their presentation and activation in the presence of fluid flow. This provides new insight into the role of integrins in mediating T-lymphocyte motility and understanding the critical role ligand composition can play in controlling the physiological response of T-lymphocytes to shear flow.

REFERENCES

1. Luster, A.D., R. Alon, and U.H. von Andrian, *Immune cell migration in inflammation: present and future therapeutic targets.* Nat Immunol, 2005. **6**(12): p. 1182-90.
2. Alon, R. and M.L. Dustin, *Force as a facilitator of integrin conformational changes during leukocyte arrest on blood vessels and antigen-presenting cells.* Immunity, 2007. **26**(1): p. 17-27.
3. Springer, T.A., *Traffic signals for lymphocyte recirculation and leukocyte emigration: the multistep paradigm.* Cell, 1994. **76**(2): p. 301-14.
4. von Andrian, U.H. and C.R. Mackay, *T-cell Function and Migration: Two Sides of the Same Coin.* N Engl J Med, 2000. **343**(14): p. 1020-34.
5. Rose, D.M., et al., *The Affinity of Integrin α4β1 Governs Lymphocyte Migration.* The Journal of Immunology, 2001. **167**(5): p. 2824-2830.
6. Jones, D.A., et al., *A two-step adhesion cascade for T cell/endothelial cell interactions under flow conditions.* The Journal of Clinical Investigation, 1994. **94**(6): p. 2443-2450.
7. Butcher, E.C. and L.J. Picker, *Lymphocyte homing and homeostasis.* Science, 1996. **272**(5258): p. 60-6.
8. Shulman, Z., et al., *Transendothelial migration of lymphocytes mediated by intraendothelial vesicle stores rather than by extracellular chemokine depots.* Nat Immunol, 2012. **13**(1): p. 67-76.
9. Steiner, O., et al., *Differential Roles for Endothelial ICAM-1, ICAM-2, and VCAM-1 in Shear-Resistant T Cell Arrest, Polarization, and Directed Crawling on Blood–*

Brain Barrier Endothelium. The Journal of Immunology, 2010. **185**(8): p. 4846-4855.

10. Valignat, M.P., et al., *T lymphocytes orient against the direction of fluid flow during LFA-1-mediated migration.* Biophys J, 2013. **104**(2): p. 322-31.
11. Lek, H.S., et al., *The spontaneously adhesive leukocyte function-associated antigen-1 (LFA-1) integrin in effector T cells mediates rapid actin- and calmodulin-dependent adhesion strengthening to ligand under shear flow.* J Biol Chem, 2013. **288**(21): p. 14698-708.
12. Alon, R., et al., *The integrin VLA-4 supports tethering and rolling in flow on VCAM-1.* J Cell Biol, 1995. **128**(6): p. 1243-53.
13. Konstantopoulos, K., et al., *Endothelial P-selectin and VCAM-1 each can function as primary adhesive mechanisms for T cells under conditions of flow.* Journal of Leukocyte Biology, 1997. **61**(2): p. 179-87.
14. Hyun, Y.M., et al., *Activated integrin VLA-4 localizes to the lamellipodia and mediates T cell migration on VCAM-1.* J Immunol, 2009. **183**(1): p. 359-69.
15. Berlin, C., et al., *α4 integrins mediate lymphocyte attachment and rolling under physiologic flow.* Cell, 1995. **80**(3): p. 413-422.
16. Stachowiak, A.N., et al., *Homeostatic lymphoid chemokines synergize with adhesion ligands to trigger T and B lymphocyte chemokinesis.* J Immunol, 2006. **177**(4): p. 2340-8.
17. Shimonaka, M., et al., *Rap1 translates chemokine signals to integrin activation, cell polarization, and motility across vascular endothelium under flow.* J Cell Biol, 2003. **161**(2): p. 417-27.

18. Hyun, Y.-M., C. Lefort, and M. Kim, *Leukocyte integrins and their ligand interactions.* Immunologic Research, 2009. **45**(2-3): p. 195-208.

19. Chan, J.R., S.J. Hyduk, and M.I. Cybulsky, *α4β1 Integrin/VCAM-1 Interaction Activates αLβ2 Integrin-Mediated Adhesion to ICAM-1 in Human T Cells.* The Journal of Immunology, 2000. **164**(2): p. 746-753.

20. May, A.E., et al., *VLA-4 (α4β1) engagement defines a novel activation pathway for β2 integrin–dependent leukocyte adhesion involving the urokinase receptor*. Blood, 2000. **96**(2): p. 506-513.

21. Sigal, A., et al., *The LFA-1 Integrin Supports Rolling Adhesions on ICAM-1 Under Physiological Shear Flow in a Permissive Cellular Environment.* The Journal of Immunology, 2000. **165**(1): p. 442-452.

22. Chan, J.R., S.J. Hyduk, and M.I. Cybulsky, *Chemoattractants Induce a Rapid and Transient Upregulation of Monocyte α4 Integrin Affinity for Vascular Cell Adhesion Molecule 1 Which Mediates Arrest: An Early Step in the Process of Emigration.* The Journal of Experimental Medicine, 2001. **193**(10): p. 1149-1158.

23. Woolf, E., et al., *Lymph node chemokines promote sustained T lymphocyte motility without triggering stable integrin adhesiveness in the absence of shear forces.* Nat Immunol, 2007. **8**(10): p. 1076-85.

24. Granger, D.N. and P. Kubes, *The microcirculation and inflammation: modulation of leukocyte-endothelial cell adhesion.* Journal of Leukocyte Biology, 1994. **55**(5): p. 662-75.

25. Koutsiaris, A.G., et al., *Volume flow and wall shear stress quantification in the human conjunctival capillaries and post-capillary venules in vivo.* Biorheology, 2007. **44**(5): p. 375-386.

26. Dominguez, G.A. and D.A. Hammer, *Effect of adhesion and chemokine presentation on T-lymphocyte haptokinesis.* Integr Biol (Camb), 2014. **6**(9): p. 862-873.

27. Ley, K., et al., *Getting to the site of inflammation: the leukocyte adhesion cascade updated.* Nat Rev Immunol, 2007. **7**(9): p. 678-689.

28. Chen, C., et al., *High Affinity Very Late Antigen-4 Subsets Expressed on T Cells Are Mandatory for Spontaneous Adhesion Strengthening But Not for Rolling on VCAM-1 in Shear Flow.* The Journal of Immunology, 1999. **162**(2): p. 1084-1095.

29. Kinashi, T., *Intracellular signalling controlling integrin activation in lymphocytes.* Nat Rev Immunol, 2005. **5**(7): p. 546-59.

30. Muller, W.A., *Mechanisms of Leukocyte Transendothelial Migration.* Annual Review of Pathology: Mechanisms of Disease, 2011. **6**(1): p. 323-344.

31. Smith, L.A., et al., *Interplay between shear stress and adhesion on neutrophil locomotion.* Biophys J, 2007. **92**(2): p. 632-40.

32. Geiger, B., et al., *Transmembrane crosstalk between the extracellular matrix--cytoskeleton crosstalk.* Nat Rev Mol Cell Biol, 2001. **2**(11): p. 793-805.

33. Ingber, D.E., *Cellular mechanotransduction: putting all the pieces together again.* FASEB J, 2006. **20**(7): p. 811-27.

34. Critchley, D.R., *Cytoskeletal proteins talin and vinculin in integrin-mediated adhesion.* Biochem Soc Trans, 2004. **32**(Pt 5): p. 831-6.

35. Choquet, D., D.P. Felsenfeld, and M.P. Sheetz, *Extracellular matrix rigidity causes strengthening of integrin-cytoskeleton linkages.* Cell, 1997. **88**(1): p. 39-48.

36. Wang, N., J.P. Butler, and D.E. Ingber, *Mechanotransduction across the cell surface and through the cytoskeleton.* Science, 1993. **260**(5111): p. 1124-7.

37. Hirata, H., et al., *Force-dependent vinculin binding to talin in live cells: a crucial step in anchoring the actin cytoskeleton to focal adhesions.* Am J Physiol Cell Physiol, 2014. **306**(6): p. C607-20.

38. Smith, A., et al., *A talin-dependent LFA-1 focal zone is formed by rapidly migrating T lymphocytes.* The Journal of Cell Biology, 2005. **170**(1): p. 141-151.

39. Manevich, E., et al., *Talin 1 and paxillin facilitate distinct steps in rapid VLA-4-mediated adhesion strengthening to vascular cell adhesion molecule 1.* J Biol Chem, 2007. **282**(35): p. 25338-48.

40. Jannat, R.A., M. Dembo, and D.A. Hammer, *Traction forces of neutrophils migrating on compliant substrates.* Biophys J, 2011. **101**(3): p. 575-84.

41. Zhu, J., et al., *Structure of a complete integrin ectodomain in a physiologic resting state and activation and deactivation by applied forces.* Mol Cell, 2008. **32**(6): p. 849-61.

42. Palecek, S.P., Loftus, J.C., Ginsberg, M.H., Lauffenburger, D.A., and A.F. Horwitz, *Integrin-ligand binding properties govern cell migration speed through cell-substratum adhesiveness.* Nature, 1997. **385**(6616): p. 537-540.

43. Pober, J.S. and R.S. Cotran, *Cytokines and endothelial cell biology.* Physiological Reviews, 1990. **70**(2): p. 427-451.

44. Henninger, D.D., et al., *Cytokine-induced VCAM-1 and ICAM-1 expression in different organs of the mouse.* J Immunol, 1997. **158**(4): p. 1825-32.

45. Porter, J.C. and N. Hogg, *Integrin Cross Talk: Activation of Lymphocyte Function-associated Antigen-1 on Human T Cells Alters α4β1- and α5β1-mediated Function.* The Journal of Cell Biology, 1997. **138**(6): p. 1437-1447.

46. Wittmann, T. and C.M. Waterman-Storer, *Cell motility: can Rho GTPases and microtubules point the way?* Journal of Cell Science, 2001. **114**(21): p. 3795-3803.

47. Ridley, A.J., et al., *Cell Migration: Integrating Signals from Front to Back.* Science, 2003. **302**(5651): p. 1704-1709.

48. Krummel, M.F. and I. Macara, *Maintenance and modulation of T cell polarity.* Nat Immunol, 2006. **7**(11): p. 1143-9.

49. Yu, Y., A.A. Smoligovets, and J.T. Groves, *Modulation of T cell signaling by the actin cytoskeleton.* J Cell Sci, 2013. **126**(Pt 5): p. 1049-58.

50. Dewey, C.F., Jr., et al., *The dynamic response of vascular endothelial cells to fluid shear stress.* J Biomech Eng, 1981. **103**(3): p. 177-85.

51. Nerem, R.M., M.J. Levesque, and J.F. Cornhill, *Vascular endothelial morphology as an indicator of the pattern of blood flow.* J Biomech Eng, 1981. **103**(3): p. 172-6.

CHAPTER 5: ADDITIONAL LIGANDS TO STUDY T-LYMPHOCYTE HAPTOKINESIS AND CHEMOKINESIS

ABSTRACT

Homing to and migration within secondary lymphoid organs (SLOs) is not only governed by the adhesive ligands ICAM-1 and VCAM-1 and the CCL19/CCL21/CCR7 chemokine axis. It is known that endothelial cells also express the chemokine CXCL12 on their apical surface that binds to CXCR4 allowing for arrest and migration to extravasate into inflamed tissues or the SLOs. Furthermore, fibronectin is known to be expressed by fibroblastic reticular cells (FRCs) within SLOs and is a common ligand encountered by T lymphocytes as well as other leukocytes. In this chapter we measured the migration of primary human T lymphocytes in response to varying fibronectin concentration (haptokinesis) and CXCL12 concentration (chemokinesis). Through the use of microcontact printing we created uniform surfaces of fibronectin of varying densities. Furthermore, we exposed T lymphocytes to varying concentrations of soluble CXCL12 on ICAM-1 surfaces. In the previous chapters, we demonstrated that exposing cells to varying concentrations of ICAM-1 and VCAM-1 as well as CCL19 and CCL21 elicits biphasic motility. In this chapter, we show that fibronectin elicits a monotonic response in motility that leads to increases speeds and persistence times as ligand concentration increases. Furthermore, CXCL12 elicits biphasic motility only on *low* concentrations of ICAM-1 similar to what is found with CCL19 and CCL21. Overall, motion on fibronectin is lower than what was observed on ICAM-1 surfaces but similar to VCAM-1 further elucidating motility observed within the SLOs.

INTRODUCTION

We have demonstrated in the previous chapters that human primary T lymphocytes are capable of spontaneous adhesion and robust migration on ICAM-1 and VCAM-1 microcontact printed PDMS surfaces. These ligands are known to be crucial for homing and migration to and within the secondary lymphoid organs (SLOs) [1-4]. Here within the organs, T lymphocytes are exposed to adhesive ligands and chemokines that facilitate the interactions between T lymphocytes and dendritic cells [5-8]. This allows for the transfer of information acquired by about foreign antigens by dendritic cells to T lymphocytes to elicit effector functions. With this said, the cell adhesion molecules ICAM-1 and VCAM-1 and the CCR7/CCL19/CCL21 chemokine signaling axis are not the only players involved this process [9-12].

Fibronectin is a ubiquitous protein found both in a soluble plasma form, and in an insoluble form that allows for cell adhesion and migration; both of these forms are from the same gene undergoing alternative splicing patterns [13]. Fibronectin is a common adhesive ligand used to study cell migration and motility. Recent studies have demonstrated that it support robust murine dendritic cell migration and can even elicit a phenotypic switch in primary human neutrophils [14, 15]. We decided to study the motility of human T lymphocytes in response to varying concentrations of fibronectin and compare the findings to the motility observed on ICAM-1 and VCAM-1 substrates. Furthermore, the chemokine CXCL12 binds to the chemokine receptor CXCR4 and is capable of inducing chemotaxis [16, 17]. It is also involved in T lymphocyte homing to SLOs and in numerous autoimmune diseases particularly those involved with the central nervous system (CNS) [12]. We performed chemokinesis studies on ICAM-1 surfaces with varying

concentrations of CXCL12 to determine if it elicits a biphasic response in motility similar to what was observed with CCR7-mediated chemokinesis. This response had been previously observed in dendritic cells [14].

In this chapter, we investigate the effects on primary human T lymphocyte motility by varying fibronectin concentrations (haptokinesis) and CXCL12 concentrations (chemokinesis). We apply standard engineering approaches and the use of microcontact printing to measure cell speed, persistence time, and the random motility coefficient on these extracellular stimuli. Our results show that T lymphocytes elicit a monotonic response in the random motility coefficient on varying fibronectin concentrations. Furthermore, we demonstrate that T lymphocytes respond biphasically to the homeostatic chemokine CXCL12 as function of ICAM-1 concentration similar to what was observed for CCR7-mediated chemokinesis.

MATERIALS AND METHODS

Cell culture and reagents

Human blood was obtained via venipuncture from healthy adult donors and collected into sterile tubes containing sodium heparin (BD Biosciences). Samples were collected with University of Pennsylvania Institutional Review Board approval from consenting adult volunteers. Blood samples were carefully layered in a 1:1 ratio of whole blood to 1-Step™ Polymorphprep (Axis-Shield). Vials were then centrifuged at 1500 rpm for 35 minutes and the mononuclear band was collected into a fresh vial. Cells were cultured in RPMI-1640 supplemented with 10% FBS and 1 μg/ml of phytohemagglutinin (PHA-M; Sigma-Aldrich) overnight. After 24 hours, the lymphocyte suspension in the PHA medium was transferred into a new flask leaving behind adherent cells. After an additional 48 hours, the cells were then cultured in RPMI-1640 with 10% FBS and 1% penicillin-streptomycin supplemented with 20 ng/ml of interleukin-2 (IL-2; Roche). Cells were used for experimentation following an additional 72 hours in culture. Other biological reagents included: protein A/G (Thermo Scientific), human ICAM-1/Fc (R&D Systems), human IgG1 (Abcam), human anti-beta2 (Calbiochem), , human anti-beta1 (BD Pharmingen), human CXCL12 (PreproTech), and Pluronics F127 (Sigma-Aldrich).

Substrate preparation

Poly(dimethylsiloxane) (PDMS) (Dow Corning,) coated coverslips were prepared from number one thickness glass coverslips (Fisher Scientific) of 25 mm diameter spin coated with degassed PDMS (10:1 base:cure by weight) and cured overnight at 65 ºC. PDMS-coated coverslips were affixed to the bottom of six-well tissue culture plates which has been laser-cut to generate a 22 mm diameter opening in the bottom of the wells.

Coverslip bonding was performed using a small amount of PDMS (10:1 base:cure by weight) and baked at 65 ºC for 30 minutes for curing.

Protein printing and blocking

Flat stamps for printing were prepared by pouring degassed PDMS mixed at 10:1 base:cure by weight over an unpatterned silicon wafer. The polymer was cured for 2 hours or longer at 65 ºC. Stamps were trimmed, sonicated in 200 proof ethanol for 10 minutes, rinsed with dH_2O, and dried in a stream of $N_2(g)$. For fibronectin haptokinesis studies, stamps 1 cm^2 were inked with 200 µl of varying concentrations of bovine fibronectin in PBS for 2 hours at room temperature. For CXCL12 chemokinesis studies, stamps 1 cm^2 were inked with 200 µl of 2 µg/ml of protein A/G in PBS for 2 hours at room temperature. The stamps were then thoroughly rinsed in H_2O and blown dry with a stream of N2. In parallel, the six-well PDMS coverslip substrate was treated with ultraviolet ozone for 7 minutes (UVO Cleaner Model 342) to render the surface hydrophilic. The stamps were then placed in conformal contact with the substrate for ~10 seconds and removed. A 0.2% (w/v) solution of Pluronics F127 was immediately adsorbed to the PDMS substrates for 30 minutes at room temperature to prevent protein adsorption to non-functionalized portions of the PDMS. The cell culture substrate was then rinsed with PBS 3X without dewetting the functionalized surface and either incubated with cells for fibronectin surfaces or followed by deposition of 200 µl of ICAM-1/Fc in PBS for 2 hours at room temperature. ICAM-1 functionalized surfaces were then rinsed with PBS 3X without dewetting before incubation with cells.

Haptokinesis and chemokinesis assay

PDMS substrates were prepared as described above. For printed CCL21 studies, 20 nM of CCL21 was inked with Protein A/G followed by stamping onto PDMS substrates. Before use, all substrates were washed 3X with phosphate-buffered saline. Each well was plated at 5 x 10^5 cells/ml in serum-free RPMI-1640 supplemented with 0.1% BSA and 2 mg/ml glucose. The substrate was then placed in a 37°C humidified atmosphere containing 5% CO_2 in air incubator for 15 minutes to allow for cell attachment. The wells were then gently washed 3X with PBS to remove non-adherent cells followed by imaging in a 5% CO_2 and 37°C environment for at least 1 hour. Cells were placed into a motorized stage and observed using a Nikon Eclipse TE_{300} phase contrast microscope. A 10X objective and 10X eyepiece were used for a final magnification of 100X. For chemokinesis assays, a CCL19 and/or CCL21 chemokine solution was dispensed into each well before imaging and performed on ICAM-1 substrates at a concentration of 0.05 µg/ml. For surface presentation of CCL21, stamps were inked with 2 µg/ml of Protein A/G and 250 ng/ml of CCL21 and printed onto the PDMS substrates before blocking and application of the Fc protein solution.

Measurement of cell trajectories and mean-squared displacements

Cell movement was tracked using the ImageJ plugin Manual Tracking. ImageJ and the plugin are both freely available through the NIH website (http://rsbweb.nih.gov/ij/). The centroid of the cell was considered to represent the cell position. Time lapse microscopy was used and images were taken every 1.5 minutes. The result was a series of (x,y) positions with time for each cell. The net displacement during the ith 1.5 minute increment, D_i, was calculated by the difference of the position at the beginning and end of

that time step. The mean-squared displacement, $\langle D^2(t)\rangle$, over time was calculated using the method of non-overlapping intervals [18]. Speed, S, can be considered as the total path length over time and persistence time, P, is the time a cell remains moving without changing direction. S and P were obtained by fitting these to the persistent random walk equation (Dunn, 1983 $\langle D^2(t)\rangle = 2S^2\left[t - P\left(1 - e^{-t/P}\right)\right]$ where *t* is the time interval, using a non-linear least squares regression analysis [19, 20]. The mean-free path length (P_L) and random motility coefficient (μ) are then calculated as $P_L = PS$ and $\mu = \frac{1}{2}S^2P$ [21, 22].

Antibody Blocking

Functional blocking antibodies against the β_1 integrin subunit (clone Mab13), β_2 integrin subunit (clone IB4), α_L integrin subunit (clone 38), and IgG_2a isotype control (clone R35-95) were used at a final concentration of 50 μg/ml. 5 x 10^5 T-lymphocytes in 500 μl of running buffer were incubated for 30 minutes with the blocking antibodies at 37ºC and 5% CO_2. Cells were then plated and allowed to adhere for 15 minutes followed by rinsing with PBS 3X and subsequent imaging in media containing blocking antibody.

RESULTS AND DISCUSSION

Microcontact printing of fibronectin and T lymphocyte adhesion

Fibronectin is a common molecule that has been printed on PDMS surfaces to support adhesion and motility of various cell types [15, 23, 24]. We use microcontact printing to prepare surfaces of fibronectin of known concentrations as determined by initial inking concentrations. The steps for microcontact printing for our experimental system are illustrated in Figure 5.1A. Alexa Fluor-488 conjugated fibronectin was stamped onto a PDMS surface to demonstrate precision of the method (Fig. 5.1B).

A

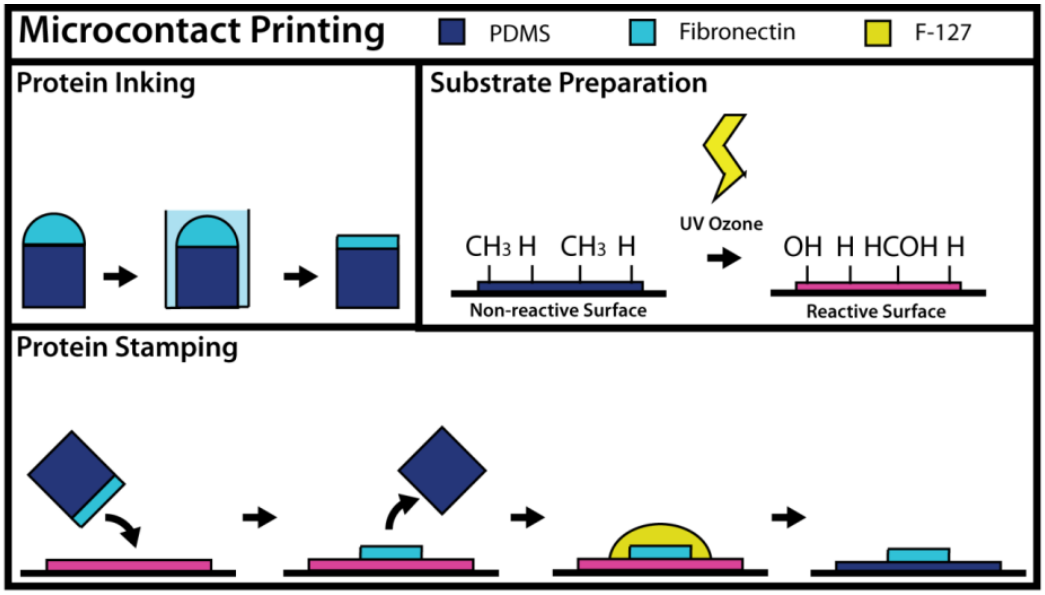

B

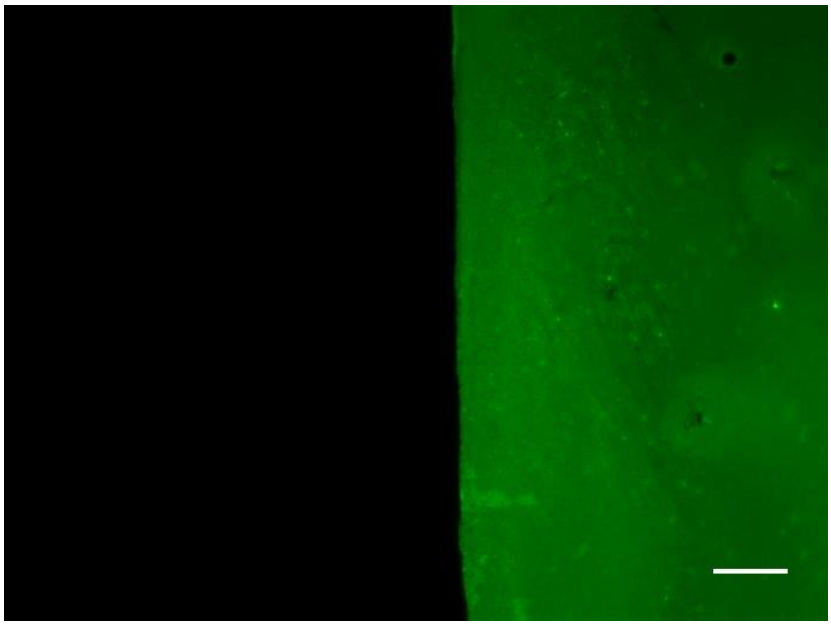

Figure 5.1. µCP fibronectin on PDMS substrates. (A) Illustration for printing fibronectin onto PDMS surfaces. (B) Alexa Fluor-488 conjugated fibronectin stamped onto a PDMS surfaces. Scale bar = 50 µm (Image courtesy of Laurel Hind).

Integrins containing the β_1 subunit are known to bind to fibronectin surfaces supporting adhesion and migration; we verified this through functional integrin blocking and quantifying adhesion (Fig. 5.2A). Blocking of the β_1 integrin chain resulted in a significant decrease in cell adhesion on fibronectin relative to the positive control without antibody present ($p < 0.01$) (Fig. 5.2B). These data led us to attribute the observed adhesion and resulting motility to the specific ligation of β_1 containing integrins binding to the fibronectin printed surfaces.

Fibronectin alone triggers T lymphocyte haptokinesis

Primary human T lymphocytes adhere and migrate on PDMS surfaces printed with fibronectin. We measured haptokinesis on fibronectin by quantifying the mean-squared displacements over a range of ligand concentration in the absence of chemokine. From the mean-squared displacements over time, we could determine the speed, persistence time, and random motility coefficient for each ligand concentration. T lymphocytes plated on fibronectin surfaces were tracked for 30 minutes. As illustrated by representative single-cell migration tracks (Fig. 5.3), T lymphocytes migrated substantial distances on both 0.5 and 5.0 μg/ml of fibronectin with no preferred direction. This remained true for all other concentrations of ligand tested.

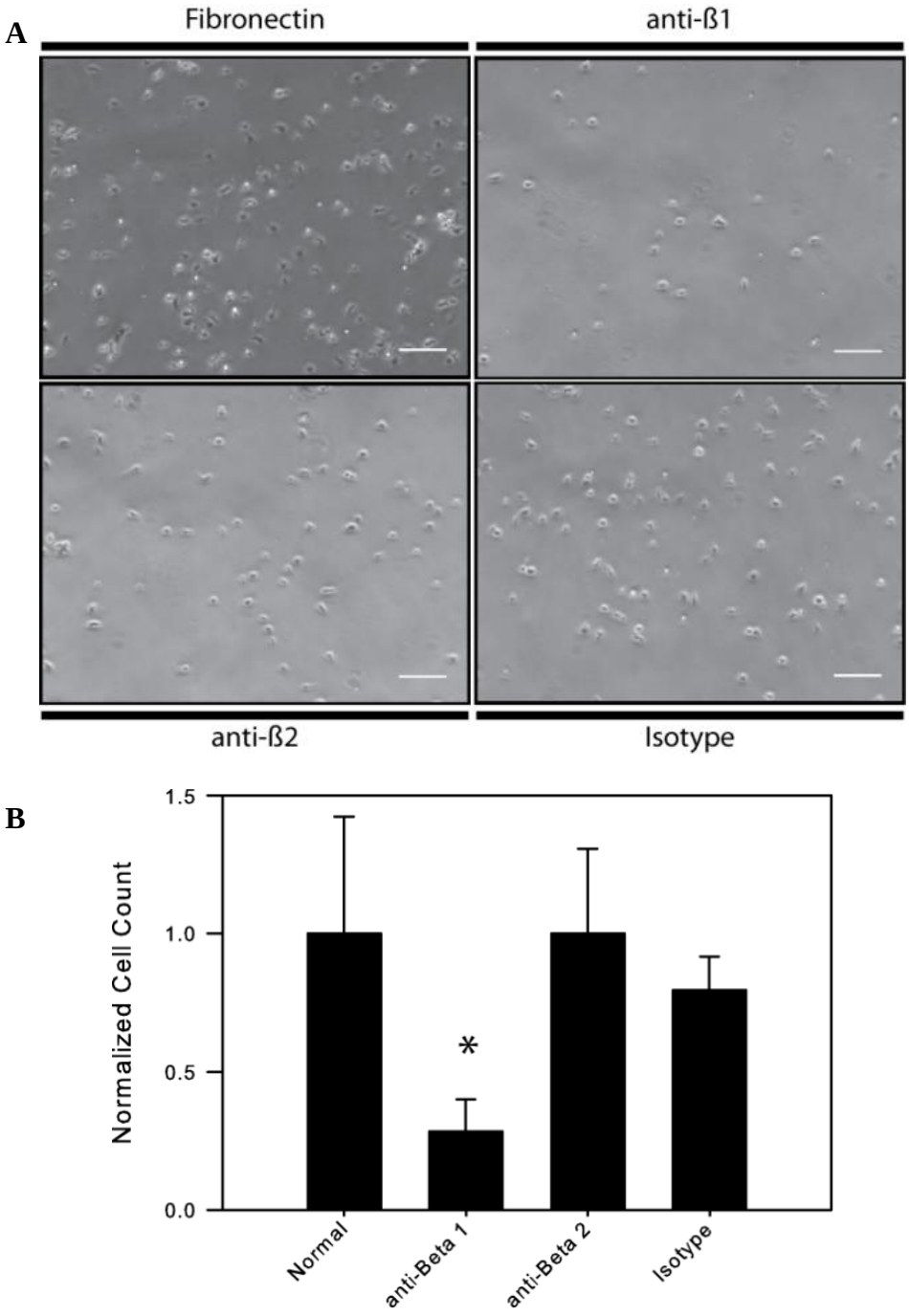

Figure 5.2. Antibody blocking against β_1 reveals discrete integrin/ligand interactions on printed fibronectin surfaces. (A) Phase contrast images of T lymphocytes blocked against $\beta_1$or β_2 integrins on fibronectin surfaces. (B) Quantification of antibody blocking against β_1 and β_2 integrins show decreased cell adhesion to fibronectin substrates; *$p < 0.05$, compared to isotype; one-sample t test.

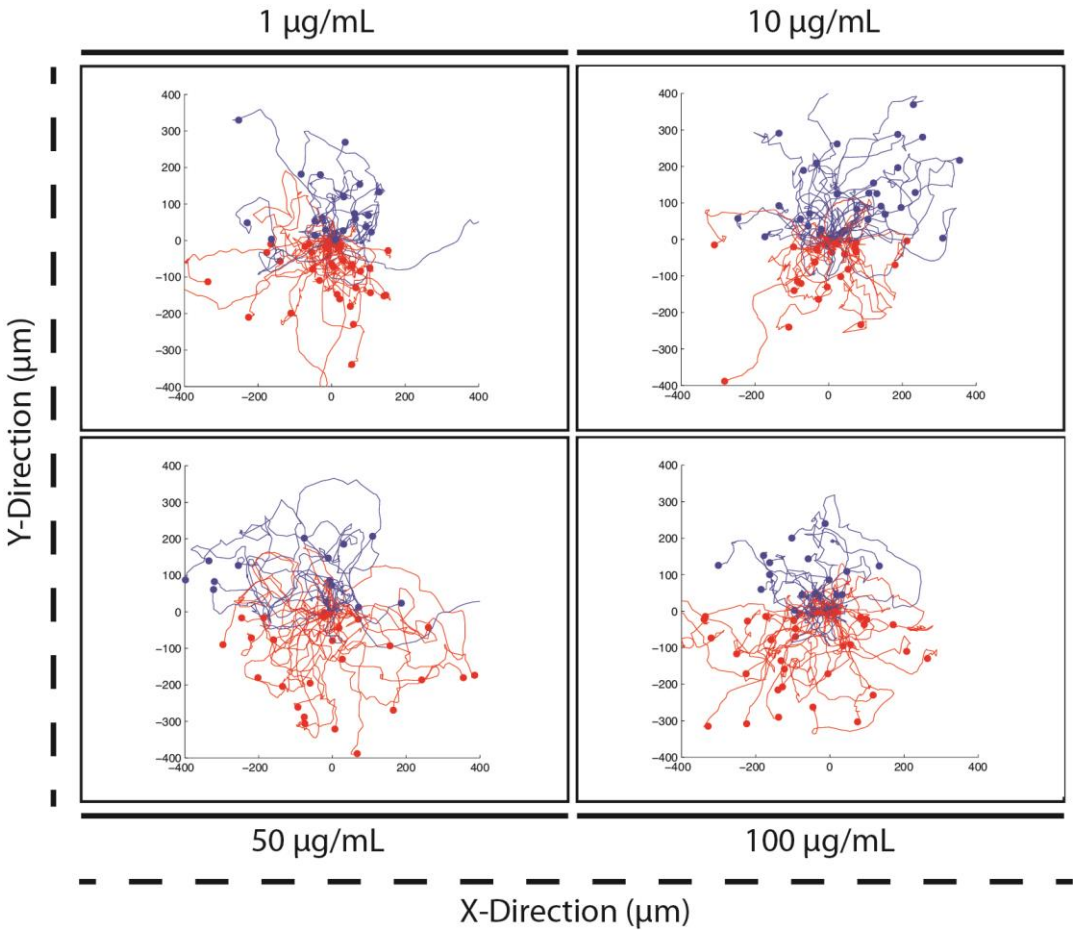

Figure 5.3. T lymphocyte cell traces on fibronectin surfaces. Representative single-cell migration tracks for T lymphocytes on 1.0, 10.0, 50.0, and 100.0 µg/ml of fibronectin showing no preferred direction in migration (haptokinesis).

Using the mean-squared displacements (MSD), we found that migrating T lymphocytes on fibronectin surfaces migrated substantial distances as observed by the linear increase of the mean-squared displacement over time (Fig. 5.4, A and B). As with LFA-1- and VLA-4-mediated motility, the use of random walk theories is common to quantify this migration. The MSDs of migration can be scaled as $x^2(t) \propto t^{\alpha}$ during $0 < t <$ 30 minutes where fitting can be used to determine the exponent α to classify the type of motion for each type and concentration of ligand. Random or Brownian motion is observed for the value of $\alpha = 1$ and ballistic motion is observed for $\alpha = 2$, while values between the two are categorized as superdiffusive motion. Cells migrating on fibronectin surfaces display an average α over all concentrations of 1.40, indicating superdiffusive motility. This value is lower than what was found on ICAM-1 surfaces ($\alpha = 1.57$) but similar to values observed on VCAM-1 surfaces ($\alpha = 1.38$). Table 3.1 shows all values of fitted α's for all concentrations of ligand tested. With this said, this data is consistent with data presented in previous chapters that T lymphocytes do not display pure diffusive motion on ICAM-1 or VCAM-1 printed substrates. Furthermore, recently we have shown that neutrophils migrate superdiffusively with a keratocye-like phenotype on fibronectin printed substrates indicating similarities between possible migration mechanisms for these two types of leukocytes [15].

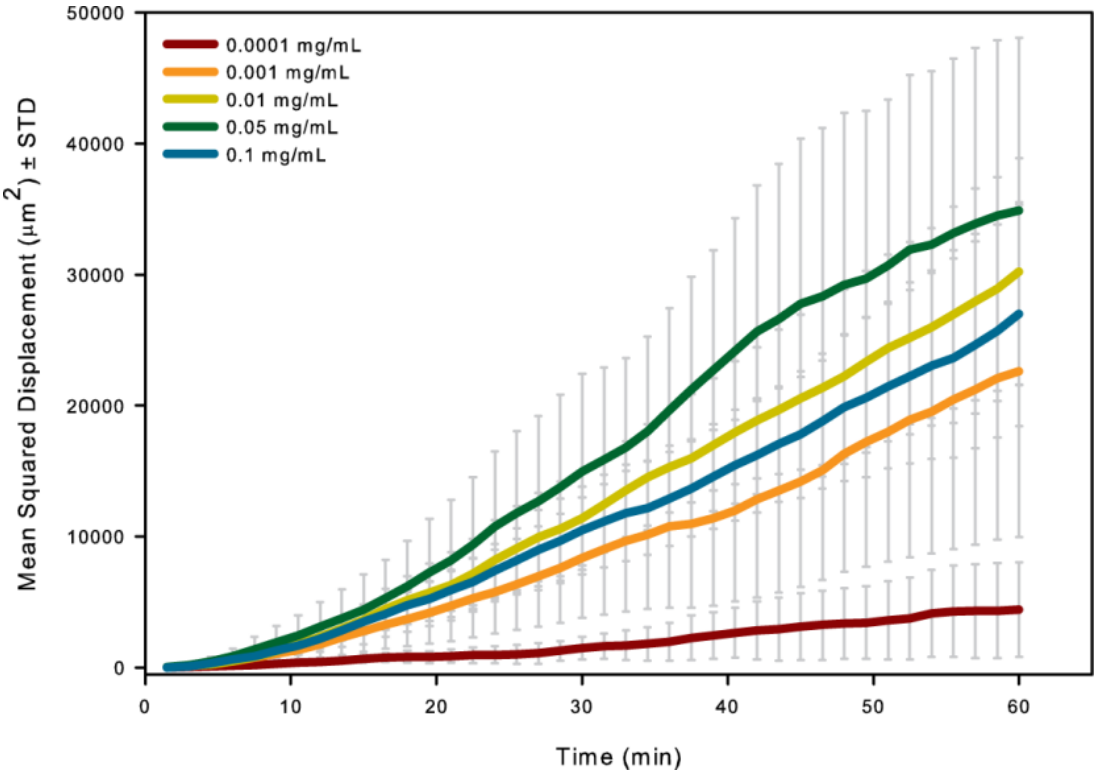

Figure 5.4. Mean-squared displacements versus time of migrating human T-lymphocytes on varying fibronectin concentrations.

Fibronectin (mg/mL)	Average α ± STD
0.00001	0.57 ± 0.17
0.0001	1.32 ± 0.03
0.001	1.42 ± 0.04
0.01	1.40 ± 0.08
0.05	1.40 ± 0.08
0.1	1.45 ± 0.16

Table 5.1. Average fitted α ± standard deviation on fibronectin. Values of fitted α's indicate superdiffusive for almost all concentration conditions on fibronectin surfaces.

By scaling the mean squared displacements to t^{α} and plotting them as slopes over time, we see that all T lymphocyte motility lies between a slope of 1 (pure diffusion motion) and a slope of 2 (pure ballistic motion) lying in the superdiffusive region on all three ligands (Fig. 5.5). We also show that the superdiffusive motility exist in three different regimes for the three ligands. T lymphocytes exhibit more diffusive-like motion on VCAM-1 surfaces compared to ICAM-1 surfaces with cell exhibiting more ballistic-like motion on fibronectin surfaces. This is the first indication, to our knowledge, that T lymphocytes exhibit superdiffusive motion on these ligands.

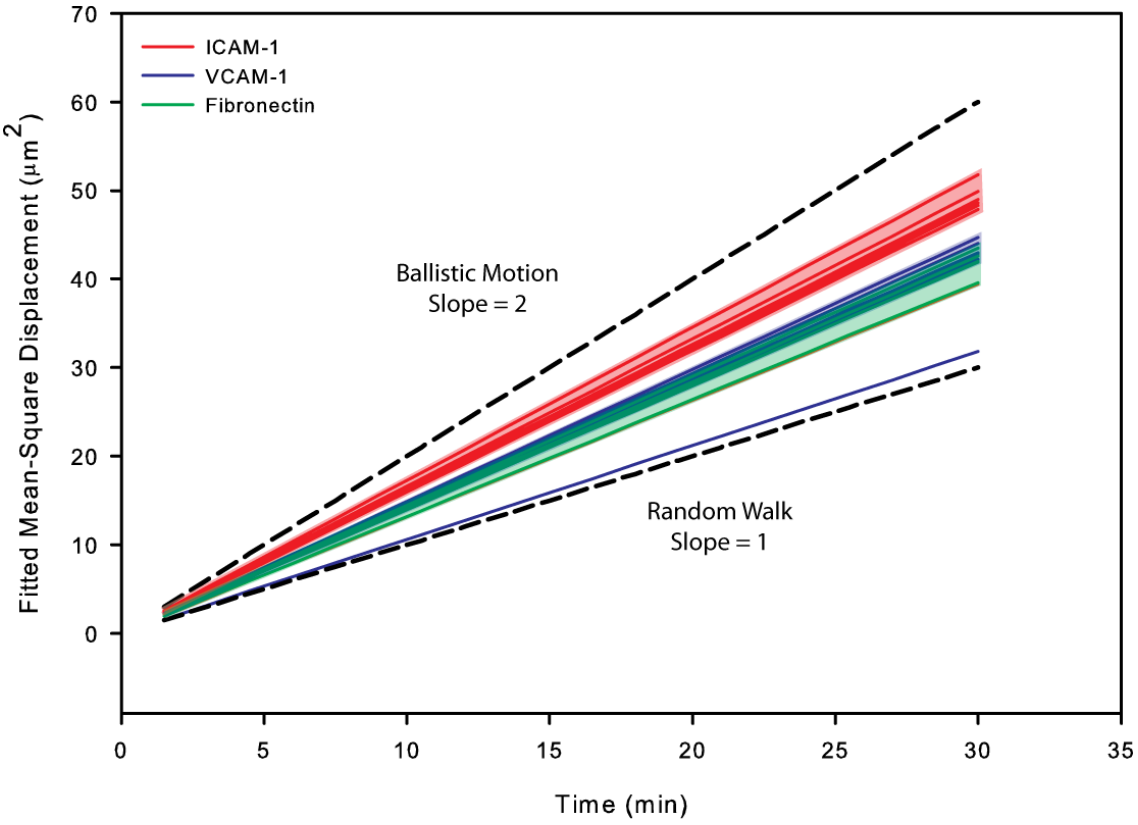

Figure 5.5. Fitted mean-squared displacements versus time on ICAM-1, VCAM-1, and fibronectin surfaces. The slopes of lines indicate the α's determined by scaling the MSD previously to t^{α}. Red lines are values on ICAM-1 surfaces, blue lines are values on VCAM-1, and green lines are on fibronectin surfaces. Slopes of the lines fall between values of 1 (pure diffusive motion) and 2 (pure ballistic motion).

To further characterize the motility of T cells on ICAM-1 and VCAM-1 surfaces, we used the experimental mean-squared displacements of each cell population with the persistent random walk model to fit for speed and persistence time. Migrating T lymphocytes average cell speeds (S) ranging between 1.55 ± 0.69 and 5.5 ± 0.78 μm/min with peak speed reached on 50.0 μg/ml of fibronectin (Fig. 5.6). These speeds were much lower than what was observed on ICAM-1 surfaces but similar to those observed on VCAM-1 (whose integrin contains the β_1 subunit). Persistence times (P) ranged from 1.25 ± 0.9 to 12.0 ± 1.5 minutes; these were much larger values that what was found on the previous two adhesion molecules.

Overall, both responses for speed and persistence time as a function of fibronectin concentration were found to be monotonic. This behavior has been observed previously on fibronectin using murine myoblasts and could be due to differences in bond strength, production of signals required for force generation, or organization of the receptors by the cytoskeleton [25, 26]. Furthermore, it is also known that fibronectin can be engaged through multiple integrin receptors: $\alpha_4\beta_1$ (VLA-4) binds the CS-1 sequence and $\alpha_5\beta_1$ (VLA-5) binds the RGD sequence; both are expressed on T-lymphocytes [27, 28]. Engagement of these receptors may lead to different downstream signaling and/or different binding of adaptor proteins leading to different responses in motility. This sort of behavior has been observed in murine epithelial cells where $\alpha_5\beta_1$ and $\alpha_v\beta_3$ both bind to fibronectin resulting in the same level of adhesion but differ in cellular morphology and motility [29].

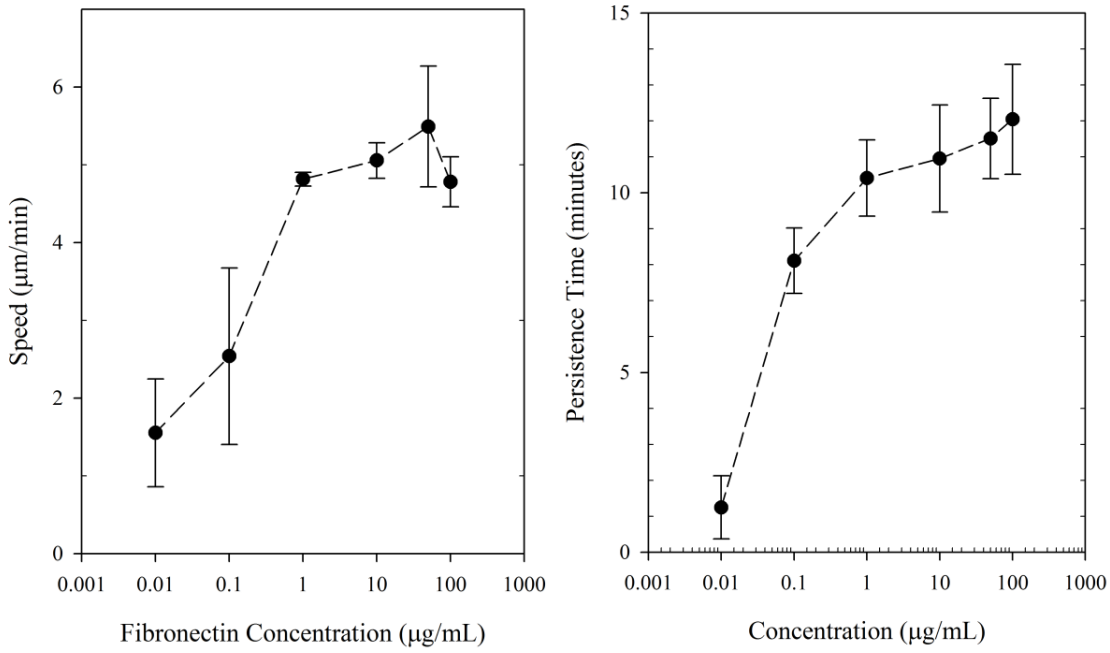

Figure 5.6. T lymphocytes elicit monotonic responses in speed and persistence time on fibronectin surfaces. T lymphocyte (A) speeds and (B) persistence times determined from using the persistent random walk model; cells have faster speeds and longer persistence times as ligand concentration increases.

As with motility on ICAM-1 and VCAM-1 surfaces, we calculated the random motility coefficient (μ). Figure 5.7 demonstrates that the random motility coefficient increases with increasing concentration of fibronectin reaching a maximum value of 141.85 ± 16.45 μm^2/min (μ_{Fibro}) on 10.0 μg/ml.

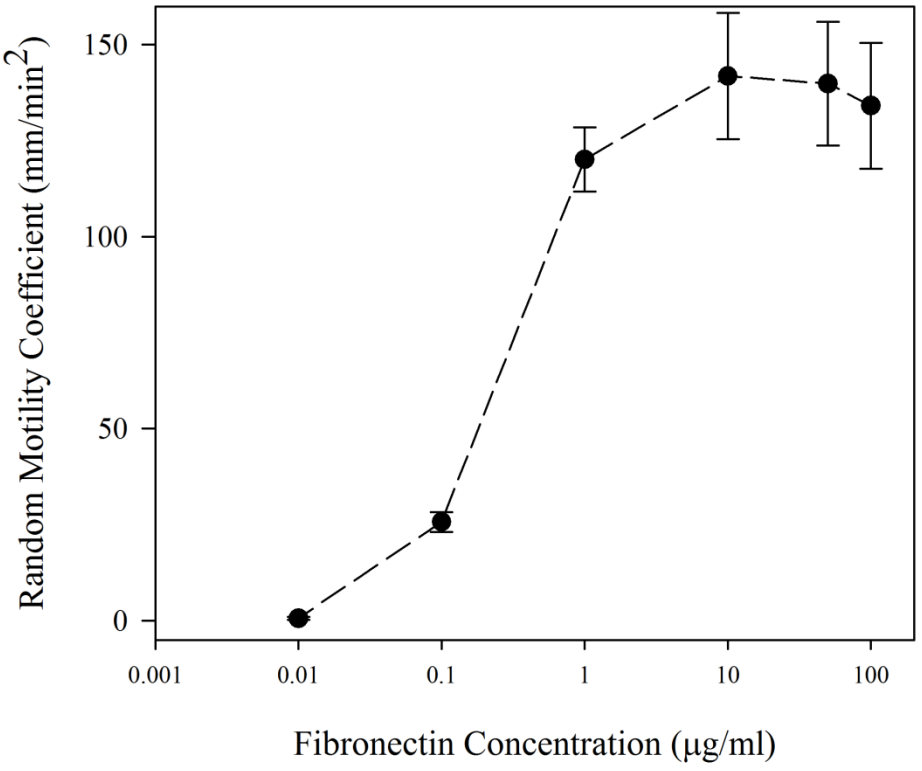

Figure 5.7. Fibronectin elicits a monotonic response in the random motility coefficient on fibronectin surfaces. Comparison of the random motility coefficients (μ) show a monotonic response in motility as a function of ligand concentration (peak μ_{Fibro} = 141.85 ± 16.45 μm^2/min). The error bars represent the standard error of the mean (s.e.m.)

Comparing the values of the random motility coefficient to our previous surfaces of ICAM-1 and VCAM-1, we observe distinct differences (Fig. 5.8). On ICAM-1, the highest random motility coefficient (μ_{ICAM-1}) is 160 μm^2/min, observed over a range of ICAM-1 concentrations between 0.5 to 10.0 μg/ml. T lymphocytes display a maximum μ_{VCAM-1} of 103 ± 16.1 μm^2/min at 0.5 μg/ml VCAM-1. Overall, we generally found that cells exhibit greater motility on ICAM-1 followed by fibronectin and then VCAM-1 ($\mu_{ICAM-1} > \mu_{Fibro} > \mu_{VCAM-1}$).

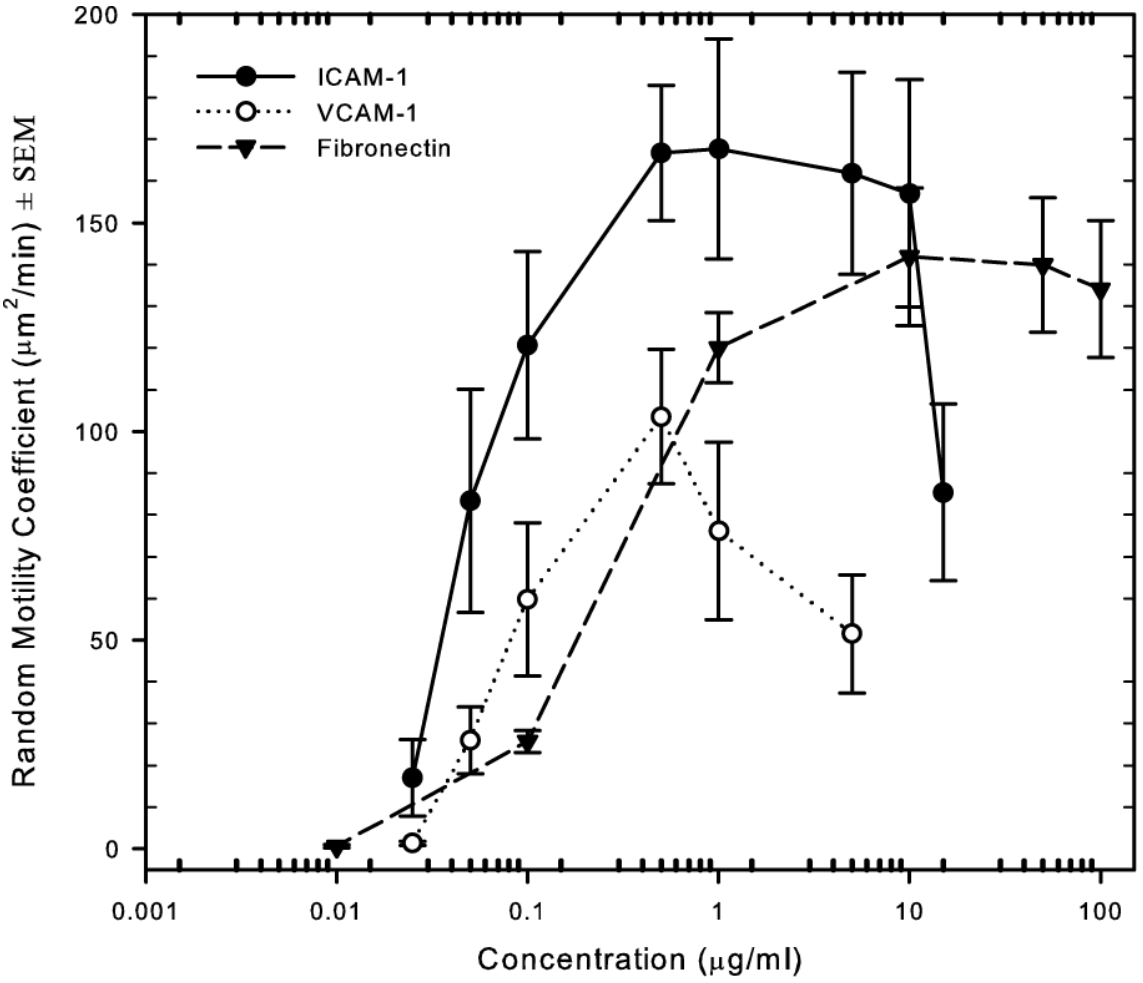

Figure 5.8. The random motility coefficients for all ligand concentrations on ICAM-1, VCAM-1, and fibronectin surfaces. Comparison of the random motility coefficients (μ) show biphasic motility as a function of ligand concentration with ICAM-1 (peak μ_{ICAM-1} = 172.77 ± 45.45 μm^2/min) promoting increased haptokinesis than VCAM-1 (peak μ_{VCAM-1} = 103.58 ± 16.06 μm^2/min) with a monotonic response on fibronectin surfaces (peak μ_{Fibro} = 141.85 ± 16.45 μm^2/min). The error bars represent the standard error of the mean (s.e.m.)

In our system, higher cell speeds were observed on ICAM-1 compared to VCAM-1 and fibronectin ($S_{ICAM-1} > S_{VCAM-1}/S_{Fibro}$) while generally cells were more persistent on fibronectin and VCAM-1 than ICAM-1 ($P_{ICAM-1} < P_{VCAM-1} < P_{Fibro}$). Previous empirical observations have showed that speed and persistence times are inversely correlated across a variety of cells types with high speeds correlating to short persistence times and vice versa [26]. Previously, we plotting the speeds and persistence times across all concentrations of ICAM-1 and VCAM-1 and observed that this inverse correlation holds true for primary human T lymphocytes. On fibronectin surfaces, this inverse correlation does not hold since as speeds increase, persistence times increase as well (Fig. 5.9). Overall, on ICAM-1 surfaces, T- lymphocytes have higher speeds with lower persistence times ($\uparrow S_{ICAM-1}$, $\downarrow P_{ICAM-1}$) and on VCAM-1 surfaces, T lymphocytes have lower speeds with higher persistence times ($\downarrow S_{VCAM-1}$, $\uparrow P_{VCAM-1}$). For cells on fibronectin, you have similar speeds to that on VCAM-1 but with much higher persistence times that trend together ($\downarrow S_{Fibro}$, $\uparrow\uparrow P_{Fibro}$). These data suggests that each ligand stimulates different adhesion signaling pathways through engagement of different integrin adhesion receptors.

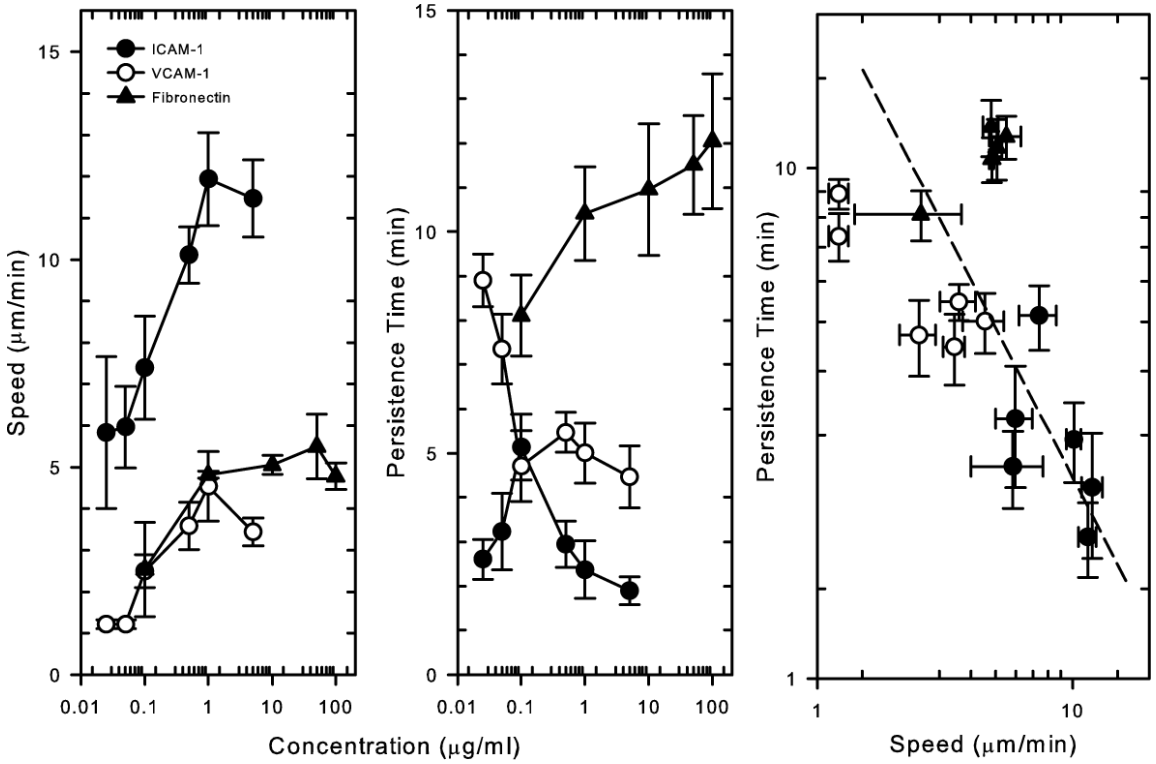

Figure 5.9. T lymphocytes elicit biphasic responses in speed and an inverse correlation with persistence time on ICAM-1 and VCAM-1 but not on fibronectin. T lymphocyte (A) speeds and (B) persistence times determined from using the persistent random walk model; cells have faster speeds and shorter persistence times on ICAM-1 with lower speeds and longer persistence times on VCAM-1 while cells on fibronectin elicit a monotonic response. (C) Across all concentrations of ligand an inverse correlation is maintained between persistence time and cell speed on ICAM-1 and VCAM-1 but not on fibronectin.

CXCL12 induces T lymphocyte chemokinesis that is dependent on ICAM-1 concentration

The chemokine CXCL12 binds to the CXCR4 receptor and is capable of driving chemokinesis and chemotaxis [11, 14]. As with previous CCL19 and CCL21 studies, transwell assays have predominantly been used to demonstrate chemokinesis and chemotaxis, but these three dimensional assays provided limited ability to directly observe cells [30-32]. We decided to investigate CXCL12 mediated chemokinesis on ICAM-1 surfaces to see if we can see a peak in the random motility coefficient as a result of CXCR4 signaling. We designated ICAM-1 concentrations of 5.0 μg/ml as *high* and 0.05 μg/ml as *low*; these two concentrations support spontaneous and robust T lymphocyte migration, as shown in Chapter 3 of this thesis. We measured the random motility coefficient for a range of CXCL12 chemokine concentrations on both *high* and *low* concentrations of ICAM-1. We observed no significant differences in the random motility coefficients as a function of chemokine concentration on the *high* ICAM-1 surface with random motility coefficients (μ_{HIGH}) ranging between 208 ± 32.2 to 262 ± 52.5 μm^2/min (Fig. 3.10). We have showed that T lymphocytes are capable of sustained motility on ICAM-1 alone without the need for chemokines; this leads us to believe that sustained signaling through LFA-1/ICAM-1 interactions at this high ligand concentration was overwhelming the signals that resulted from CXCR4 receptor engagement similar to what was observed for CCR7 mediated chemokinesis. On the *low* ICAM-1 surface, we observed a biphasic response in motility to chemokine concentrations. Statistically significant peaks in the random motility coefficients (μ_{LOW}) were observed at 100 nM for CXCL12 (43.44 ± 4.82 μm^2/min) when compared to the random motility coefficient observed on *low* ICAM-1 alone ($p < 0.05$; Fig.

5.10). The values of the random motility coefficients for CXCL12 chemokinesis on *low* ICAM-1 surfaces are much less than what was observed for CCR7-mediated chemokinesis. Empirical observations in other cell systems have estimated the K_D of the CXCR4 receptor to be between 3 - 15 nM with observable peaks in motility which is significantly far less than what we show for the peak in the random motility coefficient [33, 34]. The observed peak of motility here with CXCR4 mediated chemokines may be a unique characteristic of T lymphocytes in our experimental system.

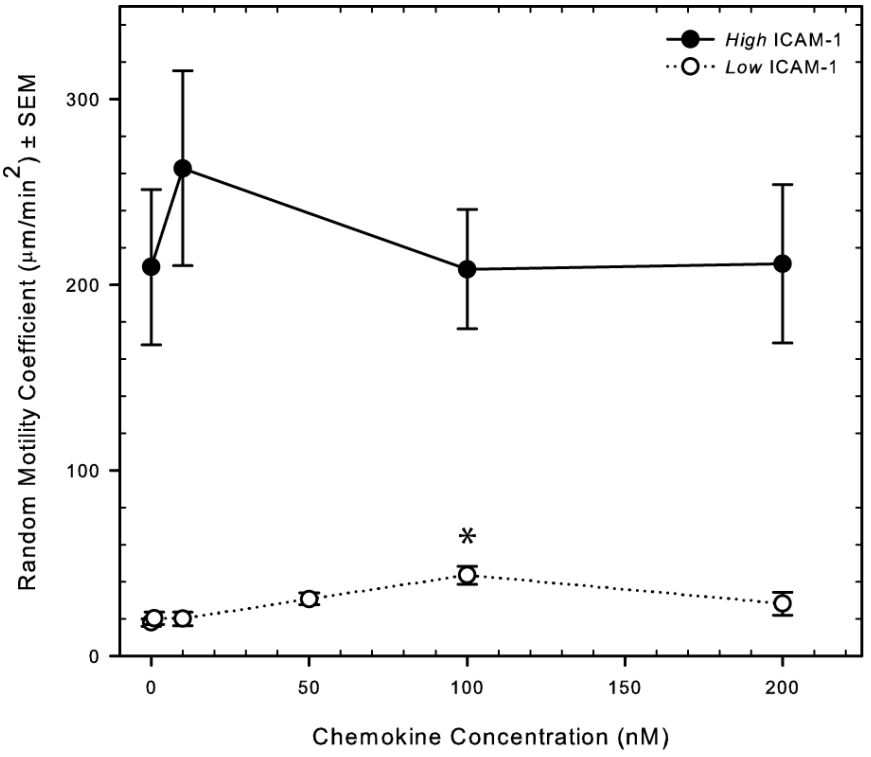

Figure. 5.10. sCXCL12 induces chemokinesis on *low* ICAM-1 surfaces. Comparison of the random motility coefficients (μ) show biphasic responses on *low* but not *high* ICAM-1 surfaces. Peak in chemokinesis observed at 100 nM with a value of 43.44 μm^2/min; *$p < 0.05$, compared to all concentrations; one-sample t test.

CONCLUSIONS

In this chapter, we measured the migration of primary human T lymphocytes on microcontact printed fibronectin PDMS surfaces and the effect of CXCL12 on ICAM-1. Our results show that T lymphocytes are capable of spontaneous and robust adhesion and migration to fibronectin in the absence of chemokine. By varying the fibronectin concentrations, we are able to modulate the speed, persistence times, and thus their random motility on these surfaces. As seen with LFA-1- and VLA-4-mediated motility, their motion is non-Brownian with superdiffusive behavior similar to what is seen on VCAM-1 surfaces. Unlike their motion on ICAM-1 and VCAM-1 surfaces, their motion is not biphasic on fibronectin surfaces but rather monotonic with both speed and persistence time increasing with ligand concentration. This leads us to believe that signaling through engagement of the three different integrins results in different modes of motility. Overall, we conclude through haptokinesis studies that ICAM-1 contributes more to motility than either VCAM-1 or fibronectin.

Furthermore, we explore chemokinesis to CXCL12 on ICAM-1 surfaces. As seen with CCL19 and CCL21, this response is dependent upon ligand concentration with T lymphocytes eliciting biphasic motility as a function of chemokine concentration on *low* ICAM-1 surfaces. We observe a peak in the random motility coefficient at a concentration of chemokine that is far greater than what has been observed before implying, perhaps, a unique response CXCL12-mediated chemokinesis in T lymphocytes.

REFERENCES

1. Springer, T.A., *Traffic signals for lymphocyte recirculation and leukocyte emigration: the multistep paradigm.* Cell, 1994. **76**(2): p. 301-14.
2. Butcher, E.C. and L.J. Picker, *Lymphocyte homing and homeostasis.* Science, 1996. **272**(5258): p. 60-6.
3. von Andrian, U.H. and C.R. Mackay, *T-cell Function and Migration: Two Sides of the Same Coin.* N Engl J Med, 2000. **343**(14): p. 1020-34.
4. Rose, D.M., J. Han, and M.H. Ginsberg, *Alpha4 integrins and the Immune Response.* Immunol Rev, 2002. **186**: p. 118-24.
5. Cahalan, M.D. and I. Parker, *Choreography of cell motility and interaction dynamics imaged by two-photon microscopy in lymphoid organs.* Annu Rev Immunol, 2008. **26**: p. 585-626.
6. Miller, M.J., et al., *T cell repertoire scanning is promoted by dynamic dendritic cell behavior and random T cell motility in the lymph node.* Proceedings of the National Academy of Sciences of the United States of America, 2004. **101**(4): p. 998-1003.
7. Bousso, P. and E.A. Robey, *Dynamic Behavior of T Cells and Thymocytes in Lymphoid Organs as Revealed by Two-Photon Microscopy.* Immunity, 2004. **21**(3): p. 349-355.
8. Bajenoff, M., et al., *Stromal cell networks regulate lymphocyte entry, migration, and territoriality in lymph nodes.* Immunity, 2006. **25**(6): p. 989-1001.
9. Miller, M.J., et al., *Two-Photon Imaging of Lymphocyte Motility and Antigen Response in Intact Lymph Node.* Science, 2002. **296**(5574): p. 1869-1873.

10. Sobocinski, G.P., et al., *Ultrastructural localization of extracellular matrix proteins of the lymph node cortex: evidence supporting the reticular network as a pathway for lymphocyte migration.* BMC Immunol, 2010. **11**: p. 42.

11. Shahabi, N.A., K. McAllen, and B.M. Sharp, *Stromal cell-derived factor 1-alpha (SDF)-induced human T cell chemotaxis becomes phosphoinositide 3-kinase (PI3K)-independent: role of PKC-theta.* J Leukoc Biol, 2008. **83**(3): p. 663-71.

12. Karin, N., *The multiple faces of CXCL12 (SDF-1alpha) in the regulation of immunity during health and disease.* J Leukoc Biol, 2010. **88**(3): p. 463-73.

13. Mao, Y. and J.E. Schwarzbauer, *Fibronectin fibrillogenesis, a cell-mediated matrix assembly process.* Matrix Biol, 2005. **24**(6): p. 389-99.

14. Ricart, B.G., et al., *Dendritic cells distinguish individual chemokine signals through CCR7 and CXCR4.* J Immunol, 2011. **186**(1): p. 53-61.

15. Henry, S.J., J.C. Crocker, and D.A. Hammer, *Ligand density elicits a phenotypic switch in human neutrophils.* Integrative Biology, 2014. **6**(3): p. 348-356.

16. Cherla, R.P. and R.K. Ganju, *Stromal cell-derived factor 1 alpha-induced chemotaxis in T cells is mediated by nitric oxide signaling pathways.* J Immunol, 2001. **166**(5): p. 3067-74.

17. Cyster, J.G., *Chemokines and Cell Migration in Secondary Lymphoid Organs.* Science, 1999. **286**(5447): p. 2098-2102.

18. Dickinson, R.B. and R.T. Tranquillo, *A stochastic model for adhesion-mediated cell random motility and haptotaxis.* Journal of Mathematical Biology, 1993. **31**(6): p. 7.

19. Othmer, H.G., S.R. Dunbar, and W. Alt, *Models of dispersal in biological systems.* Journal of Mathematical Biology, 1988. **26**(3): p. 263.

20. Dunn, G.A., *Characterising a kinesis response: time averaged measures of cell speed and directional persistence.* Agents and Actions Supplements, 1983. **12**: p. 19.

21. Stokes, C.L., D.A. Lauffenburger, and S.K. Williams, *Migration of individual microvessel endothelial cells: stochastic model and parameter measurement.* J Cell Sci, 1991. **99 (Pt 2)**: p. 419-30.

22. Ford, R.M. and D.A. Lauffenburger, *Measurement of bacterial random motility and chemotaxis coefficients: II. Application of single-cell-based mathematical model.* Biotechnology and Bioengineering, 1991. **37**(7): p. 661-672.

23. Desai, R.A., et al., *Subcellular spatial segregation of integrin subtypes by patterned multicomponent surfaces.* Integr Biol (Camb), 2011. **3**(5): p. 560-7.

24. Rodriguez, N.M., et al., *Micropatterned Multicolor Dynamically Adhesive Substrates to Control Cell Adhesion and Multicellular Organization.* Langmuir, 2014. **30**(5): p. 1327-1335.

25. Goodman, S.L., G. Risse, and K. von der Mark, *The E8 subfragment of laminin promotes locomotion of myoblasts over extracellular matrix.* J Cell Biol, 1989. **109**(2): p. 799-809.

26. Lauffenburger, D.A. and J.J. Linderman, *Receptors: Modeling for Binding, Trafficking, and Signaling*. 1996, New York: Oxford University Press.

27. Laffon, A., et al., *Upregulated expression and function of VLA-4 fibronectin receptors on human activated T cells in rheumatoid arthritis.* J Clin Invest, 1991. **88**(2): p. 546-52.

28. Rodriguez, R.M., et al., *T lymphocyte adhesion to fibronectin (FN): a possible mechanism for T cell accumulation in the rheumatoid joint.* Clin Exp Immunol, 1992. **89**(3): p. 439-45.

29. Truong, H. and E.H. Danen, *Integrin switching modulates adhesion dynamics and cell migration.* Cell Adh Migr, 2009. **3**(2): p. 179-81.

30. Yoshida, R., et al., *EBI1-ligand chemokine (ELC) attracts a broad spectrum of lymphocytes: activated T cells strongly up-regulate CCR7 and efficiently migrate toward ELC.* International Immunology, 1998. **10**(7): p. 901-910.

31. Frow, E.K., J. Reckless, and D.J. Grainger, *Tools for anti-inflammatory drug design: In vitro models of leukocyte migration.* Medicinal Research Reviews, 2004. **24**(3): p. 276-298.

32. Campbell, J.J., et al., *6-C-kine (SLC), a Lymphocyte Adhesion-triggering Chemokine Expressed by High Endothelium, Is an Agonist for the MIP-3β Receptor CCR7.* The Journal of Cell Biology, 1998. **141**(4): p. 1053-1059.

33. Oberlin, E., et al., *The CXC chemokine SDF-1 is the ligand for LESTR/fusin and prevents infection by T-cell-line-adapted HIV-1.* Nature, 1996. **382**(6594): p. 833-5.

34. Laguri, C., et al., *The novel CXCL12gamma isoform encodes an unstructured cationic domain which regulates bioactivity and interaction with both*

glycosaminoglycans and CXCR4. PLoS One, 2007. **2**(10): p. e1110.

CHAPTER 6: CONCLUSIONS AND FUTURE WORK

SPECIFIC AIMS

The research presented in this work shows that we were able to successfully characterize primary human T lymphocyte motility in response to three different adhesion ligands (haptokinesis), three different chemokines (chemokinesis), and fluid shear flow (mechanotaxis) on microcontact printed PDMS substrates.

Aim 1a: Characterize the motility of primary human T-lymphocytes on microcontact printed PDMS surfaces.

Aim 1b: Characterize the chemokinetic behavior of primary human T-lymphocytes in response to the homeostatic chemokines CCL19 and CCL21.

Aim 2: Quantify the motility of primary human T-lymphocytes on ICAM-1, VCAM-1 and combined ICAM-1/VCAM-1 PDMS surfaces under shear flow.

SPECIFIC FINDINGS

T Lymphocyte haptokinesis on ICAM-1, VCAM-1, and fibronectin substrates

We have investigated the effects of ligand concentration on T lymphocyte motility through quantification of the speeds, persistence times, and random motility coefficients. Through the use of microcontact printing, we printed PDMS spin coated glass coverslips with either protein A/G for Fc-containing ligands or fibronectin. All ligands were capable of supporting spontaneous adhesion and robust migration in the absence of chemokine. The use of ICAM-1/Fc and VCAM-1/Fc allows for quantification of motility elicited by engagement of their sole integrin binding partner LFA-1 ($\alpha_L\beta_2$) and VLA-4 ($\alpha_4\beta_1$),

respectively [1]. The observed motility on these substrates was biphasic with peaks in the random motility coefficients that is dependent upon ligand concentration. Furthermore, T lymphocytes maintained an inverse relationship between speed and persistence time that is typically seen in other cell types (Fig. 6.1) [2]. When cells were plated on varying concentrations of fibronectin, cells displayed a monotonic response with increasing speeds and persistence times with increasing ligand concentrations. Observed speeds for cells on fibronectin were similar to those quantified on VCAM-1 substrates; these similarities may lie in the fact that the engaged integrins are both β_1 containing. We also determined that T lymphocytes exhibit superdiffusive motion on these substrates which has recently been observed in vivo and in human neutrophils [3, 4]. Overall, T lymphocytes are more active on ICAM-1 than VCAM-1 or fibronectin surfaces, and ligand composition and concentration are essential in controlling their motility. Understanding how the three ligands affect T lymphocyte motility can provide insight into migration to and within secondary lymphoid organs (SLOs).

Quantifying chemokinesis using the homeostatic chemokines CCL19, CCL21, and CXCL12

Along with varying ligand composition, T lymphocytes are exposed to various chemokines that are required for migration and entry to SLOs [5, 6]. These homeostatic chemokines are known as CCR7-binding CCL19 and CCL21 and CXCR4-binding CXCL12. Initially, T lymphocytes were exposed to uniform concentrations of chemokine on ICAM-1 surfaces. There was no observable peak in motility leading us to conclude that the ligand concentration was too high thus preventing a response to chemokine. After repeating the experiments with a concentration that was two orders of magnitude lower, T

lymphocytes exhibited biphasic responses in the random motility coefficient to CCL19, CCL21, and CXCL12. The peak in the random motility coefficient corresponds to the K_D of each receptor [7]. CCR7 has a peak around 20 nM which is similar to what is found in literature [8, 9]. CXCR4, on the other hand, had a peak around 100 nM – a value that has not been previously observed.

Along the blood endothelium and within the SLOs, CCL19 and CCL21 are known to work together to drive homing and migration through simultaneous engagement of the CCR7 receptor [10]. This led us to ask whether combined chemokinesis of CCL19 and CCL21 would synergize and increase motility further. By combining both in solution, T lymphocyte motility was increased to levels above what was observed by each chemokine individually. However within the body, CCL21 is expressed on the blood endothelium and presented to cells on the surface rather than in soluble form [11, 12]. This led us to create surfaces of printed CCL21 with ICAM-1 and repeat the chemokinesis assay with varying concentrations of soluble CCL19. This resulted in T lymphocytes exhibiting random motility greater than what was observed by exposing to both soluble chemokines, combined or individually. Here, we demonstrated that CCL19 and CCL21 were capable of enhancing the motion of T lymphocytes and that enhancement was dependent upon the presence of an adhesive ligand.

T Lymphocyte migration under shear flow is dependent upon the presentation of ICAM-1 and VCAM-1

During T lymphocyte homing, cells must adhere and migrate along the blood endothelium to undergo diapedesis into the site of inflammation or SLO [13, 14]. These steps are mediated through the integrins LFA-1 and VLA-4. Previously, it was shown that demonstrated that naïve and effector T lymphocytes orient their migration against the direction of flow on ICAM-1 surfaces [15]. This effect was shown to be dependent upon shear rate with higher shear leading to an increased bias in upstream migration. We decided to investigate this further by quantifying T lymphocyte migration on ICAM-1 and VCAM-1 surfaces alone and on combinations of the two under varying shear rates. For T lymphocytes on ICAM-1 surfaces, upstream migration was found to not be dependent upon ligand concentration but rather shear rate with increasing shear rate resulting in an increase in preferred migration direction. For cells on VCAM-1, migration was downstream with fluid flow and found to be dependent upon ligand concentration and, to a lesser extent, shear rate.

Since extravasation requires LFA-1 and VLA-4 for transient and firm adhesion and migration, we created surfaces that present varying densities of the ligands ICAM-1 and VCAM-1 [16, 17]. For cells exposed to low shear rates, the resulting migration showed varying preferences either upstream or downstream of fluid flow that appeared to be dependent upon the densities of the ligand used. Upon exposure to high shear flow, a switch in migration was observed with cells orienting their migration upstream of fluid flow indicating a possible preference in utilizing LFA-1-ICAM-1 interactions to drive motility. This was further supported upon qualitative assessment of adhesion strength

mediated through LFA-1, VLA-4, or LFA-1/VLA-4 engagements. Increased shear resistance was observed on ICAM-1 containing surfaces when compared to VCAM-1. Furthermore, it is known that VLA-4 engagement can regulate β_2-mediated adhesion, and our data further indicates synergy of these two integrins to facilitate migration under shear on two-dimensional substrata [18, 19].

FUTURE WORK

Shear sensing: what is the intracellular signal?

Our flow chamber work has shown that T lymphocytes respond to shear in a ligand and shear rate specific manner. We ask the question – what is allowing the cell to sense this mechanical stress? There has been some exploration into what signaling molecules permit cell adhesion under flow but not specifically what controls the migration. We have performed some preliminary experiments using small molecule inhibitors against known signaling molecules involved in cell motility and adhesion; the molecules targeted include actin (Cytochalasin D), myosin II (blebbistatin), ROCK (Y-27632), PI3K (LY294002), and Rac (NSC23766). These molecules are known to be compartmentalized within T lymphocytes with ROCK and myosin II being concentrated at the rear of the cell and required for actomyosin contractility [20, 21]. Rac and PI3K are known to be in the front of the cell with Rac being required for stable actin polymerization while PI3K has been implicated in the sensing of the chemical gradients [22-24]. Upon disruption of actin filaments using Cytochalasin D, no cells adhered to the surface and thus no quantification of motility was permitted (data not shown). Figure 6.1 shows that all the inhibitors caused decreased upstream migration under 100 s^{-1} but increased upstream migration on 800 s^{-1}.

Furthermore, migration speeds were also not what we expected with increased speeds for some inhibitors under 100 s^{-1} compared to static (Fig. 6.2). These data is inconclusive and indicates that another signaling pathway is most likely involved in shear sensing leading to directional migration upstream of fluid flow. It would also be advantageous to do fluorescent labeling of candidate molecules or western blots to measure their distribution and amount.

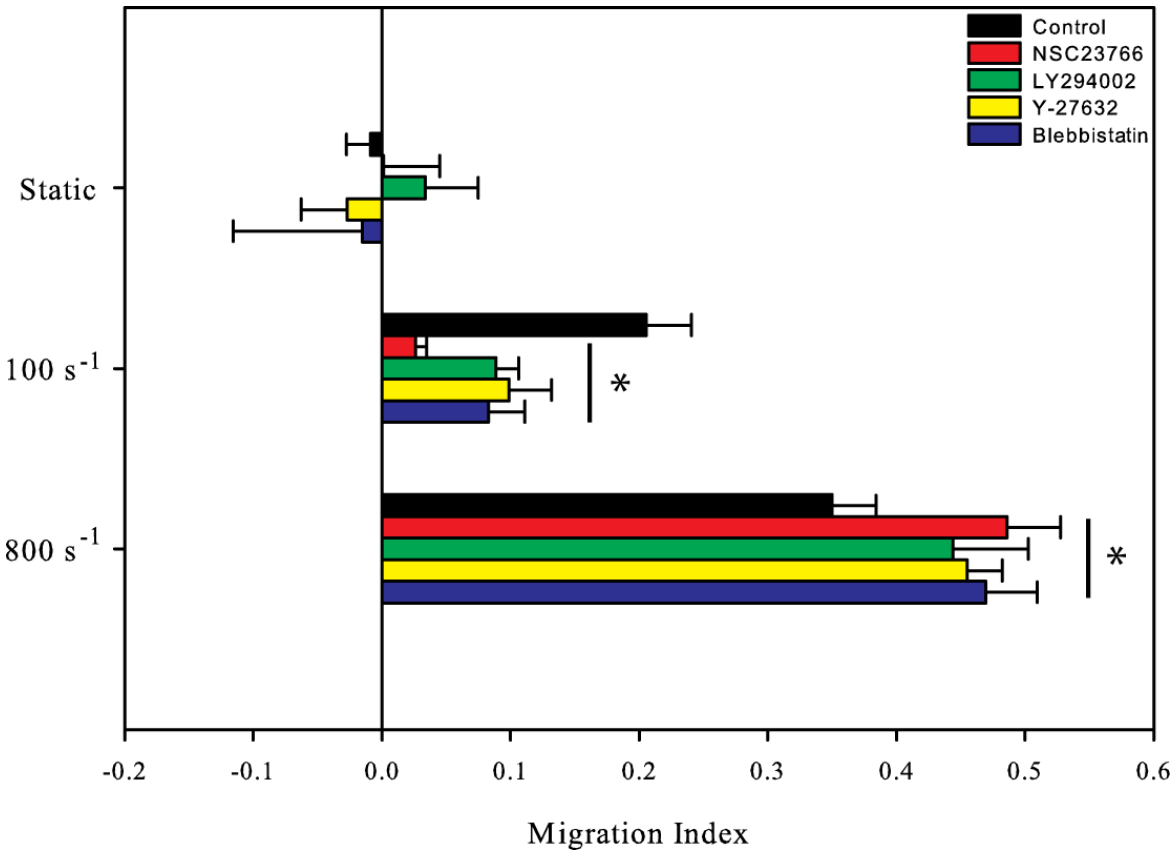

Figure 6.1. Effect of pharmacological inhibitors on the orientation of T-lymphocyte migration under shear flow. The effect of pharmacological inhibitors on the migration index for static, low, and high shear conditions.

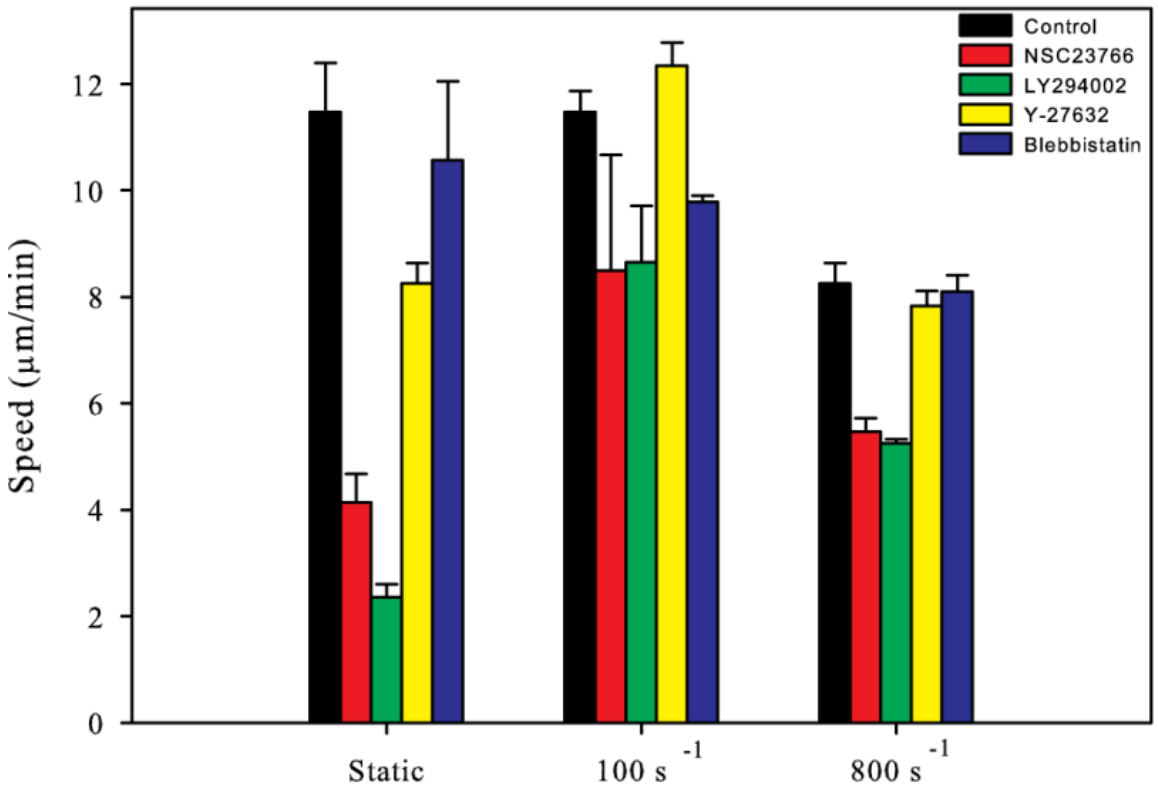

Figure 6.2. Effect of pharmacological inhibitors on the speed of T-lymphocyte migration under shear flow. The effect of pharmacological inhibitors on the speed for static, low, and high shear conditions.

Another possible target for inhibition in determining the mechanosensing in T lymphocytes is Vav1. Evidence has shown that Vav1, a guanine exchange factor (GEF) for the Rho family GTPases Rac and Cdc42, is involved in mechanosensing in murine neutrophils under shear flow. In Vav1 deficient murine neutrophils, cells lost the ability to migrate perpendicular to fluid flow [25]. A known Rac inhibitor, 6-Thio-GTP, is known to block the activity between Vav1 and Rac and could prove useful to study Vav1's involvement in migration under shear flow. The previously used Rac inhibitor NSC23766 blocks the activity between Rac and another GEF known as Tiam1 which is know to be involved in other processes [26-28].

Geometric patterning substrates for migration

It is well known that ligand geometry affects cell behavior [29, 30]. We would like to quantify the effects of ligand geometry on T lymphocyte migration in the absence and presence of shear flow on ICAM-1, VCAM-1, and fibronectin surfaces. Through the use of microcontact printing and the "stamp-off" method, we can create patterned lined substrates of varying widths ranging from 3 to 25 μm and larger (Fig. 6.3) [31-33].

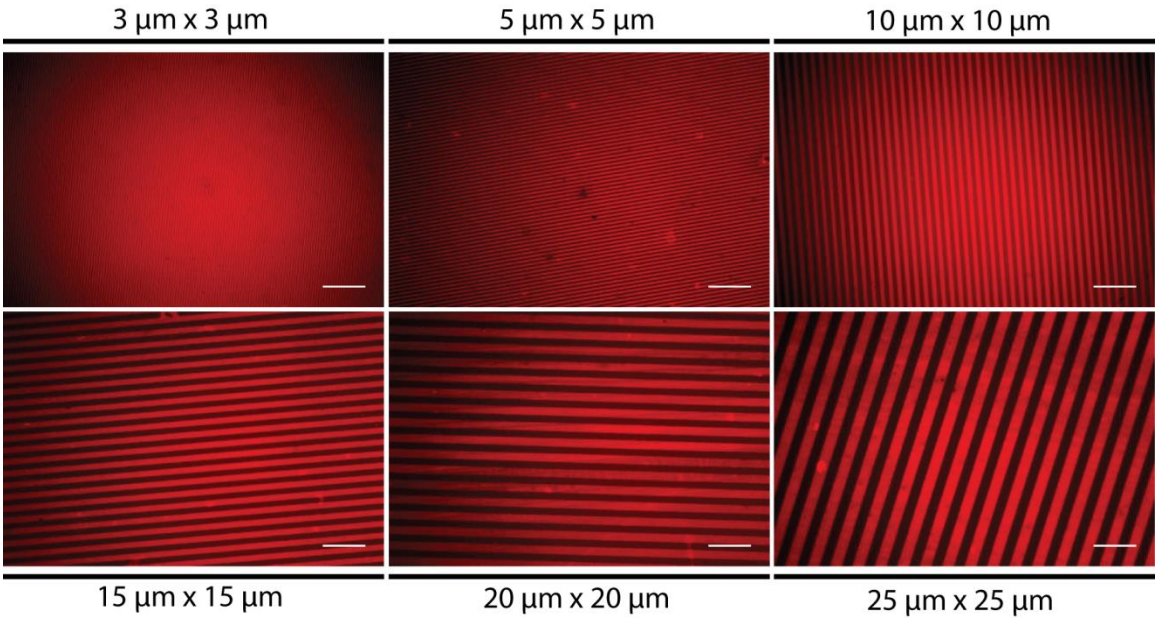

Figure 6.3. Patterned substrates of protein A/G with varying line widths. Surfaces were prepared using the stamp-off method with Alex Fluor-555 conjugated Protein A/G.

Preliminary experiments show that T lymphocytes plated on these substrates exposed to 100 s^{-1} of fluid flow display a bias in migration depending upon line orientation – either orthogonal or parallel to fluid flow (Fig. 6.4).

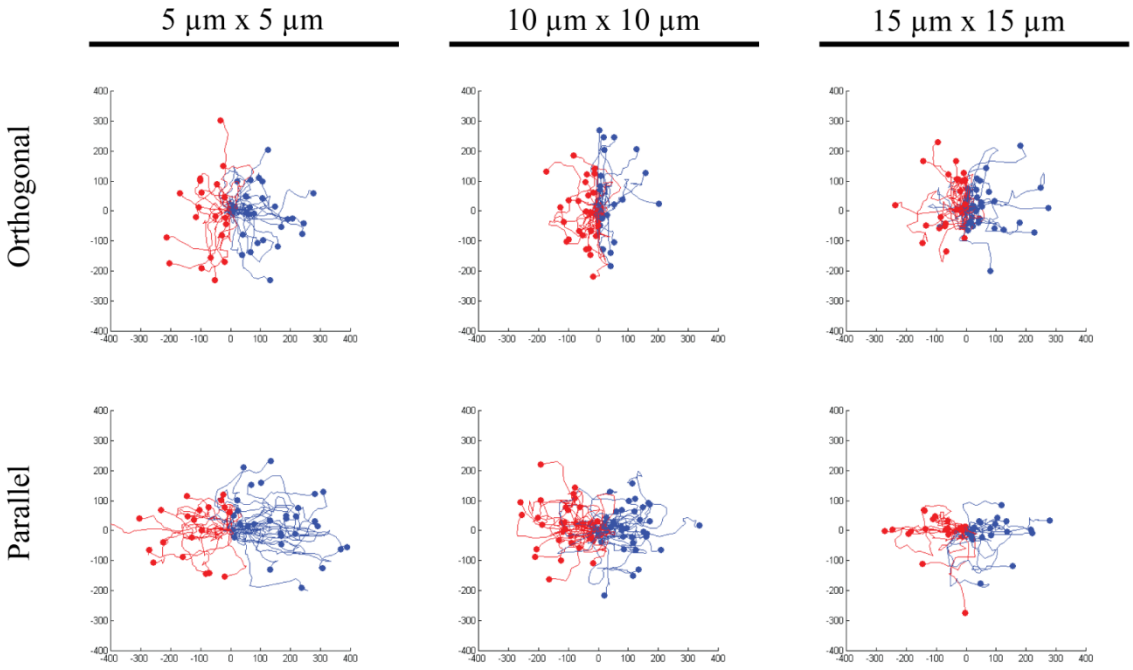

Figure 6.4. Traces of cell migration paths on patterned substrates of ICAM-1. T lymphocytes were allowed to crawl under 100 s^{-1} on ICAM-1 lined substrates.

Use of the stamp off method for microcontact printing allows for surface functionalization with multiple ligands. Cells have been shown to respond differently to patterned substrates with multiple ligands [32]. This technique would prove useful to study the effects of exposing T lymphocytes to ligand in alternating patterns. In this thesis, we have discussed that T lymphocytes migrate differently in response to various ligands; we would thus like to quantify this migration on spatially segregated ligands. Figure 6.5 shows that we can create alternating patterns of Alexa Fluor-488 conjugated fibronectin and Alexa Fluor-555 conjugated protein A/G at the smallest resolution of lines available (3 μm X 3 μm). Dual presentation of ligands in an ordered geometric pattern would provide further insight into how cell adhesion molecules control T lymphocyte migration under static conditions and under shear flow.

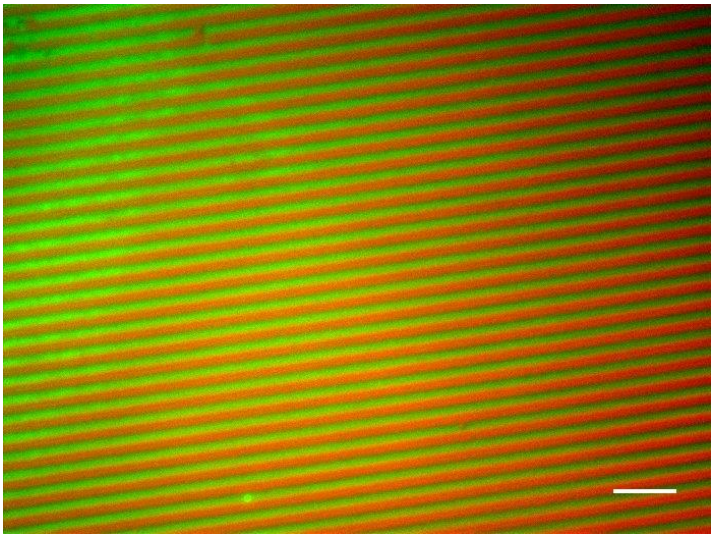

Figure 6.5. Alternating lines of fibronectin and protein A/G. 3 μm x 3 μm lines of alternating fibronectin (green) and protein A/G (red). Scale bar = 25 μm @ 40X

Haptokinesis on combined surfaces of ICAM-1 and VCAM-1 and LifeAct GFP transfection

Finally, we would like to expand upon our work of combined ligand surfaces of both ICAM-1 and VCAM-1. By repeating the experiments under static conditions, we could explore the signaling dynamics that occur upon engagement of both ligands allowing us to have increased insight about their migration under fluid flow. By performing western blots, we could identify the level of integrin activation downstream of receptor engagement as a function of ligand concentration for all combinations of ICAM-1 + VCAM-1. Furthermore, we would like to virally transduce cells to express the LifeAct-GFP construct for actin visualization. We believe this would allow us to better characterize the migration of T lymphocytes on ICAM-1 and VCAM-1 under fluid flow.

FINAL THOUGHTS

Homing and migration of leukocytes is at the heart of the immune system. Specifically, T lymphocytes are required to adhere and migrate on adhesive ligands, respond to chemokines, and withstand the hemodynamic forces present in order for them to reach sites of inflammation and lymphoid tissue. While we only focused on a specific aspect of controlling T lymphocyte migration, we believe this work contributes to the field of immunology and cell migration. Through our work, we have gained further insight into the dynamics of T lymphocyte motility on three different physiological ligands, how homeostatic chemokines govern their motility, and the effects that shear flow has on their ability to adhere and migrate. We hope this work will continue on engineered substrates to control migration and inspire future ideas and projects.

ACKNOWLEDGMENTS

Thanks to Eric Johnston for technical support as well as the entire Hammer Lab for helpful discussions, suggestions, and support throughout the past 6 years. We also acknowledge financial support from the National Academies Ford Foundation Predoctoral Fellowship, Fontaine Fellowship, and the National Institutes of Health Grant AI082292.

REFERENCES

1. Hyun, Y.-M., C. Lefort, and M. Kim, *Leukocyte integrins and their ligand interactions.* Immunologic Research, 2009. **45**(2-3): p. 195-208.
2. Lauffenburger, D.A. and J.J. Linderman, *Receptors: Modeling for Binding, Trafficking, and Signaling*. 1996, New York: Oxford University Press.
3. Harris, T.H., et al., *Generalized Levy walks and the role of chemokines in migration of effector CD8+ T cells.* Nature, 2012. **486**(7404): p. 545-548.
4. Henry, S.J., J.C. Crocker, and D.A. Hammer, *Ligand density elicits a phenotypic switch in human neutrophils.* Integrative Biology, 2014. **6**(3): p. 348-356.
5. von Andrian, U.H. and C.R. Mackay, *T-cell Function and Migration: Two Sides of the Same Coin.* N Engl J Med, 2000. **343**(14): p. 1020-34.
6. Worbs, T., et al., *CCR7 ligands stimulate the intranodal motility of T lymphocytes in vivo.* J Exp Med, 2007. **204**(3): p. 489-95.
7. Farrell, B.E., R.P. Daniele, and D.A. Lauffenburger, *Quantitative relationships between single-cell and cell-population model parameters for chemosensory migration responses of alveolar macrophages to C5a.* Cell Motil Cytoskeleton, 1990. **16**(4): p. 279-93.
8. Ricart, B.G., et al., *Dendritic cells distinguish individual chemokine signals through CCR7 and CXCR4.* J Immunol, 2011. **186**(1): p. 53-61.
9. Yoshida, R., et al., *Secondary Lymphoid-tissue Chemokine Is a Functional Ligand for the CC Chemokine Receptor CCR7.* Journal of Biological Chemistry, 1998. **273**(12): p. 7118-7122.

10. Miller, M.J., et al., *Autonomous T cell trafficking examined in vivo with intravital two-photon microscopy.* Proc Natl Acad Sci U S A, 2003. **100**(5): p. 2604-9.

11. Stein, J.V., et al., *CCR7-mediated physiological lymphocyte homing involves activation of a tyrosine kinase pathway.* Blood, 2003. **101**(1): p. 38-44.

12. Warnock, R.A., et al., *The Role of Chemokines in the Microenvironmental Control of T versus B Cell Arrest in Peyer's Patch High Endothelial Venules.* The Journal of Experimental Medicine, 2000. **191**(1): p. 77-88.

13. Springer, T.A., *Traffic signals for lymphocyte recirculation and leukocyte emigration: the multistep paradigm.* Cell, 1994. **76**(2): p. 301-14.

14. Butcher, E.C. and L.J. Picker, *Lymphocyte homing and homeostasis.* Science, 1996. **272**(5258): p. 60-6.

15. Valignat, M.P., et al., *T lymphocytes orient against the direction of fluid flow during LFA-1-mediated migration.* Biophys J, 2013. **104**(2): p. 322-31.

16. Alon, R., et al., *The integrin VLA-4 supports tethering and rolling in flow on VCAM-1.* The Journal of Cell Biology, 1995. **128**(6): p. 1243-53.

17. Shimonaka, M., et al., *Rap1 translates chemokine signals to integrin activation, cell polarization, and motility across vascular endothelium under flow.* J Cell Biol, 2003. **161**(2): p. 417-27.

18. Rose, D.M., et al., *The Affinity of Integrin α4β1 Governs Lymphocyte Migration.* The Journal of Immunology, 2001. **167**(5): p. 2824-2830.

19. Chan, J.R., S.J. Hyduk, and M.I. Cybulsky, *α4β1 Integrin/VCAM-1 Interaction Activates αLβ2 Integrin-Mediated Adhesion to ICAM-1 in Human T Cells.* The Journal of Immunology, 2000. **164**(2): p. 746-753.

20. Smith, A., et al., *LFA-1-induced T cell migration on ICAM-1 involves regulation of MLCK-mediated attachment and ROCK-dependent detachment.* J Cell Sci, 2003. **116**(Pt 15): p. 3123-33.

21. Takesono, A., Heasman, S. J., Wojciak-Stothard, B., Garg, R. and A. J. Ridley, *Microtubules Regulate Migratory Polarity through Rho/ROCK Signaling in T Cells.* PLoS One, 2010. **5**(1): p. 15.

22. Ward, S.G., *Do phosphoinositide 3-kinases direct lymphocyte navigation?* Trends in Immunology, 2004. **25**(2): p. 67-74.

23. Ward, S.G., *T lymphocytes on the move: chemokines, PI 3-kinase and beyond.* Trends in Immunology, 2006. **27**(2): p. 80-87.

24. Ward, S.G. and F.M. Marelli-Berg, *Mechanisms of chemokine and antigen-dependent T-lymphocyte navigation.* Biochem J, 2009. **418**(1): p. 13-27.

25. Phillipson, M., et al., *Vav1 is essential for mechanotactic crawling and migration of neutrophils out of the inflamed microvasculature.* J Immunol, 2009. **182**(11): p. 6870-8.

26. Gerard, A., et al., *The Rac activator Tiam1 controls efficient T-cell trafficking and route of transendothelial migration.* Blood, 2009. **113**(24): p. 6138-47.

27. Hamelers, I.H., et al., *The Rac activator Tiam1 is required for (alpha)3(beta)1-mediated laminin-5 deposition, cell spreading, and cell migration.* J Cell Biol, 2005. **171**(5): p. 871-81.

28. Van Leeuwen, F.N., et al., *Rac activation by lysophosphatidic acid LPA1 receptors through the guanine nucleotide exchange factor Tiam1*. J Biol Chem, 2003. **278**(1): p. 400-6.

29. Chen, C.S., et al., *Geometric Control of Cell Life and Death.* Science, 1997. **276**(5317): p. 1425-1428.

30. Nelson, C.M., et al., *Tissue Geometry Determines Sites of Mammary Branching Morphogenesis in Organotypic Cultures.* Science, 2006. **314**(5797): p. 298-300.

31. Desai, R.A., N.M. Rodriguez, and C.S. Chen, *Chapter 1 - "Stamp-off" to Micropattern Sparse, Multicomponent Features,* in *Methods in Cell Biology*, P. Matthieu and T. Manuel, Editors. 2014, Academic Press. p. 3-16.

32. Desai, R.A., et al., *Subcellular spatial segregation of integrin subtypes by patterned multicomponent surfaces.* Integr Biol (Camb), 2011. **3**(5): p. 560-7.

33. Rodriguez, N.M., et al., *Micropatterned Multicolor Dynamically Adhesive Substrates to Control Cell Adhesion and Multicellular Organization.* Langmuir, 2014. **30**(5): p. 1327-1335.